

Evaluation of Storm Surge Components at Saldanha Bay

by
Johan Louw Wahl

*Thesis presented in fulfilment of the requirements for the degree of
Master of Engineering (Research) in the Faculty of Civil Engineering at
Stellenbosch University*



Supervisor: Prof JS Schoonees

December 2016

Declaration

By submitting this thesis electronically, I declare that the entirety of the work contained therein is my own, original work, that I am the owner of the copyright thereof (unless to the extent explicitly otherwise stated) and that I have not previously in its entirety or in part submitted it for obtaining any qualification.

December 2016

Copyright © 2016

Stellenbosch University All rights reserved

Abstract

Extreme sea levels are made up of many different components – the most noteworthy of these include tides, tsunamis, seiches, wave setup, runup and storm surge. The latter is often considered to be the most significant contributing component. Accordingly, some of the most severe coastal floods globally have been as direct result of storm surge. Storm surge is the increase (or decrease) in sea levels resulting mainly from wind setup and the inverse barometer effect (pressure setup). Wind setup usually makes up the majority component. With this in mind, it is vast shallow coastlines in areas frequented by strong winds that are most vulnerable to storm surge. Many scholars have essentially ruled out the possibility of large storm surges along the South African coast on the basis that the coastal shelf is too deep and that winds are too moderate to agitate significant wind setup. As a result, storm surge heights for the South African coast, specifically, has never been thoroughly researched or documented. Yet, in the absence of definitive literature on this matter, storm surge is often quoted as the scapegoat for coastal damages. Furthermore, when it comes to engineering designs, indiscreetly estimated values are often used.

This study, focussing on Saldanha Bay as a test case, gains knowledge into the actual range of values for storm surge to be taken into account in engineering designs. This is done primarily by means of time series analyses of available water level data. Methods by which to easily calculate such results are also looked at. These methods include analytical calculations and numerical modelling.

The data available for this study included water level data (tide gauge) from SANHO and weather data from TNPA. Weather data was used for the comparison with water level data. Data sets span approximately 5 years in total (January 2010 to March 2015) although large and frequent gaps are present. The time series analyses included a Fourier analysis, cross correlation analyses, regression analyses and filtering. Correlations were sought out between wind and pressure, and the measured water levels, so as to attribute certain components of the total measured fluctuations to storm surge. Subsequent to the time series analysis, a hindcast of the storm surge components was done using analytical calculation techniques as well as a numerical model. Analytical techniques used include the formulae as prescribed by Bretschneider and Kamphuis. The numerical modes made use of DHI's MIKE HD module. Furthermore, NCEP data was sourced, validated and used for the calculation of extreme storm surges.

The study results indicate that values for wind setup and pressure setup at Saldanha Bay are in the order of 31 to 64mm and 91-268mm respectively. The extreme value analysis performed on the NCEP data suggests that the maximum expected values for wind setup and pressure setup are 163mm and 386mm respectively. From the results it is concluded that the wind setup component of storm surge is small enough to be ignored for most practical applications. An exception to this rule would apply to extreme

shallow water bodies such as large lagoons and estuaries where it is estimated that wind setup could reach heights of up to 1.5m. The pressure component of storm surge is regarded as more significant and (for design purposes) may be assigned a fixed maximum value of 390mm along the entire south and southwestern coast. In cases (possibly outside the coastal area considered in this study) where detailed calculations are needed, the appropriate guidelines of this study may be taken into account. On the methods for calculating storm surge, it was found the MIKE 21 model yields good results for static conditions, but that very little of the expected dynamic effects of storm surge is revealed. The accuracy of the analytically calculations was not conclusively determined. However, there was strong evidence to suggest that, provided the assumptions and limitations of these formulae are respected, the analytical formulas provide satisfactory results.

Opsomming

Ekstreme seevlakke bestaan uit verskillende komponente waarvan getye, tsoenami's, "seiches", golfopstuwing, oloop en stormopstuwing die vernaamste is. Laasgenoemde word allerweë as die belangrikste bydraende komponent beskou en sommige van die ergste kus-verwante vloede wat al wêreldwyd plaasgevind het, is 'n direkte gevolg van stormopstuwing. Stormopstuwing is die toename (of afname) in seevlakke, hoofsaaklik as gevolg van windopstuwing en die omgekeerde barometer effek (lugdrukopstuwing). Windopstuwing is normaalweg die grootste komponent. Teen hierdie agtergrond is die groot, vlak kuslyne in gebiede waar sterk winde gereeld voorkom, besonder kwesbaar vir stormopstuwing. Baie navorsers het in die verlede die moontlikheid van groot stormopstuwings langs die Suid-Afrikaanse kus vir alle praktiese doeleindes buite rekening gelaat, aangesien die kusplat te diep is en die winde te matig, om betekenisvolle windopstuwing te veroorsaak. Die gevolg hiervan is dat die hoogte van stormopstuwing langs die Suid-Afrikaanse kus nog nooit deeglik nagevors en gedokumenteer is nie. Nietemin, ten spyte van die gebrek aan toepaslike literatuur, word stormopstuwing dikwels as die sondebok beskou wanneer dit kom by stormskade langs die Suid-Afrikaanse kus. Verder, wanneer daar ingenieursontwerpe in hierdie verband gedoen word, word daar dikwels, op onoordeelkundige wyse, van geskatte waardes gebruik gemaak.

Hierdie studie, wat vir toets doeleindes op Saldanhaabaai fokus, is 'n poging om kennis in te win oor die werklike stel waardes wat vir stormopstuwing in berekening gebring behoort te word by die opstel van ingenieursontwerpe. Dit word primêr gedoen deur die ontleding van tydreekse wat uit die beskikbare watervlak data geneem word. Daar word gekyk na metodes waarvolgens hierdie tipe resultate redelik maklik bereken kan word. Hierdie metodes sluit onder meer analitiese berekeninge en numeriese modellering in.

Die beskikbare data vir hierdie studie sluit in: watervlak data (getymeter) van SANHO en weer data van TNPA. Weer data is gebruik as deel van 'n proses van vergelyking met watervlak data. Datastelle strek oor ongeveer 5 jaar in totaal (Januarie 2010 tot Maart 2015), maar is ongelukkig nie heeltemal volledig nie en bevat 'n aantal opvallende gapings. Die ontledings van tydreeks sluit onder meer die volgende in: 'n Fourier analise, 'n kruiskorrelasie analise, 'n regressie analise en 'n filterproses. Daar is gesoek na korrelasies tussen wind, lugdruk en die gemete watervlakke met die oog daarop om sekere komponente van die totale gemete fluktuasies aan stormopstuwing toe te skryf. Die ontleding van tydreeks is opgevolg met 'n naskatting van die stormopstuwing komponente, deur gebruikmaking van analitiese berekeningstegnieke, sowel as 'n numeriese model. Van die analitiese tegnieke wat gebruik is, sluit die formules in wat deur Bretscheider en Kamphuis voorgeskryf is. Die Numeriese model wat gebruik is, maak gebruik van DHI se MIKE HD module. NCEP data is ook verkry, gevalideer en gebruik vir die berekening van ekstreme stormopstuwing.

Die studieresultate dui aan dat waardes vir windopstuwing en lugdrukopstuwing by Saldanhabaai wissel van 31 tot 64 mm en van 91 tot 268 mm onderskeidelik. Die ekstreme waarde analise wat op die NCEP data toegepas is, dui op 'n maksimum verwagte waarde van 163 mm vir windopstuwing en 386 mm vir lugdrukopstuwing. Vanuit hierdie resultate word die gevolgtrekking gemaak dat die windopstuwing komponent van stormopstuwing vir alle praktiese doeleindes klein genoeg is om geïgnoreer te word. 'n Uitsondering op hierdie reël is wanneer daar met watermassas, soos strandmere en riviermondings, gewerk word waarin die water baie vlak is en waar die windopstuwing vlakke van so hoog as 1.5m kan bereik. Die lugdruk komponent van stormopstuwing word as meer betekenisvol beskou en vir ontwerpdoeleindes mag 'n vaste maksimum waarde van 390mm hieraan toegeken word. Dit geld in die algemeen vir die hele suid- en suidwes kus. In gevalle waar gedetailleerde berekeninge benodig word (moontlik in ander kusgebiede as die area waarop daar in hierdie studie gefokus is), kan die betrokke riglyne van hierdie studie in aanmerking geneem word. Wat die metodes betref vir die berekening van stormopstuwing, is daar bevind dat die MIKE 21 model goeie resultate lewer vir statiese toestande, maar dat baie min van die verwagte dinamiese effekte van stormopstuwing na vore kom. Die akkuraatheid van die analitiese berekeninge kon nie bo alle twyfel vasgestel word nie. Daar was nogtans sterk aanduidings dat die analitiese formules wel bevredigende resultate lewer, indien dit met inagneming van die relevante aannames en beperkinge toegepas word.

Acknowledgements

The following individuals and institutions provided valuable and much appreciated assistance and contributions towards the outcome of this thesis:

CSIR	<i>Facilitating data collection</i>
SANHO	<i>Supply of tide gauge data and records of calculated tides</i>
TNPA	<i>Supply of ultrasound water level data, weather data and bathymetry data</i>
DHI	<i>Academic licence for MIKE 21 modelling software</i>
Mr G Toms	<i>Study supervisor and lecturer (2014)</i>
Prof JS Schoonees	<i>Study supervisor and lecturer (2015 – 2016)</i>
John Wahl	<i>Proof reading and editing</i>

A sincere thanks to all of the above, especially to my dad, John, who genuinely went the extra mile to assist with proof reading and editing at the last minute.

Furthermore, and most importantly, I want to extend my most sincere gratitude and thanks to my close friends and family who endured with me for 3 rough years of full time work and part time study. Your support and encouragement has been inspirational and invaluable.

Table of Contents

Declaration.....	i
Abstract.....	ii
Opsomming.....	iii
Acknowledgements.....	v
Table of Contents.....	vi
List of Figures.....	x
List of Tables.....	xii
Abbreviations.....	xiv
1 Introduction.....	1
1.1 Background.....	1
1.2 Thesis Objectives.....	3
1.3 Thesis overview & Structure.....	4
1.4 Clarifications and Initial Assumptions.....	4
2 Literature Review.....	6
2.1 Meteorology and Weather Systems of South Africa.....	6
2.2 Storm Events.....	9
2.3 Previous Work in South Africa Relating to Storm Surge.....	11
2.4 Storm surge theory and Analytical Methods.....	15
2.4.1 Typical Storm Surge Conditions (Global).....	15
2.4.2 Mechanics of Storm Surge.....	16
2.4.3 Analytical Solutions.....	16
2.5 Signal Processing Theory.....	20
2.5.1 Signal Processing Theory: Frequency Transforms and the Fourier Analysis.....	20
2.5.2 Sampling Theory.....	21
3 Analysis of Measured Time Series Data.....	23
3.1 General.....	23
3.2 Data Overview and Preliminary Analysis.....	23

3.2.1	Discussion of available data.....	23
3.2.2	Defining Wind Directions.....	26
3.2.3	Length of Data Records	27
3.2.4	Data Quality Control.....	29
3.2.5	Preliminary Analysis of Residual Water Levels	31
3.3	Spectral analysis of residual water levels	34
3.3.1	Methodology	34
3.3.2	Results.....	34
3.4	Data Filtering	43
3.5	Comparitive Analysis.....	49
3.5.1	Methodology	49
3.5.2	Results.....	52
3.6	Discussion of Results.....	57
3.6.1	Component breakdown	57
3.6.2	Summary of Residual Components: Saldanha Bay	60
3.6.3	Storm Surge: Saldanha Bay	65
4	Extreme Water Levels Based on NCEP Data.....	67
4.1	General.....	67
4.2	Validation of NCEP Data.....	68
4.2.1	Validation of NCEP Wind Data.....	68
4.2.2	Validation of NCEP Pressure Data.....	72
4.3	Extreme Value Analysis of NCEP data	73
4.3.1	EVA Theory and methodology	73
4.3.2	Results.....	74
5	Analytical Computations of Storm Surge	76
5.1	General.....	76
5.2	Calculation Of Wind Setup.....	78
5.2.1	Selecting Suitable Test Positions for Calculating Wind Setup	78
5.2.2	Selecting Wind Velocities for use in calculations.....	80

5.3	Calculation Of Pressure Effects	81
5.4	Results.....	81
5.5	Discussion of Results	88
5.5.1	Results Comparison: Different Analytical Equations	88
5.5.2	Results Comparison: Analytical Equations vs Time Series Analysis	89
6	Numerical Modelling of Storm Surge.....	92
6.1	General.....	92
6.2	Model Description	92
6.2.1	Model Setup	93
6.2.2	Model Outputs	95
6.3	Model Calibration	96
6.3.1	Discussion	96
6.3.2	Calibration Scenarios: Domain Size Sensitivity	97
6.3.3	Calibration Scenarios: Wind Drag Coefficient Sensitivity	99
6.3.4	Calibration Scenarios: Bottom Friction Coefficient Sensitivity	100
6.3.5	Calibration Scenarios: Wind Data Time-step Size Sensitivity.....	101
6.3.6	Calibration Scenarios: Pressure	102
6.3.7	Calibration Scenarios: Local Wind Set-up.....	103
6.4	Model Results and Discussion	108
6.4.1	Comparison with Results of Analytical Calculations	112
7	Discussion of Results.....	115
7.1	General.....	115
7.2	Discussion and Comparison of Results.....	115
7.2.1	Static Storm Surge vs. Dynamic Storm Surge	115
7.2.2	Storm Surge heights	116
7.2.3	Application of Study Outcomes	118
8	Conclusions and Recommendations	120
8.1	Study Conclusions and Application of Results.....	120
8.2	Recommendations for Future Studies	121

9 References..... 123

List of Figures

Figure 1: Map of South Africa. Position of Saldanha Bay indicated with red marker	5
Figure 2: Overview of typical global weather patterns (Watts 2004 Modified)	7
Figure 3: Typical passage of a cold front along the south Western Cape coast (Tyson & Preston-Whyte 2000 modified).....	7
Figure 4: Cyclone tracks for 1952 to 2007 (Mavume et al. 2009 Modified)	8
Figure 5: sea level pressure analysis for 18 March 2007, 18h00 UTC (Hunter et al. 2007 Modified). 10	
Figure 6: Photograph showing storm damage along the Durban coast, 2007 (Hunter et al. 2007 Modified)	10
Figure 7: Brundrit's results of separating high frequencies from low frequencies.....	12
Figure 8: Sea levels, Pressure and wind at Lamberts Bay (De Cuevas 1985 Modified).....	13
Figure 9: Aerial imagery of Saldanha Bay.....	25
Figure 10: Plot of wind directions for the Saldanha Bay wind data set. Direction is in degrees. South is 180 degrees and north is 0 or 360.	27
Figure 11: Time intersection plot for the various data sets available for Saldanha Bay	28
Figure 12: Complete residual data set for all available tide gauge data from January 2010 to March 2015	32
Figure 13: Summary plot of Data Series 1 showing water levels (measured, predicted and residuals) as well as ambient wind and pressure measurements. Start time is 2014-03-14 15:20 and end time is 2014-05-20 07:10	36
Figure 14: Summary plot of Data Series 2 showing water levels (measured, predicted and residuals) as well as ambient wind and pressure measurements. Start time is 2010-01-01 00:00 and end time is 2010-03-05 00:00	37
Figure 15: Summary plot of Data Series 3 showing water levels (measured, predicted and residuals) as well as ambient wind and pressure measurements. Start time is 2014-06-29 17:40 and end time is 2014-08-11 19:10	38
Figure 16: Spectrum plot of for residual water levels for Saldanha data series No. 1. Red lines indicate the spectra for each 1-week window. The black line is the average spectrum over 10 windows.	39
Figure 17: Spectrum plot of for predicted tides	40
Figure 18: Spectrum plot of for residual water levels for Saldanha data series No. 2. Red lines indicate the spectra for each 1-week window. The black line is the average spectrum over 9 windows.	41
Figure 19: Spectrum plot of for residual water levels for Saldanha data series No. 3. Red lines indicate the spectra for each 1-week window. The black line is the average spectrum over 7 windows.	42
Figure 20: Results of preliminary filtering for Saldanha data set No.1 (a) unfiltered (red) vs. filtered data(black) (b) isolated tide lag component 1.97 cpd (c) isolated noise of frequencies greater than 20.4 cpd.....	44
Figure 21: Comparison plots of residual components (frequencies 8.9 to 21.4 cpd) and onshore (south) wind speeds. (a), (b) and(c) represent data series 1, 2 and 3 respectively.	45
Figure 22: Comparison plots of smoothed residual components (frequencies 8.9 to 21.4 cpd) and onshore wind for data series No.1. (a) 12 hour moving average (b) 1 day moving average (c) 2 day moving average.....	46

Figure 23: Comparison plots of smoothed residual components (frequencies 8.9 to 21.4 cpd) and onshore wind for data series No.2. (a) 12 hour moving average (b) 1 day moving average (c) 2 day moving average.....	47
Figure 24: Comparison plots of smoothed residual components (frequencies 8.9 to 21.4 cpd) and onshore wind for data series No.3. (a) 12 hour moving average (b) 1 day moving average (c) 2 day moving average.....	48
Figure 25: Cross correlation between maximum tidal heights and filtered residual water levels. (a) Cross Correlation (b) Auto correlation for maximum tidal height (red), filtered residuals (blue) and their product (black dash) (c) Time integral of autocorrelation functions	51
Figure 26: Pressure (a) and Filtered residuals (b) for data set No.3 (2014-06-29 to 2014-08-11).....	53
Figure 27: Scatter plot of filtered residual water levels against pressure at Saldanha Bay for data set No. 1	54
Figure 28: Comparison plots of Filtered residual water levels with and without adjustment for inverse barometer effect. (a) Data series No.1 (2014) (b) Data series No.2 (2010) (c) Data series No.3 (2014)	55
Figure 29: Summary plot of storm surge components in Saldanha Bay data series No. 1	62
Figure 30: Summary plot of storm surge components in Saldanha Bay data series No. 2	63
Figure 31: Summary plot of storm surge components in Saldanha Bay data series No. 3	64
Figure 32: Total storm surge componts at Saldanha Bay for (a) Data series no.1 (b) No.2 and (c)No. 3 as determined in the time series analysis	66
Figure 33: NCEP (Red) and measured (Black) wind speed at Saldanha Bay. (a) Data set No.1 (b) No.2 (c) No.3	68
Figure 34: Rose Plot of measured wind (20 minute average at 10 aMSL) for the full duration of measured data (from Jan 2010 to Jan 2015)	70
Figure 35: Rose Plot of NCEP wind (6 hour average at 10 aMSL). Data subset is from Jan 2010 to Jan 2015	71
Figure 36: Visual comparison of NCEP pressure data (red) vs measured pressure data (black) for (a) Data set No.1, (b) Data set No. 2 and (c) Data set No. 3.	72
Figure 37: Visual comparison of NCEP pressure data (red) vs measured pressure data (black) for data spanning Jan 2010 to Jan 2015	73
Figure 38: Probability plot for Extreme Value analysis of NCEP Wind speeds.....	74
Figure 39: Probability plot for Extreme Value analysis of NCEP Pressure data.....	75
Figure 40: Schematic of wind setup parameters for the open coast.....	77
Figure 41: Test scenarios for analytical wind setup calculations.....	78
Figure 42: Bathymetry cross sections for test lines used in analytical calculations	79
Figure 43: Results of analytical calculations for wind setup at test position no.1 using the Kamphuis equation (Equation (17)).....	82
Figure 44: Results of analytical calculations for wind setup at test position no.2 using the Kamphuis equation (Equation(17)).....	83
Figure 45: Results of analytical calculations for wind setup at test position no.3 using the Kamphuis equation (Equation (17)).....	84
Figure 46: Results of analytical calculations for wind setup at test position no.4 using the Kamphuis equation (Equation (17)).....	85

Figure 47: Results of analytical calculations for wind setup at test position no.5 using the Kamphuis equation (Equation (17)).....	86
Figure 48: Comparison of calculated wind setup heights	89
Figure 49: Saldanha bay numerical model mesh (magnification of port and lagoon area).....	94
Figure 50: Saldanha Bay numerical model boundary conditions: (red) open boundary (green) zero normal velocity land boundary.....	95
Figure 51: Selected points for time series model outputs	96
Figure 52: Extents of different domains used in sensitivity analysis. (a) Maximum available domain (b) Inner bay and 15 of offshore bathymetry (c) Inner bay only	98
Figure 53: Modelled wind set-up results for 3 test runs of varying domain sizes. (a) Wind setup heights for different domain sizes (b) Wind input data set.....	98
Figure 54: Modelled results for wind setup (Y-axis shows height in mm) for 3 different test runs whereby varying only the wind drag coefficient in each run.....	99
Figure 55: Modelled wind setup height (in mm) compared with storm surge as determined in the data analysis of Chapter 3 (dynamic effects included).....	100
Figure 56: Modelled wind set up (Height in mm) for 3 different test runs whereby varying only the bottom friction coefficient	101
Figure 57: Modelled wind set up (Height in mm) for 3 different test runs whereby the wind input series are averaged over varying times	102
Figure 58: Modelled wind set up (Height in mm). (a) Model results shown against comparison series (b) Model results shown against pressure input.....	103
Figure 59: Modelled wind set up (Height in mm for data set No.1. The comparison series (black) consists of wind setup components only.....	105
Figure 60: Modelled wind set up (Height in mm for data set No.2. The comparison series (black) consists of wind setup components only.....	106
Figure 61: Modelled wind set up (Height in mm for data set No.3. The comparison series (black) consists of wind setup components only.....	107
Figure 62: Modelled wind set up for data series no.1(top), no.2(middle) and no.3(bottom). Different colours represent results from different test points.....	110
Figure 63: spatial distribution of wind setup heights for a strong summer event.....	111
Figure 64: spatial distribution of wind setup heights for a strong winter event.....	111
Figure 65: Comparison of modelled- and analytically-calculated wind setup heights	114

List of Tables

Table 1: Extreme value analysis of Cape Town tide gauge residuals (PRDW 2010 Modified).....	14
Table 2: Example of an incremental numerical solution as suggested by Kamphuis (2000).	19
Table 3: Technical summary of data available for Saldanha Bay.....	26
Table 4: Summary of gaps and continuous data segments in the water level data sets	30
Table 5: Summary of the 3 data sets that were selected for spectral analyses at Saldanha Bay	35

Table 6: Summary of frequency groups in Saldanha Bay residual water level data and their respective filtering requirements.....	43
Table 7: List of data series pairs on which cross correlation analysis were performed.....	52
Table 8: Results of cross correlation analysis.....	56
Table 9: Summary of sampling error components in residual water levels at Saldanha Bay	57
Table 10: Summary of high frequency noise components in residual water levels at Saldanha Bay ...	58
Table 11: Summary of wind components in residual water levels at Saldanha Bay	59
Table 12: Summary of pressure components in residual water levels at Saldanha Bay	59
Table 13: Summary of dynamic effects components in residual water levels at Saldanha Bay	60
Table 14: Summary of percentage contributions from storm surge components. Saldanha Bay	61
Table 15: Tabulated results of Extreme Value Analysis of NCEP Wind speeds (in m/s)	74
Table 16: Tabulated results of Extreme Value Analysis of NCEP Pressure data (in mbar). Values are read off from the probability plot (followed by actual corrected values in brackets)	75
Table 17: Description of test point positions selected for analytical wind setup calculations	79
Table 18: Wind speed in m/s. Wind speeds are maximum measured wind speeds (20min average at 10m) for data sets 1 to 3.....	80
Table 19: Summary of maximum NCEP wind speeds (m/s at 10m) as determined using the MIKE Zero EVA tool (best fit estimates).....	81
Table 20: Wind set-up (in mm) calculated from maximum wind speeds in data set 1 to 3 using the Kamphuis equation (Equation (17)).....	87
Table 21: Wind set-up (in mm) calculated from maximum wind speeds in data set 1 to 3 using the Bretschneider equation (Equation(18)).....	87
Table 22: Wind set-up (in mm) calculated for selected return periods using the Kamphuis equation (Equation (17)).....	87
Table 23: Wind set-up (in mm) calculated for selected return periods using the Bretschneider equation (Equation (18)).....	88
Table 24: Pressure setup (in mm) calculated for selected return periods as determined from 36 years of NCEP data.....	88
Table 25: Summary of calculated wind setup: Tip of Caisson 25 (Extract from Table 20)	89
Table 26: Comparison of wind setup results as calculated analytically and as determined from the time series analysis (Time series analysis results extracted from Table 11).....	90
Table 27: Calibration results for modelled wind setup as compared with wind components of the time series analysis (Time series analysis results (B) extracted from Table 11)	108
Table 28: summary of modelled wind setup elevations at various points	112
Table 29: Summary of comparison of modelled results and analytically calculated results	113

Abbreviations

aMSL – *Unit for elevation – meters above mean sea level*

CD – *Chart Datum*

CPD – *Cycles per day*

CSIR – *Council for Scientific and Industrial Research*

EVA – *Extreme Value Analysis*

FFT – *Fast Fourier Transform*

HAT – *Highest Astronomical Tide*

LLD – *Land levelling datum*

NCEP – *NCEP data refers to data of the NCEP/DOE Reanalysis II project*

NOAA – *National Oceanic and Atmospheric Administration (US)*

SANHO – *South African Navy Hydrographic Office*

SLOSH - *Sea, Lake, and Overland Surges from Hurricanes*

SWL - *Still water level – elevation of the water if no gravity waves were present*

TNPA – *Transnet National Ports Authority*

UTC – *Universal time coordinated*

CHAPTER 1

1 Introduction

1.1 BACKGROUND

Determining extreme high sea levels is an important process for many coastal engineering applications, ranging from the design of coastal structures to the risk mitigation and planning related to coastal flooding. In recent years, the study of extreme sea levels has also become increasingly popular from a climate change perspective. Extreme sea levels can be made up of a combination of components such as astronomical tides, tsunamis, seiches, wave setup, runup and storm surges. The latter of these, storm surge, is often considered to be one of the governing components of extreme sea levels and accordingly, some of the most devastating coastal flooding damages worldwide have been inflicted as a direct result of storm surges. Many sources claim that storm surges can reach heights of 8 meters and more (CERC 1984; Gonnert et al. 2001). Accordingly, some of the most devastating flooding events worldwide have been a direct result of storm surge. The 1970 Bhola cyclone that devastated Bangladesh and resulted in the death of over 300,000 people (Karim & Mimura 2008), is a single tragic example of such a severe storm surge event.

It is true that for storm surges to reach extreme heights, several conditions must be satisfied. Vast shallow coastal shelves along coastlines frequented by large storms are particularly prone to storm surges. Contrary to these ideal storm surge conditions, the South African coast is characterized, predominantly, by deep waters and is relatively free of extreme storm events such as cyclones. As such, the country is in fact relatively well protected against the effects of storm surge. Against this background many scholars who have performed studies on extreme high sea levels along the SA coast, have refrained from quantifying sea level fluctuations specifically owing to storm surge. It is in this relative absence of published storm surge heights in SA literature that, in practice, this parameter is often estimated based on rudimentary assumptions.

Under normal conditions, sea level fluctuations owe largely to the effects of astronomical tides, but on top of that, are typically the superimposed fluctuations resulting from meteorologically induced processes. Broadly speaking, these meteorologically driven, extra-tidal fluctuations are categorized as storm surge. However, amongst coastal engineers the general consensus seems to point towards

categorising as storm surge, only those positive sea level fluctuations owing exclusively to wind setup and pressure effects. Other meteorologically induced phenomena are accordingly not included into the engineering definition for storm surge.

Astronomical tide components can be predicted with great accuracy. These tide components usually make up the greater part of sea level fluctuations. With this mind, it appears as common practice in SA to subtract only this known tidal component from observed sea levels and by assumption accepting the mean remaining components (called the residual) as storm surge. An example of where such an approach is followed is seen in PRDW (2010). This approximation of storm surge may be put to question, considering that besides the contribution of storm surge to sea level fluctuation, there are also the contributions of other coastal processes. These include wind setup, wave setup, trapped long waves, seiches, pressure effects, shelf waves, edge waves and tsunamis – all of which have been recognised along the SA coast, but not all of which are related to storm surge. This begs the question of how correct it is, then, to allocate the entire residual to storm surge, if it is not known, at least, that storm surge is the majority component.

The two core components of storm surge, wind setup and pressure effects, can both be calculated analytically for static conditions and are explained, respectively, as the uplift in still water level resulting from wind stress on the water's surface and uplift in still water level in response to variations in atmospheric pressure from the mean. The latter is also known as the inverse barometer effect. Set down is the opposite of set up and is equally common for both wind and pressure. Wind setup is proportional to wind speed and inversely proportional to water depth. The inverse barometer effect is proportional to variation in atmospheric pressure at sea level. While storm surge reacts fairly statically to local wind and pressure, its propagation and interaction with other phenomena and geographical features is complex and dynamic.

As mentioned above, South African literature is rather void of content directly related to storm surge. However, several of the other processes which constitute sea level fluctuations are covered extensively. For example, there is evidence in literature of the existence of a phenomenon called shelf waves (or coastal trapped waves). Shelf waves, in the South African context, is typically not categorised as storm surge as such, although it certainly bears a strong resemblance to storm surge, particularly in that it shares similar forcing mechanisms. Shelf waves are explained as low frequency fluctuations in sea level resulting from the interacting effects of coastal lows and large scale atmospheric systems. It is the movement of these atmospheric systems that is believed to be the forcing mechanism for shelf waves (Wijnberg 1993). Another phenomenon that is being researched extensively is trapped long waves and their associated seiches in bays and harbour basins. Contrary to shelf waves, long waves bear no real resemblance to storm surge. It is believed to be associated with the groupiness of gravity waves and not directly with meteorological systems as such. Wave setup too, a process that also contributes to sea

level fluctuations, is not considered as being at all related to storm surge. Another interesting phenomenon that has received some attention in SA literature, and that also contributes to sea level fluctuations, is edge waves (also called meteo tsunamis). Edge waves are associated with very specific pressure pulses that occur in resonance with gravity waves over a particular water depth. Edge waves too are not really related to storm surge. Furthermore, conventional tsunamis result from tectonic disturbances and also bear no resemblance to storm surge. Despite most of these abovementioned phenomena not relating directly to storm surge as such, it is nevertheless important to be able to identify their effects in order to close in on the true effects storm surge.

Having a further look into existing literature, and more specifically studies relating to combined sea levels, it is seen that several studies have been done pertaining to long term trends in sea level fluctuations around the SA coast (Brundrit et al. 2011; Brundrit 1995; Mather et al. 2009; Mather & Stretch 2012; Brundrit 2008; Wijnberg 1993). However, these studies have aimed to resolve long term and seasonal fluctuations only and do not provide explanations to shorter scale fluctuations in sea level owing specifically to the likes of storm surge. The handful of studies covering the subject of design sea levels (Wijnberg 1993; Jury et al. 1986; De Cuevas 1985) essentially wrote off the noteworthy occurrence of storm surge along the SA coast on the basis of unsatisfactory weather and coastal shelf conditions. Yet, there is evidence from the work of Mather & Stretch (2012) that SA has been subjected to storm surges of up to 70cm in past storm events.

Considering the importance of accurately quantifying storm surge, and the relative void in literature pertaining to this phenomenon in SA, it is clear that there is a need for more careful research into its occurrence in SA and its associated magnitude and frequency as well as looking critically at the methodologies which may be used to obtain such information. It is shown that there is already fairly good knowledge of the various processes (or building blocks) which make up the composite sea levels as observed along the SA coast, but that storm surge is yet to be examined and studied in isolation from the rest of its co-existing counterparts.

1.2 THESIS OBJECTIVES

The objective of this study is to quantify storm surge components at Saldanha Bay. In addition, this study is an effort to gauge, by means of comparison, the accuracies of different methods of determining storm surge. These methods include time series analyses, analytical calculations and numerical modelling.

1.3 THESIS OVERVIEW & STRUCTURE

Chapter 2 opens with a literature review of work relating to storm surge. This is done with the emphasis on literature pertaining to South Africa. Chapter 3 deals with the analysis of time series data to determine storm surge. Included within this chapter is a review of the available data. The analytical and numerical modelling of storm surges follows next. This includes the review of an alternative set of data, namely NCEP data (Chapter 4, Chapter 5 and Chapter 6). The results are then thoroughly discussed in Chapter 7 and conclusions and recommendations are made in Chapter 8.

1.4 CLARIFICATIONS AND INITIAL ASSUMPTIONS

Several aspects regarding the content of the study are clarified below:

A note to the reader regarding the engineering definition of storm surge:

Although the engineering definition of storm surge is discussed in depth later on, it may be noted here that for the purpose of this study, storm surge is considered as consisting of only the effects of wind setup and the inverse barometer effect. This is very much in line with common engineering practice even though some texts prefer to define storm surge more broadly. Other components that are sometimes linked to storm surge include wave setup, rainfall and Coriolis effects. However, these components fall outside the scope of this study and are therefore not included.

On Saldanha Bay as a suitable test site for a study on storm surge:

The study is done in the context of South Africa as a whole, but analyses are only completed for Saldanha Bay as being selected as the test site for the study. The selection of Saldanha Bay as test site for determining Storm Surge is a conservative selection if viewed in the context of South Africa. It represents the rare case of a (relatively) shallow enclosed bay; a condition which typically favours the agitation of storm surge. False Bay being perhaps the only comparable counterpart. It may therefore be assumed that storm surge values, as determined at Saldanha Bay, will not easily be overlooked if placed in the context of the broader South African coast.

The locality of Saldanha Bay is indicated on **Figure 1**.

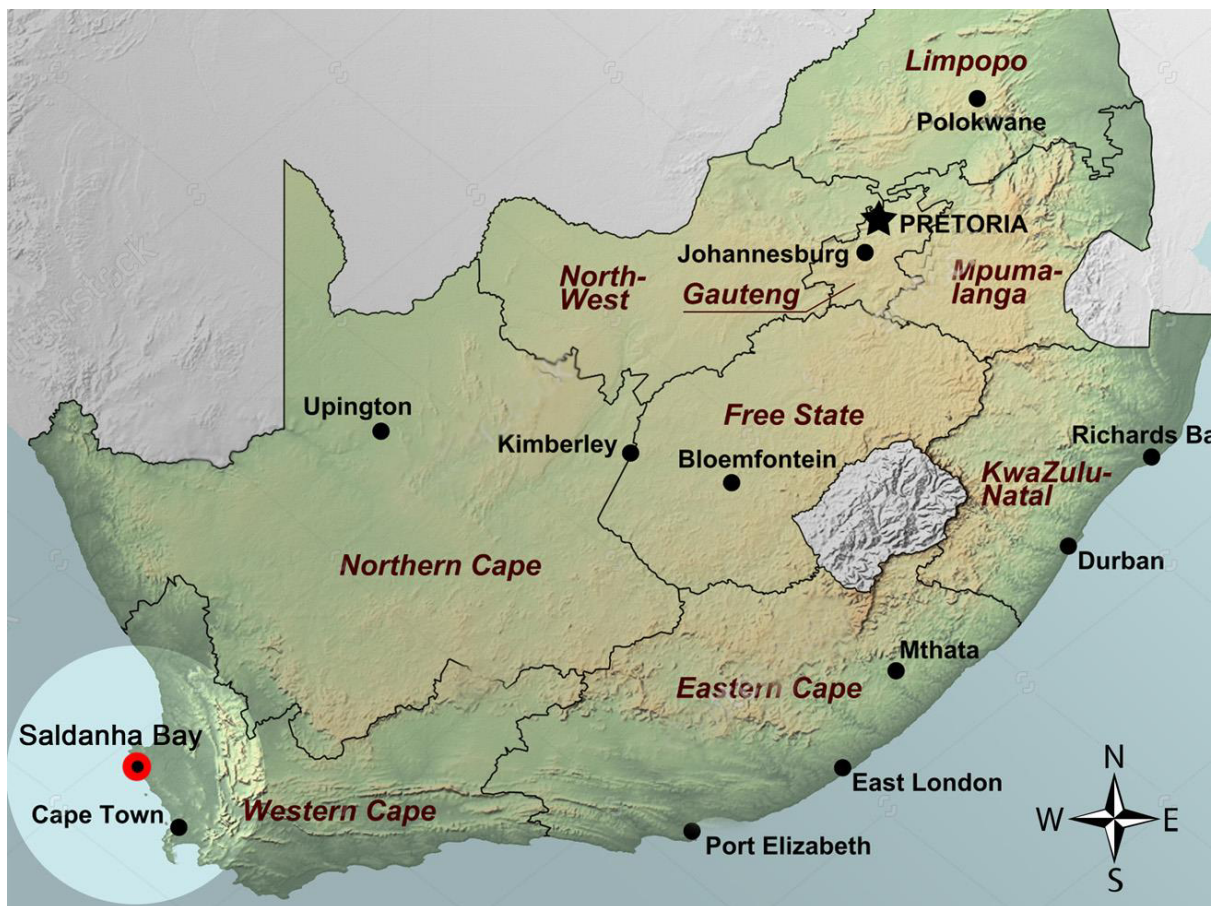


Figure 1: Map of South Africa. Position of Saldanha Bay indicated with red marker

CHAPTER 2

2 Literature Review

2.1 METEOROLOGY AND WEATHER SYSTEMS OF SOUTH AFRICA

South African meteorology and weather patterns are well documented in several comprehensive books and publications (Watts 2004; Tyson & Preston-Whyte 2000). A short summary is given here of the meteorological conditions that typically have an impact on the South African coastline with particular focus on those applicable to Saldanha Bay.

Air movement within the atmosphere follows a generally recognisable pattern as illustrated in **Figure 2** below. Movement of air, including depressions and fronts, is driven by the interaction between large air masses from different source regions (MacHutchon 2006). Alongside southern Africa are two such source regions, the South Atlantic Ocean Marine Tropical (mT) and the Southern Indian Ocean mT off the west coast and the east coast respectively (Watts 2004). When heated air rises from the tropics, it is driven to the south and descends at roughly 30°S, forming the so called Hadley cell. It is the downward-driven air from within the Hadley cell which causes the two aforementioned semi-permanent high pressure systems on either side of the sub-continent in the region known as the Sub Tropical Belt (MacHutchon 2006). The air circulation around these two high pressure source regions is anti-clockwise.

South of the Sub Tropical Belt, easterly spiralling movements from the Ferrel Cell called the Ferrel westerlies, may be found. Irregularities in the Ferrel westerlies results in the formation of low pressure systems off the South Atlantic. Once formed, the low pressure systems are driven east by the Ferrel winds. These depressions and their associated cold fronts are characterised by strong clockwise wind fields (Rossouw 1989).

The low pressure systems described above regularly pass by the southern tip of Africa but in winter months, when the whole system shifts northwards, these depressions are often intersected by the south western tip of Africa. These winter encounters between the low pressure systems and the south western and southern cape coast are accompanied by NW winds. These NW winds usually decreases rapidly

and swings through its initial NW to SW and SE during the passage of a cold front (Rossouw 1989).

Figure 3 below illustrates the passage off a typical cold front system as described above.

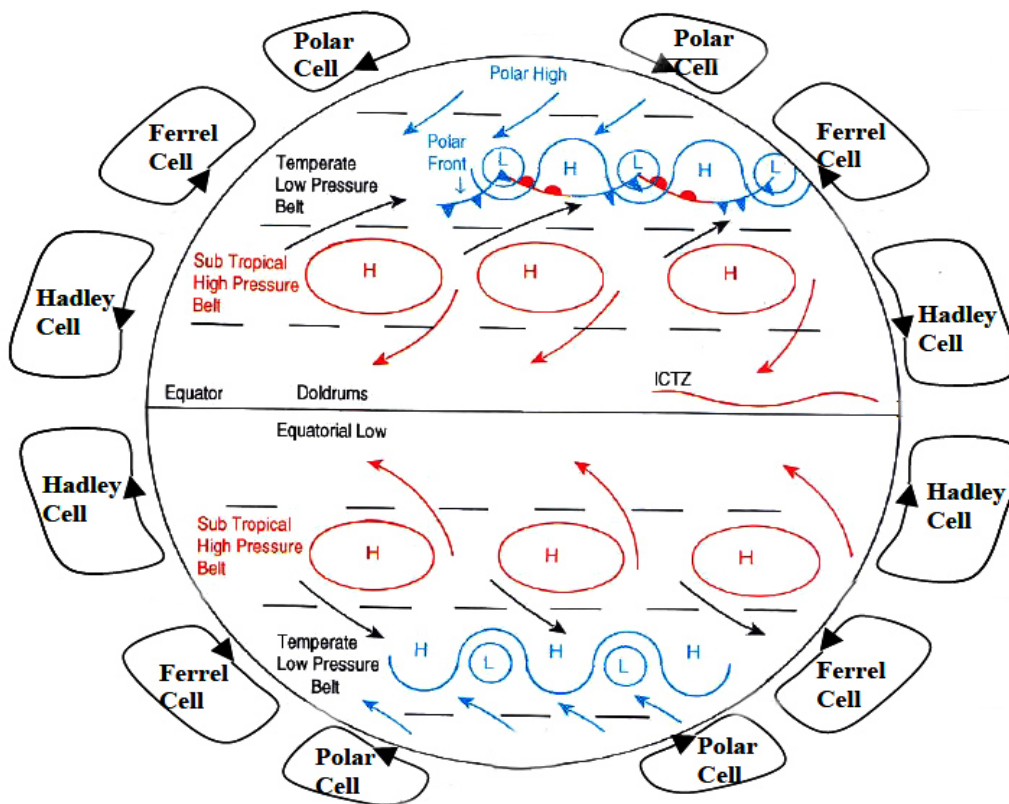


Figure 2: Overview of typical global weather patterns (Watts 2004 Modified)

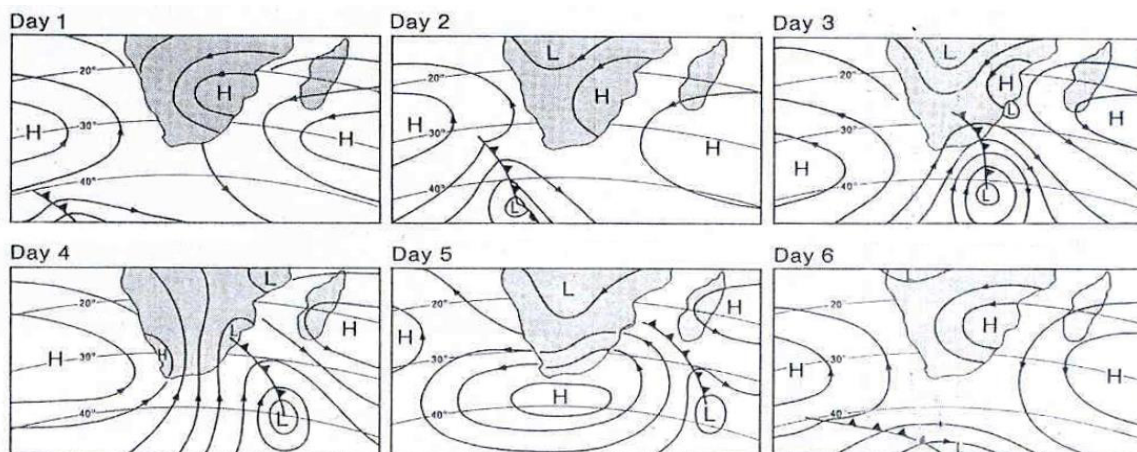


Figure 3: Typical passage of a cold front along the south Western Cape coast (Tyson & Preston-Whyte 2000 modified)

Saldanha Bay, as a matter of interest for this thesis, is affected by the winter cold fronts as described above. As cold fronts move east, their intensity usually reduce after passing Port Elizabeth. Furthermore, the South Indian Ocean high also plays a role in deflecting the cold front away from the coast when it reaches as far east as Port Elizabeth (Rossouw 1989) which explains how, for instance, Algoa Bay is also affected by the winter cold fronts, but to a lesser extent than Saldanha Bay.

The east coast of South Africa is affected by less frequent systems; particularly cut-off lows (Rossouw 1989). Cut-off lows are low-pressure systems that become displaced (or cut-off) from the usual westerly moving Ferrel winds and then move independently. Cut-off lows are often associated with high rainfall. Singleton & Reason (2007) explains that cut-off are usually formed when troughs of cold, high latitude air in the upper troposphere become cut off from its source region. Occasionally, however, the northern Natal coast is affected by tropical cyclones. Tropical cyclones originate in the Inter Tropical Convergence Zone (ITCZ on **Figure 2**) where the conditions favourable for the genesis of these systems are said to be erratic and difficult to predict (Fearon 2014). Tropical cyclones have a distinct characteristic structure consisting of an eye, eyewalls and spiralling rain bands. The eyewall, at approximately 50 to 100 km from the eye, is where the strongest wind exists (Fearon 2014). Winds associated with Tropical Cyclones along the South African east coast have been recorded to reach well in excess of 20m/s (10 min average) (Mather & Stretch 2012).

Figure 4 shows the areas of frequently tracked tropical cyclones around the world. Although the likelihood of tropical cyclones affecting the study-areas for this thesis, Saldanha Bay, may be ruled out on the basis of the abovementioned figure, the effects of tropical cyclones should still be considered when looking at storm surge along the South African coastline as a whole.

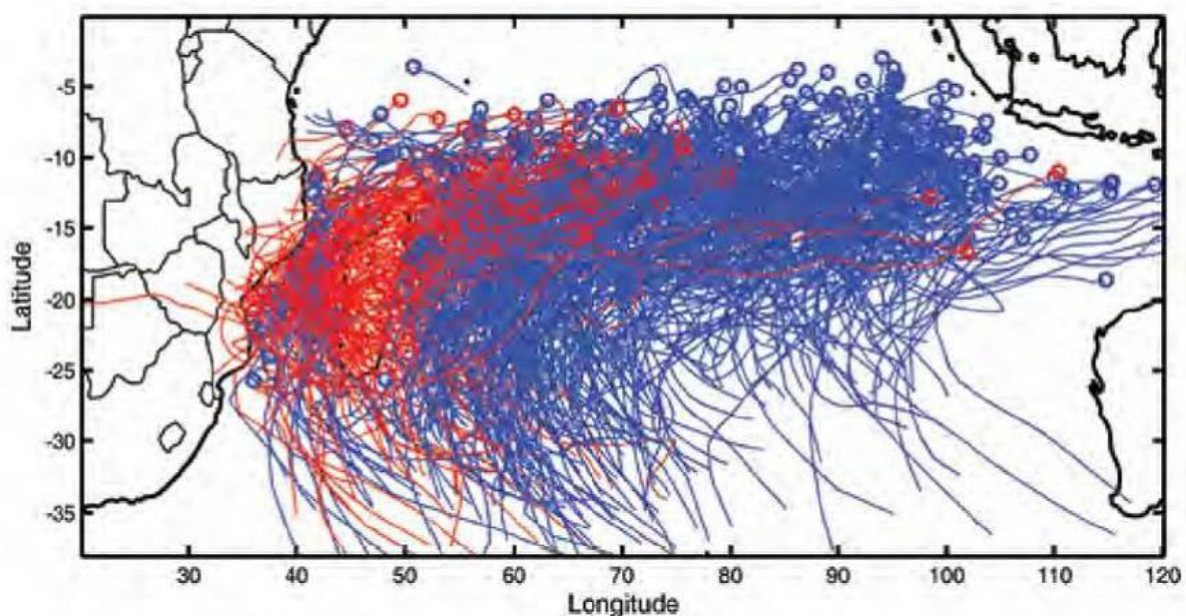


Figure 4: Cyclone tracks for 1952 to 2007 (Mavume et al. 2009 Modified)

2.2 STORM EVENTS

To gain some measure of understanding of the potential risk associated with storm surges, reference is made here of a number of recorded extreme storm surge events around the globe.

Amongst the earliest accounts, is a 6.5m storm surge that was measured at Groote Eylandt in Australia's Gulf of Carpentaria caused by the Douglas Mawson cyclone in March 1923 (Nelson 1975). In 1970, between 300,000 and 550,000 people were killed in the Bay of Bengal by a storm surge which measured 10.6m (Karim & Mimura 2008). Typhoon Joe, in 1980, drove a 5.9m storm surge at Nandu Station, China (Fengshu & Xinian 1989). Hurricane Katrina, 2005, resulted in surges of over 8m along the US coast (Knabb et al. 2005). All of the abovementioned storm surges occurred in regions which, due to its shallow coastal waters and exposure to extreme tropical cyclone events, render themselves vulnerable to large surges as will be explained later on.

One example of how countries with such storm surge prone conditions are advancing in its response to storm surge is the developing of systems by which to make themselves storm ready. The U.S. has developed a comprehensive storm surge prediction model called SLOSH (acronym for Sea, Lake, and Overland Surges from Hurricanes). SLOSH is a numerical storm surge model, able to forecast real time, storm surges in 38 coastal areas along the Atlantic and Gulf of Mexico coasts of the U.S.; Oahu, Hawaii; Puerto Rico; and the Virgin Islands (Glahn et al. 2009).

In South Africa, a number of extreme high sea level events as well as general storm damages are documented, but little mention is made of damage or high sea levels as a direct result of storm surge. In 1997, a cut-off low system resulted in 9.3m waves off the coast of East London. Similar wave heights were observed in the region during the 1984 cyclone Imboa as well as during a severe storm in 1966 (Mather & Stretch 2012). In more recent years, and perhaps the trigger event for the bulk of the recent work carried out with respect to sea level rise risk mitigation, is the well-documented and thoroughly reviewed storm of 2007. Mather & Stretch (2012) explains how the storm was the result of a cut-off low-pressure system off the east coast of South Africa. On the 18th of March, wind speeds reached peak hourly speeds of 11.9m/s and a peak 10min speed of 22.1 m/s. Significant waves height was measured at 8.5m with a peak single wave height of 14m. On the morning of the 19th of March the highest astronomical tide of the year was predicted at 2.284m above MSL, a mere 20mm less than the predicted Highest Astronomical Tide (HAT) for Durban. Damages were intensified as a result of this extreme high astronomical tide coinciding with the storm. According to the South African Weather Service (SAWS), the majority of the damages during the storm was caused by the storm surges associated with the cut-off low (Hunter et al. 2007). Storm surges during this storm is further documented as having peaked 0.7m (Smith et al. 2013; Mather & Stretch 2012). Furthermore, wave run-ups of up to 10.5m were recorded, causing extensive damages to the value of almost R1billion (Hunter et al. 2007).

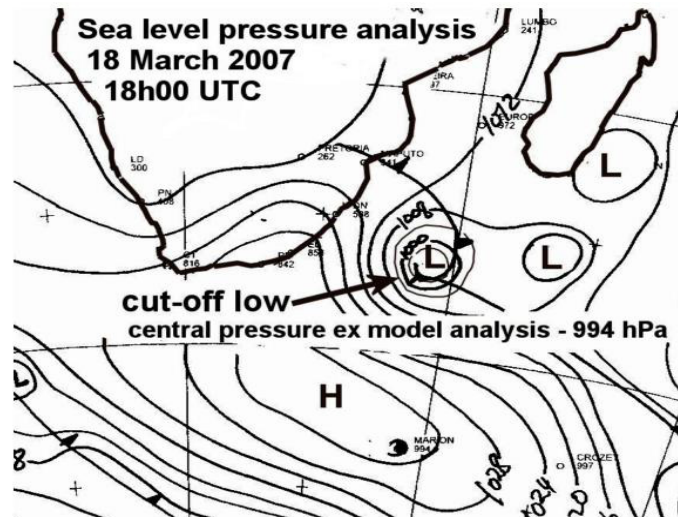


Figure 5: sea level pressure analysis for 18 March 2007, 18h00 UTC (Hunter et al. 2007 Modified)



Figure 6: Photograph showing storm damage along the Durban coast, 2007 (Hunter et al. 2007 Modified)

In the south western parts of the country, several large storm events have been documented with respect to extreme high significant wave heights recorded at the Slangkop wave-buoy. However, little mention is made of damage as direct result of storm surge. In 1984 a depression south west of Cape Town is stated to have led to “an extreme storm with hurricane force winds” (Brundrit 2009). In 2001, a uncharacteristic cut off low south west of Cape Town resulted in “strong” winds and large waves (Brundrit 2009). In August/September 2008 a storm from the south west resulted in significant waves heights of over 10m. Two factors which contributed to the severity of this storm are that it coincided with a spring high tide (the previous day) and that the storm had a longer than usual duration of over 12h. Water levels were recorded to be higher than those predicted (Mather & Theron 2012). Mather and

Theron attribute this residual to the possibility of storm surge. Residuals of 0.5m and 0.7m were measured in Cape Town and Algoa Bay respectively. This storm has subsequently been classified as a storm with a return period of 10 years with respect to wave heights (Brundrit 2009; Mather & Theron 2012).

Another case of high recorded sea levels, this time slightly more unconventional, is reported in a study by Okal et al. (2014) for the town of Dwarskersbos, some 50km north of Saldanha. In 1969, in the absence of seismic activity or meteorological events, severe run-up of up to 2.9m was documented. Okal et al. (2014) goes on to attribute this extreme high sea level event to the effects of a meteo tsunami. According to Proudman (1953), meteo tsunamis such as this one is made possible by exceptionally slow gravity waves in relatively shallow bathymetry, and propagation of pressure fronts at velocities unusually fast for meteorological events at the earth's surface.

2.3 PREVIOUS WORK IN SOUTH AFRICA RELATING TO STORM SURGE

Several scholars have researched water levels around the Southern African Coast (Brundrit et al. 2011; Brundrit 1995; Mather et al. 2009; Mather & Stretch 2012; Brundrit 2008; Wijnberg 1993; Cloete 2012; Theron 2016) The majority of these studies were aimed at resolving a long term trends in sea levels related to climate change. Despite not always focusing on storm surge components directly, these studies reveal aspects of importance with regards to methods for analysing water level data, typical storm severity along the South African coast and insight into the available water level data.

Brundrit (1984) examined the extra tidal water level fluctuations from various tide gauges along the Southern African coast on a monthly scale. Apart from high frequency noise which he related to the short term effects of synoptic events, Brundrit also noted the occurrence of larger scale periodic seasonal variations which he connected to seasonal wind patterns and long term trends in seasonal temperature anomalies. The formerly mentioned noise, which Brundrit was not able to resolve on a monthly scale, is where this study will aim to seek results for storm surge components. However, the larger scale seasonal variations are also of considerable interest when attempting to isolate storm surge. In the following decade Brundrit (1995) once again completed a study on monthly trends in sea level data from Southern African tide-gauge sites, this time doing a somewhat complex statistical analysis to identify trends in the data. The Box-Jenkins statistical model was used to separate various components of the fluctuations in sea levels and to estimate underlying trends. The aim of Brundrit's study was to

identify long-term trends related to climate change, but the methods used are nevertheless interesting for the purpose of the current study.

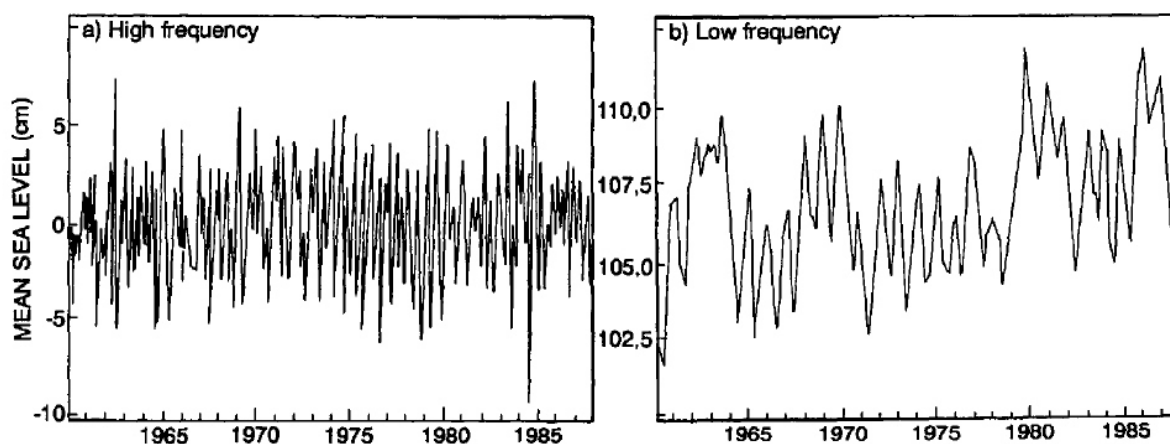


Figure 7: Brundrit's results of separating high frequencies from low frequencies

Mather et al. (2009) also studied Southern African sea level trends on a monthly scale, focussing on correcting the available data by means of primarily separating out the inverse barometer effect from the available data. Here it was found that water levels vary a mere 5.71mm to 7.67mm for every 1mbar in pressure change, which is considerably less than the theoretical 10mm. A similar study was done by De Cuevas (1985). However, this study suggested, in contrast to Mather's study, that the water level response to pressure changes at some South African ports is in fact higher than the theoretical 10mm response.

Mather & Stretch (2012), in a study to map risk-prone areas along the Durban coast, claims a recorded peak (3-minute average) storm surge of 70cm at SANHO's Durban tide gauge during the severe storm event of 2007. This being perhaps the only directly stated storm surge height in published literature for South Africa's coast.

With regards to published design sea levels, it appears that the vast majority of work done to exclusively report on design sea levels, including that which is contributed towards by storm surge, has been documented in commercial, industry related consultant studies and reports. The sole academically published piece in this regard seems to be a study by Wijnberg (1993) on design sea levels for Southern Africa. Wijnberg looked at using a probabilistic approach to derive design sea levels taking into consideration the statistical distribution for an array of contributing components to extreme sea levels but not storm surge. Wijnberg cites the work of De Cuevas (1985) to motivate that onshore wind has insignificant impact on sea levels in South Africa. **Figure 8** below shows Wijnberg's reproduction of De Cuevas' findings at Lamberts Bay on the West coast. South Africa has a relatively steep sloping coastal shelf resulting in deep water fairly close to the shore. On the basis that wind setup is inversely proportional to water depth, Wijnberg did not devote much attention to wind setup quantification and

therewith storm surge. It was mentioned however, that Saldanha Bay is an area likely to experience notable storm surge effects as a result of its shallow bathymetry.

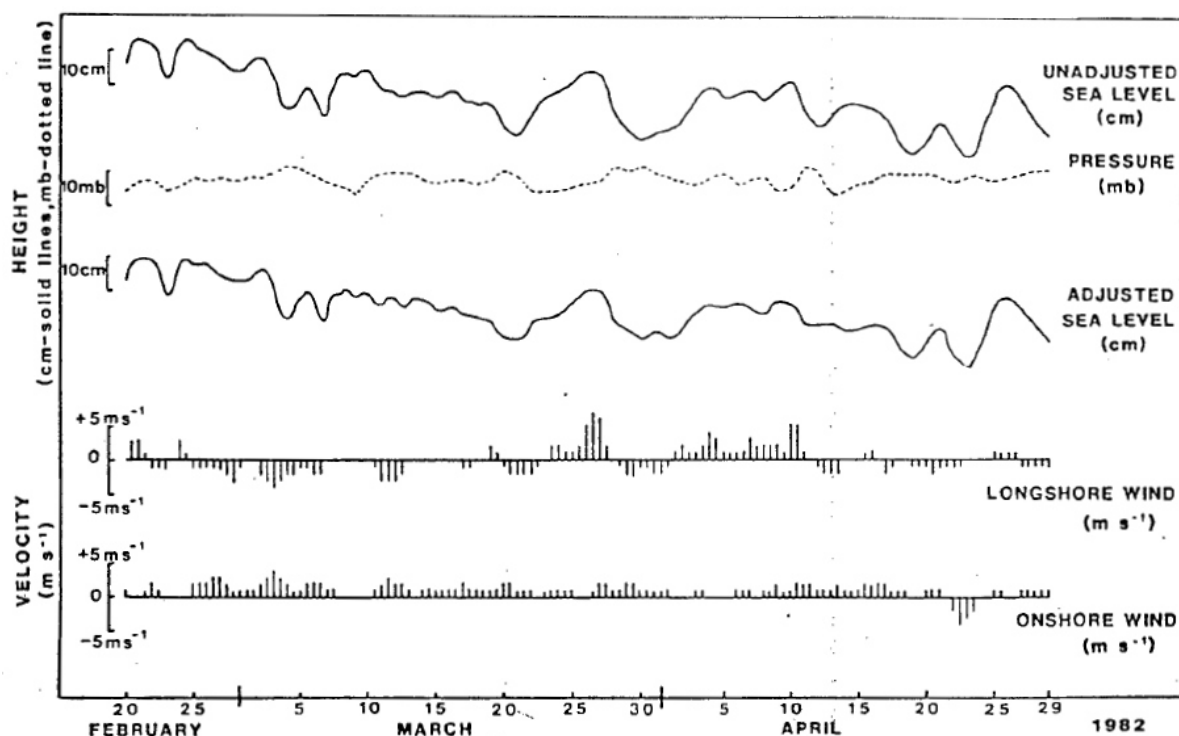


Figure 8: Sea levels, Pressure and wind at Lamberts Bay (De Cuevas 1985 Modified)

Theron (2016), in a comprehensive study on coastal setback lines for the South African coast, notes that it is not uncommon to encounter wind setup of 0.15m in the south east coast of South Africa. It is further noted that wind setup heights have been predicted to reach up to 0.5m in False Bay and that annual wind setup heights of 0.2m to 0.3m can be reasonably expected. Theron refers to a study done by Raposeiro et al (2013) in which the combined wind setup and pressure setup height for the Portuguese coast had been determined at 0.52m. Theron notes that the Portuguese coast closely resembles that of the Cape and therefore similar wind and pressure setup heights may be deemed reasonable.

Without going into the finer details of results obtained from unpublished work and consultant studies, a few results are worth pointing out. A study commissioned by the City of Cape Town (LaquaR Consultants CC 2008) cites Jury et al. (1986) to have documented a “storm surge and wave setup” of 1.2m at Cape Town during a 1984 storm. Also commissioned by the City of Cape Town, was a study in which (PRDW 2010) performed an extreme value analysis on the positive residuals from Cape Town. These results are shown in **Table 1**.

Table 1: Extreme value analysis of Cape Town tide gauge residuals (PRDW 2010 Modified)

Return Period [years]	Best estimate positive residual [m]	Upper 95% confidence positive residual [m]
20	0.64	0.71
50	0.70	0.80
100	0.74	0.87

Looking further yet in published literature related to South Africa, one finds several studies vaguely related to the sea level problem, but focussed specifically on individual phenomena or processes such as long waves, shelf waves and edge waves. Shelf waves, interestingly, is a phenomenon closely related to storm surge in that they share similar forcing mechanisms, namely pressure and wind, (shelf waves are sometimes referred to as coastal trapped waves). Shelf waves are low frequency sea level disturbances with periods in the order of 2 days to 20 days and with heights, along the SA coast, of up to 50cm (Wijnberg 1993). These waves are generated by synoptic scale events over the subcontinent's inner continental shelf. The hydrodynamics and forcing mechanism theories for shelf waves are somewhat complex and will not be explained in depth here. It is useful to note, however, that the generation of shelf waves may be attributed to the interaction of coastal lows with the prevailing large scale atmospheric systems at play on the inner continental shelf (De Cuevas 1985). In summer months, the almost permanent longshore wind associated with the South Atlantic Tropical high acts to enhance the atmospheric effect of coastal lows and drives the propagation of these pressure induced disturbances in a westerly direction. In winter months when the South Atlantic high moves several degrees north, there is more variability in the direction of winds along the coast - a factor that reduces the frequency of shelf wave events. There is thus a distinct seasonal variability associated with the sea level response to shelf waves (De Cuevas 1985).

Shelf waves have been found to propagate down the west coast and around to the greater part of the south and south east coast (Schumann 1989), but does not extend much further north than Port Elizabeth. This discontinuity of the shelf wave's propagation may be attributed the counteracting effects of the poleward flowing Agulhas current (Schumann 1989) as well as the obvious narrowing of the continental shelf north of Port Elizabeth (Schumann 1989).

In respect of identifying or recognising shelf waves by means other than its characteristic height and period, the following coinciding synoptic conditions have been identified:

Wijnberg (1993) found that typically associated with events of large shelf waves, is the precedence of a forcing frontal system to lead the peak height of the shelf wave by 5 to 24 hours. Therefore, during the winter months, one may expect to observe shelf waves a short while after the occurrence of a low pressure and high wind speed event.

In a study done by Cloete (2012), an attempt was made to determine storm surge values in northern False Bay. Water level data and wind data from Simon's Town and Cape Town International Airport were used respectively. However, the study concluded that the available data was not appropriate for determining storm surge as wind from the airport site was found not to be representative of the site where water levels had been measured.

2.4 STORM SURGE THEORY AND ANALYTICAL METHODS

Having looked specifically at literature concerning storm surge matters in a South African context, the focus for the remainder of the literature review is shifted towards reviewing theory pertaining to storm surge as a general case as well as theory pertaining to the analysis thereof.

The U.S. Army Corps of Engineers (1986), defines storm surge as the rise or possible fall of the normal water level in coastal waters due to the interaction between a storm and the underlying water surface. This same definition of storm surge is echoed throughout most of the available storm surge literature. It is widely accepted, furthermore, that the largest contributing component of storm surge is wind setup (CERC 1984). Aside from the obvious contribution of wind setup, other factors which contribute to storm surge include atmospheric pressure effects (also known as pressure effects or inverse barometer effects), effect of earth's rotation (known as Coriolis effects), rainfall effects and wave setup effects (U.S. Army Corps of Engineers 1986).

2.4.1 Typical Storm Surge Conditions (Global)

Most studies and texts on the topic of storm surge, connect the occurrence of storm surges to storms that are classified as hurricanes and typhoons (Northern hemisphere) or tropical cyclones (Southern hemisphere) (Gonnert et al. 2001). Generally, a storm is simply an atmospheric disturbance characterized by one or more low pressure centres and high winds (U.S. Army Corps of Engineers 1986). Storms are further classified as tropical storms if they originated in the tropics and extratropical storms if they resulted from the interaction between warm and cold fronts. Cyclones (and hurricanes/hurricanes) are classified specifically as storms with wind speeds exceeding 33.5m/s (75mph) (U.S. Army Corps of Engineers 2002). Cyclones developing in the western part of the North Pacific ocean are known as typhoons (OCDI 2002).

Places around the globe that are known as being particularly susceptible to extreme storm surges include (but are not limited to) the likes of the east coast of the US, Florida, the Gulf of Mexico, the east coast of Canada, the Bay of Bengal, some parts of Australia, some parts of the western Pacific such as the coasts of China and Japan, some parts of Europe such as the North Sea and the Baltic sea (Gonnert et al. 2001). All of the above-mentioned coasts are known to be frequented by cyclones, hurricanes or typhoons (depending on the location). In the work of Gonnert et al. (2001) titled *Global Storm Surges*,

a very comprehensive summary is given of recorded storms and storm surges around the globe. It is interesting to note that whenever storm surges are discussed in the abovementioned publication, it is always described and related to the characteristics of the cyclone that had caused the surge. Recall that for the bigger part of the South African coast, cyclones are not present and thus such typical descriptions and discussions of storm surges are not of much relevance to this study. It is further noticeable in the abovementioned publication that South Africa is not mentioned at all as a country prone to storm surge.

2.4.2 Mechanics of Storm Surge

The mechanics of wind setup is explained by considering wind blowing over the water surface. The wind exerts a horizontal force on the surface water and in shallow water induces a current in the general direction of the wind (CERC 1984). The force exerted on the water by the wind is partly due to variations of air pressures on the upwind and downwind side of gravity waves and partly due to shearing stresses at the water surface (U.S. Army Corps of Engineers 1986). In the case where wind is blowing perpendicular to the shore, the current travels perpendicular to the shore and water is transported in the upper layers of the water column over the continental shelf towards the coast. At the same time, water is returned seaward along the bottom layers of the water column. Water returning seaward under the influence of gravity is slower as it is being impeded by the bottom friction of the sea bed. Because of this variation in current speed through the water column, a gradient is induced at the water surface with increase in water level towards the coast. This phenomenon is known as wind setup (CERC 1984).

Because practically all of the parameters relevant to the process as described above are highly variable by nature, the wind setup problem is complex to calculate. One of the early pioneers of storm surge theory, Charles L. Bretschneider, warned that the wind setup problem is complicated and is best solved using numerical methods. Analytical solutions, he warned, usually lead to an oversimplification of the problem (Bretschneider 1967). It is therefore no surprise that recent studies pertaining to storm surge make extensive use of numerical modelling to solve storm surge related problems (Gonnert et al. 2001). Most modern texts seem to echo this sentiment that storm surge problems are complex and preferably be resolved numerically. However, due to the time-cost implications of numerical modelling, it is of benefit for coastal engineers to estimate simplified solutions for wind setup using analytical methods.

2.4.3 Analytical Solutions

The generic differential equation for hydrodynamic motion in two directions appropriate for the calculation of storm surge is given in the Shore Protection Manual (CERC 1984) as

$$\frac{\partial U}{\partial t} + \underbrace{\frac{\partial M_{xx}}{\partial x} + \frac{\partial M_{xy}}{\partial y}}_{\text{advection of momentum}} = \underbrace{fV}_{\text{coriollis}} - \underbrace{gD \frac{\partial S}{\partial x}}_{\text{surface slope}} + \underbrace{gD \frac{\partial \xi}{\partial x}}_{\text{inverse barometer}} + \underbrace{gD \frac{\partial \zeta}{\partial x}}_{\text{astro. tide potential}} + \frac{\tau_{sx}}{\rho_w} + \frac{\tau_{bx}}{\rho_w} + \underbrace{W_x P}_{\text{Rainfall rate}} \quad (1)$$

Where U is volume transport per unit width in the x direction; M is momentum transport quantities; $f = 2\omega \sin \varphi = \text{Coriollis parameter}$; D is water depth; ω is the angular velocity of earth; φ is geographical latitude; g is gravitational acceleration; ξ is atmospheric pressure deficit in head of water; ζ is astronomical tide potential in head of water; τ_s is surface wind stress; τ_b is bottom stress; ρ is mass density of water; W is wind speed and P is precipitation rate (depth/time)

Equation (1) above is the generic differential equation for hydrodynamic motion in a direction perpendicular to the shoreline. Similarly, in a direction parallel to the shore the expression reads

$$\frac{\partial V}{\partial t} + \frac{\partial M_{yy}}{\partial y} + \frac{\partial M_{xy}}{\partial x} = -fU - gD \frac{\partial S}{\partial y} + gD \frac{\partial \xi}{\partial y} + gD \frac{\partial \zeta}{\partial y} + \frac{\tau_{sy}}{\rho_w} + \frac{\tau_{by}}{\rho_w} + W_y P \quad (2)$$

Parameters are as define for Equation XX and V is the volume transport per unit width in the y direction

Should one consider only the terms applicable to wind setup, the expression follows as

$$\underbrace{gD \frac{\partial S}{\partial X}}_{\text{surface slope}} = \frac{\tau_{sx}}{\rho_w} \quad (3)$$

Where D is the water depth; S , free surface height above still water level; $\frac{\partial S}{\partial X}$, slope of wind induced gradient; τ_s , surface wind stress; ρ_w , water density.

Additionally, if one were to consider the effects of bottom stress, as is often preferred when computing wind setup, then the expression changes to

$$\frac{\partial S}{\partial X} = \frac{(\tau_s + \tau_b)}{gD\rho_w} \quad (4)$$

Where τ_b is the bottom stress. All other parameters are as defined for Equation (3)

Equation (4) is also the base expression that is used throughout literature for deriving analytical solutions for the wind setup problem.

The Shore Protection Manual thus gives good insight into the foundations of computational theory related to wind setup, but provides little in the form of analytical solutions to the problem.

Early work in developing and approximating solutions to the wind setup problem included studies by Hellstrom (1941), Langhaar (1951) and Keulegan (1951; 1952). Hellstrom developed an analytical method for calculating wind set up in a closed rectangular basin. Keulegan added to the former by including shape factors to account for basins of various shapes. Bretschneider (1967), using field data, developed equations for calculating wind setup in open coasts. A detailed summary of the early work and findings is given in Bretschneider (1967) and in Ippen & Eagleson (1966). The contents of these texts seem to form the basis of the analytical methods commonly used in an array of popular coastal engineering textbooks and tool-packages used today.

Bretschneider provides various formulae relevant to a range of different classifications of the wind setup problem. Most relevant here is the formula for wind setup normal to a coastline with a bottom of constant slope

$$S = \frac{kV^2F \cos \varphi}{g[D_0 - D_c - S]} \ln \frac{D_0}{(D_c + S)} \quad (5)$$

Where k is a dimensionless constant accounting for surface shear stress, bottom shear stress and water density. k is typically taken as 3.2×10^{-6} ; V is the wind velocity measured at 10m above SWL; F is the fetch length; φ is the winds angle of deviation from normal to the coastline; D_0 is the depth at the shore and D_c the depth at some distance, F from the coast.

Taking a closer look at the more modern engineering resources it is noted, interestingly, that many authors shy away from giving explicit analytical solutions to the wind setup problem. For example, the Shore Protection Manual (CERC 1984) goes as far as expressing the generic differential equation for hydrodynamic motion, but does not go into the integration for simplified analytical solutions. The more modern successor of the Shore Protection Manual, the Coastal Engineering Manual, also neglects to provide explicit solutions to the wind setup problem (U.S. Army Corps of Engineers 2002). In fact, wind setup is hardly mentioned in the latter text. Another popular coastal engineering design resource, the Rock Manual (CIRIA et al. 2007), does provide a simple analytical solution for calculating wind set-up in a closed rectangular basin of constant depth, but it does not go further to include solutions for the open coast. The lack of explicit analytical solutions in these popular texts highlight the dilemma that storm surge problems are complex by nature and are more commonly preferred to be solved numerically.

There are some (less popular) texts that do in fact provide explicit solutions for wind setup. These solutions all seem to repeat the findings that were documented by Bretschneider (Kamphuis 2000; Sorensen 1997; Dean & Dalrymple 2002; OCDI 2002). Dean and Dalrymple (2002) provide a formula for calculating wind setup over a flat continental shelf. This same expression is also given in Sorenson (1997) and is shown in Equation (6) below:

$$S = h \left(\sqrt{\frac{2kU^2x}{gh^2} + 1} - 1 \right) \quad (6)$$

Where k is the wind stress coefficient typically given by 3.3×10^{-6} . U is wind speed and h is the water depth over the flat continental shelf. S is storm surge

CRESS, an initiative of the Netherlands Ministry of Infrastructure and Environment, is an online engineering tool which contains a collection of short routines and formulae commonly used in coastal engineering (Netherlands Ministry of Infrastructure et al. n.d.). The same expression as given in Equation (6) is also used in the CRESS routine for wind setup calculations.

The formula given by Kamphuis (2000) relates back to the basic differential equation as expressed in Equation (4). Here, surface stress, bottom stress and water density are expressed in terms of wind speed and a coefficient k .

$$\frac{dS}{dx} = \frac{k(U \cdot \cos \varphi)^2}{gD} \quad (7)$$

All parameters in equation (7) are as defined in Equation (6).

For simple numerical integration of this problem, Kamphuis suggests solving the problem incrementally at intervals, dx , starting from some distance offshore where S is assumed zero. An example is taken from Kamphuis' text to illustrate the use of this basic incremental integration (Refer to **Table 2**).

Table 2: Example of an incremental numerical solution as suggested by Kamphuis (2000).

Section	1	2	3	4	5	6
Δx (km)	3	2	2	1	1	1
d (m)	15	10	5	2.8	1.9	1.4
D (m)	15.0	10.03	5.05	2.90	2.05	1.61
Δs (km)	0.026	0.026	0.052	0.045	0.064	0.081
S (m)	0.03	0.05	0.10	0.15	0.21	0.29

The inverse barometer effect is the change in sea level, locally, as a result of a deviation in the ambient air pressure from the normal. A drop in pressure results in an increase in water level and, similarly, an increase in air pressure results in a drop in water level. The expression in Equation (8) below shows the theoretical amount by which the sea level responds to the pressure change (Kamphuis 2000):

$$\Delta h = -\frac{\Delta p}{\rho g} \quad (8)$$

Where Δh is the change in water surface level; Δp is the pressure change (usually taken as the pressure's deviation from the normal, where the normal pressure at sea level is around 1013 mbar). ρ is the water density and for sea water, is typically taken at around 1027kg/m³ but this may vary based on salinity and temperature.

From Equation (8), and assuming typical water densities, it can be seen that a pressure change of 1 mbar results in inverse sea level response of roughly 1cm.

2.5 SIGNAL PROCESSING THEORY

In the analysis of storm surge, it is common to analyse water level data obtained from tide gauges (OCDI 2002). Essentially, such analyses are classified as time series analyses. The various functions and computation techniques relating to time series analyses are widely and thoroughly discussed by many literature sources, in many different contexts (many of which are not even related to coastal engineering). Therefore, a compressive discussion of common time series analysis techniques will not be covered here. However, one particular component of time series analysis that is worth discussing here is the analysis of data in its frequency domain. Frequency domain analysis will be used extensively in this study and as such, this section serves to highlight some of the key concepts which will be employed in analyses that follow later in the study (Chapter 3).

Frequency domain analysis is a component of time series analysis but moreover it falls specifically under the umbrella of signal processing. The topic of signal processing is a broad and complex topic in its own right and is covered in a vast range of literature sources. Signal processing is most popularly applied in the field of electrical engineering, but its applications stretch as far and wide as the field of economy.

2.5.1 Signal Processing Theory: Frequency Transforms and the Fourier Analysis

Most time series may be considered as consisting of periodic components and aperiodic components superimposed on a long term trend and random noise (Thomson & Emery 2001). It is possible to express the variability of a data series in terms of those dominant periodic functions present. When a data series is expressed as frequency and not in time, it is referred to as a spectrum.

The most common method of expressing a time series as a spectrum is by the well-known Fourier analysis. In the Fourier analysis, a resultant series, called the Fourier series, is explained as a linear summation of cosines and sines. The relative contribution of a sinusoidal component to the total variance of a series defines the importance of that particular frequency component in the total signal

(Thomson & Emery 2001). This concept is also central to most other spectral analysis techniques. A Fourier series is expressed as follows.

$$y(t) = \overline{y(t)} + \sum_p [A_p \cos \omega_p t + B_p \sin \omega_p t] \quad (9)$$

A_p , and B_p are the Fourier coefficients and define the contribution that each oscillatory component, ω_p , makes to the total “energy” of the observed signal (Thomson & Emery 2001). The resulting (power-) spectrum, or periodogram, is the energy per unit frequency bandwidth of the time series.

The Fourier technique may be applied directly or through the Fourier transform of the autocorrelation function. Both of these techniques have strenuous computational overheads. Therefore, the common modern application method of the Fourier analysis is through the Fast Fourier Transform (FFT). This algorithm, pioneered by Danielsson and Lanczos (1942), has a far higher computational speed than its formerly mentioned alternatives. The FFT function is extensively documented throughout signal processing literature and is commonly and readily available in a wide range of modern analysis software packages (Microsoft Excel, R, Matlab, Mike Zero by DHI, to name a few) and thus the mathematics will not be further looked at in depth for the purposes of this summary.

Although the Fourier analysis is by far the most popular analysis technique, it also has its limitations. The limitation of the Fourier transform in the application of sea level studies, that causes the greatest concern, is that it assumes that periodic components have fixed or slowly varying amplitudes (i.e the periodic components are stationary). If a series is strictly non-stationary, then there are other transform techniques that are better suited. These include the Hilbert transform, the wavelet transform and the S-transform (Thomson & Emery 2001). Wavelet analysis in particular has been used in a number of oceanographical studies. Percival & Mofjeld (1997) studied use of wavelet analysis techniques in coastal engineering application involving the study of non-stationary processes, including storm surge and reports good results. Recently, MacHutchon (2015) used the wavelet method extensively in a study of long wave characteristics for selected South African ports. However, apart from the work of MacHutchon, it would appear that all previous studies relating to water surface elevations in South Africa, made exclusive use of the Fourier Transform, for example De Cuevas (1985) and Wijnberg (1993).

2.5.2 Sampling Theory

With respect to the Fourier analysis, which is used extensively in this study, the following considerations relating to sampling theory are of significant practical importance:

A time series of duration T , must be expressed as a discrete series $y(t_n)$ with a total of $N = T/\Delta_t$ sample intervals and $N + 1$ sample points so that $y(t_n) = y(n\Delta_t) \equiv y_n (n = 0, 1, \dots, N)$ where Δ_t is

the sampling interval. In the Fourier analysis the original series $y(t_n)$ is reproduced as the sum of sines and cosines of varying amplitudes and phases. The specific characteristics of these sines and cosines define the transform's harmonics. The harmonics are essentially the functions that, when added together, compose the Fourier series. The first harmonic has a frequency of $f = 1/T$, the second harmonic $f = 2/T$ and so forth. The first harmonic is also the lowest possible frequency that can possibly be resolved in the series' resulting spectrum (or periodogram) and is known as the fundamental frequency. On the other end of the spectrum, the highest frequency that can be resolved is the $N/2$ harmonic which has a frequency of $f_N = (N/2)/N\Delta_t = 1/2\Delta_t$. The $N/2$ harmonic is also known as the Nyquist frequency or the folding frequency of the series.

The Nyquist frequency remains the highest resolvable frequency on the basis that at least 2 sampling intervals (and 3 sampling points) are required to resolve a sinusoidal type oscillation. However, for practical purposes, 4 or more sampling points are required to realistically resolve an oscillation without incurring aliasing.

CHAPTER 3

3 Analysis of Measured Time Series Data

3.1 GENERAL

The time series analysis performed for this study involved 5 processes namely: (1) Preliminary analysis, (2) spectral analysis, (3) filtering, (4) comparative analysis and (5) formulation of results.

The preliminary analysis included an overview and quality control of the data sets available for the study. A spectral analysis was done to aid in identifying the processes contributing to water level fluctuations in Saldanha Bay. Those processes identified in the spectral analysis were then filtered out, followed by an examination of the correlation between them and the known meteorological processes. Based on the correlation findings, data series were subsequently modified to more accurately represent an approximation of the isolated components of storm surge.

3.2 DATA OVERVIEW AND PRELIMINARY ANALYSIS

3.2.1 Discussion of available data

The data available for use in the time series analysis may be placed in two categories:

- (1) Sea level data; and
- (2) Weather data.

The available data was provided by Transnet National Ports Authority (TNPA) and the South African Navy Hydrographic Office (SANHO). The Council for Scientific and Industrial Research (CSIR) played a key role in facilitating the collection of data from TNPA.

(1) Sea level Data

Water level data for Saldanha Bay was available from two sources: Tide gauge data (SANHO) and ultrasound water level meter data (TNPA).

SANHO provided data sets of predicted tides as well as measured water levels for the port of Saldanha. The measured data was obtained from a port tide gauge. This same data has been used in previous studies by reputable scholars such as Mather (Mather & Stretch 2012; Smith et al. 2007; Mather et al. 2009) This data was thus considered to be of a very high standard. Nevertheless, basic checks were performed to ensure the quality and reliability of the data. The tide data is expressed relative to Chart Datum (CD) in sampling increments varying between 1- and 3 minutes.

The dataset of predicted tidal heights has been derived mathematically by SANHO and thus contains not erroneous data points or datum shifts. It was therefore accepted with great certainty that this data set is perfectly accurate and calibrated.

TNPA's water level data was measured with an ultrasound level sensor. This ultrasound sensor was originally commissioned by TNPA to aid in studies of long wave action in the Port. A similar sensor is also installed at the Port of Ngqura near Port Elizabeth. Both the Ports of Saldanha and Ngqura experience problems with mooring under the influence of long waves and hence the motivation for collecting such data. The data from these ultrasound level sensors are relatively new and therefore not much certainty is guaranteed regarding its quality and calibration. One other study, in which this same data (or at least a portion thereof) is used, is a study by Charles & Stuart (2013) on the characteristics of long waves in the port of Ngqura.

Due to uncertainty surrounding the quality of this ultrasound data set from TNPA, careful quality control was performed to assess the validity of the data for use in the time series analysis. The quality control of this data set is discussed in more detail later.

The TNPA ultrasound dataset was measured relative to LLD and at measuring intervals of 3 seconds. **Figure 9** shows the position of the ultrasound measuring instrument in the Port of Saldanha.

(2) Weather Data

The available weather data consists of wind speed, wind direction and air pressure, all of which have been measured locally. The position of the weather station is indicated on **Figure 9**. Measurements are averaged over 20 minutes for all category (2) data.

Table 3 provides a technical summary of the available data sets.



Figure 9: Aerial imagery of Saldanha Bay

Table 3: Technical summary of data available for Saldanha Bay

Data set	Source	Δt	Position	% missing	Datum	Additional information available
Ultrasound water levels	TNPA	3 s	33.0356S, 17.9825 E at the tip of Caisson 25	39.35	LLD to accuracy of approx. 5cm.	Recording instrument used: LOG_aLevel (by General Acoustics)
Tide gauge water levels	SANHO	3 min	Approximately 33.025S, 17.962 E near small craft harbour	50.95	CD	
Predicted Tides	SANHO	10 min	Inside of port	-	CD	
Wind data	TNPA	20min	33.028 S, 17.963 E. 14m above ground	7.21	UTC Time zone	Includes wind direction and gust speed
Pressure data	TNPA	20min	33.028 S, 17.963 E. 14m above ground	7.25	UTC Time zone	
Bathymetry data	TNPA					

3.2.2 Defining Wind Directions

Saldanha Bay is a large and complex bay, particularly as a result of the position of the dry bulk and oil terminals. This, along with the way in which the breakwater connects Marcus Island to the mainland, results in the bay effectively being divided up into a number of smaller bays, each with its own narrow entrance. Any given wind direction will thus be in an onshore direction somewhere in the greater Saldanha bay and will force setup in some part of the bay and set down in another part. It is therefore important, for the purpose of this thesis, to define a particular wind direction as onshore. For such purposes a southerly wind is selected as “onshore” (northerly wind as “offshore”) and easterlies/westerlies “cross shore”. The selection of southerly winds as onshore is motivated as follows:

- The data sets that are available for this study, i.e. the water level data and weather data, have been recorded exclusively in and around the northern part of the bay i.e. the smaller bay that is formed by the Marcus Island breakwater to the west and the oil jetty to the east. If one considers this smaller northern bay as the primary study area for this thesis and particularly for the time series analysis that is done initially, then it makes sense to define southerly winds as onshore as this particular portion of the bay is open to the south
- Taking a closer look at the wind data sets, it is clear that the prevailing wind is from the south (slightly SW). A scatter plot of wind direction “spot shots” is shown in **Figure 10**. With the prevailing wind from the south, it adds to the benefit of selecting this wind direction as the

“onshore” wind direction for the study. This way, it would not be necessary to calculate the vector components for wind speeds in other directions which may be defined as onshore.

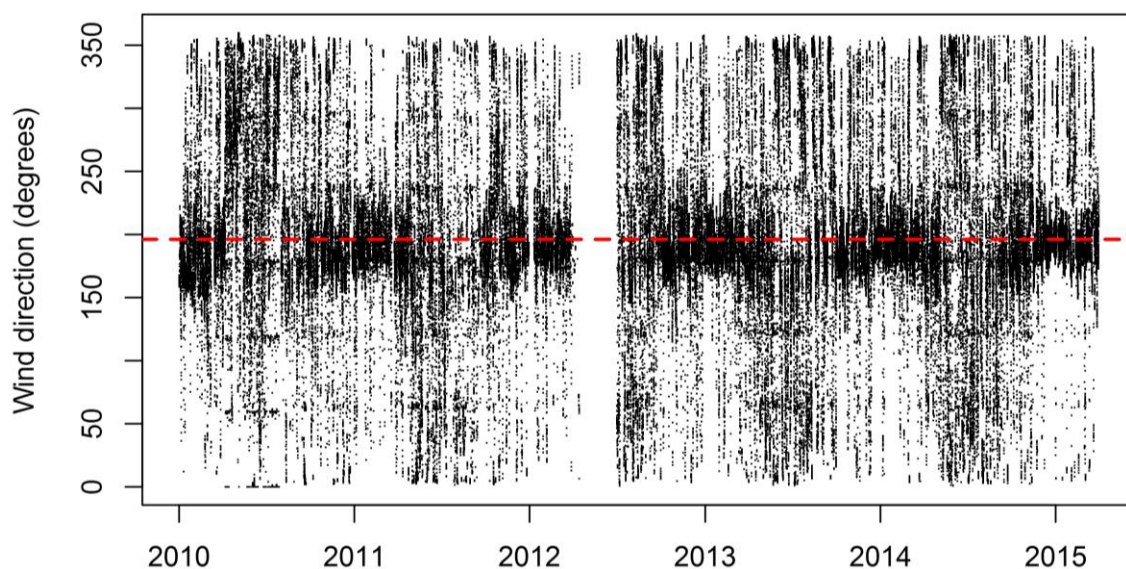


Figure 10: Plot of wind directions for the Saldanha Bay wind data set. Direction is in degrees. South is 180 degrees and north is 0 or 360.

3.2.3 Length of Data Records

SANHO’s tide gauge data was made available for a period spanning approximately 8 years (2008 to 2015). The predicted tidal water levels were provided in a data set spanning 2010 to 2015, although this could easily have been obtained for an infinitely long time span, seeing that these levels are determined mathematically. However, the weather data (TNPA) was provided in data sets spanning only from 1 January 2010 to 31 March 2015.

Having looked at the available data, the next important step was to determine the times of intersection of the various data sets, in other words, the time overlaps for the various data parameters. Ultimately, one is only able to perform time series analyses on data sets when all of the parameters in question are sampled simultaneously. For this reason, only the records from January 2010 to March 2015 were considered for the study as the weather data is not available beyond these times. However, even within these five years of intersecting data, many gaps are found in the data. **Table 3** already shows that large portions of the data are missing. **Figure 11** further goes on to illustrate the distribution of the gaps and the times of intersection of the various data sets.

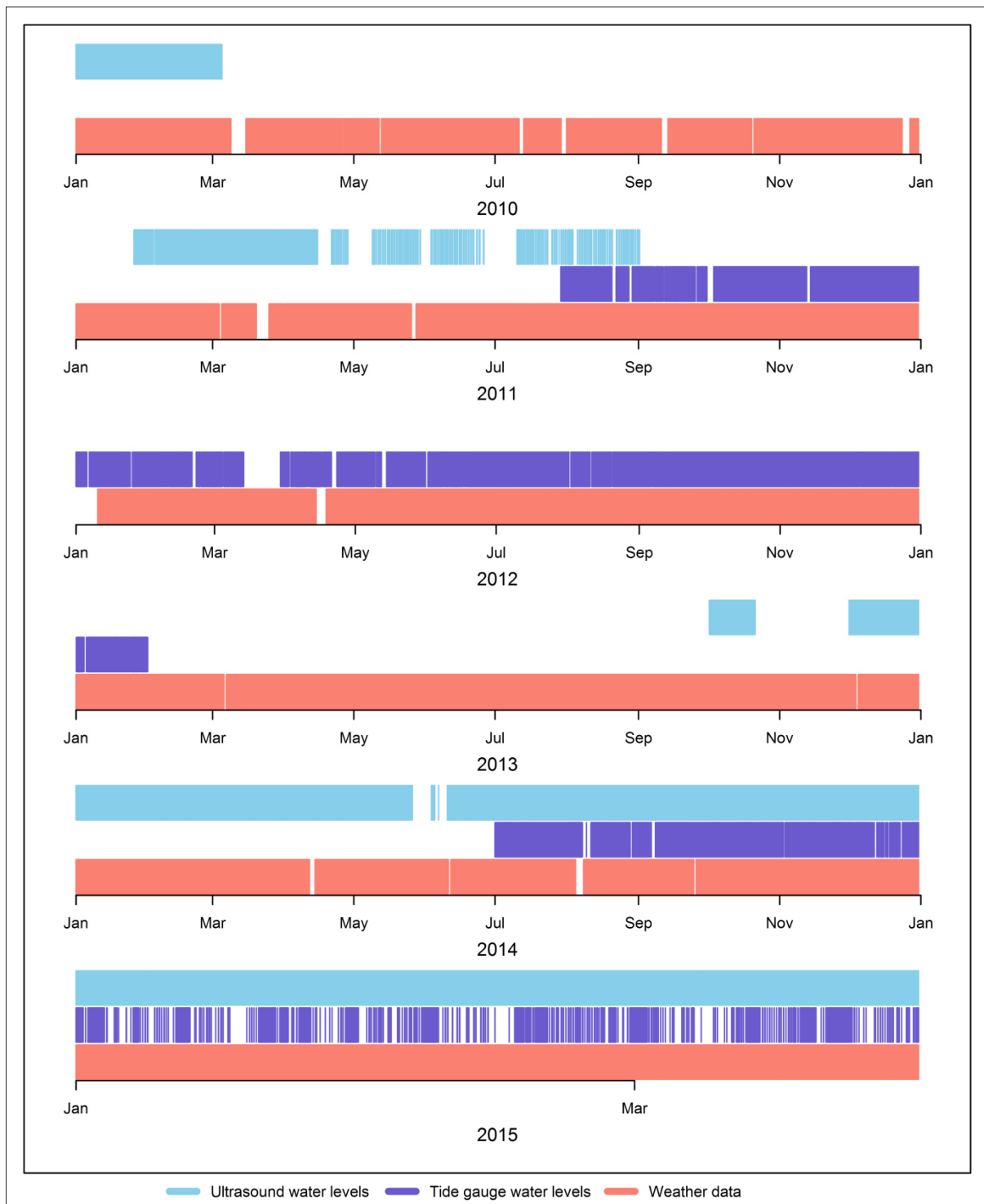


Figure 11: Time intersection plot for the various data sets available for Saldanha Bay

3.2.4 Data Quality Control

Already at first glance, it was possible to spot several defects and anomalies in the data sets:

- It would appear that TNPA's ultrasound datasets were in their raw form and had undergone no pre-processing. There were many instances of spikes, gaps and datum changes.
- A few gaps and spikes were present in SANHO's measured data sets. These could easily be corrected.
- The weather data sets from TNPA appear to have been cleaned up previously as no spikes were present in the data and there were few gaps present.

Four aspects were considered for the quality control of the various data sets:

- resampling
- gap-filling
- outliers
- calibration and datum corrections.

These four aspects are discussed in some detail below:

(a) Resampling

Weather data, at 10 minute intervals, had to be compared and used in calculations with 3 second -, 3minute- and 5-minute data from the various other available data sets. The data sets had to be re-sampled to a common sampling interval, Δt , in order to be used in the time series analysis.

If all data sets are down-sampled to the sampling interval of the weather data, i.e. 10 minutes, then the maximum frequency that can be resolved in the time series analysis¹ is:

$$f_N = \frac{1}{2\Delta t} = \frac{1}{2(60 \times 10)} = \frac{1}{1200} \text{ cps}$$

This corresponds to a minimum resolvable period of 20minutes and is accepted as a suitable minimum period to resolve, as the expected periods in which storm surge would occur is a few hours to a few days.

Down-sampling was done by averaging and decimating. Visual observation of the raw water level data revealed that at sampling increments of 3s, the data was too noisy for direct decimation and that direct

¹ Also known as the Nyquist (or folding) frequency of the data set

decimation might lead to the misrepresentation of the data set as a whole. Consequently, the following resampling measures were taken:

- i) Raw 3 second ultrasound water level data was averaged to 1 minute intervals: A 20 point moving average centred on multiples of 1 minute was used.
- ii) Raw 3-minute tide gauge water level data was interpolated linearly to 1 minute intervals.

At this point all water level data had been converted (resampled) to 1 minute intervals.

- iii) As and when down sampling was required, the now 1-minute interval water level data was decimated to the respective slower increments by simply keeping the data points at the desired increments and dropping the rest of the data points.

(b) Gap-filling

As recalled from the review of sampling theory, the longest period (or the lowest frequency) oscillation in sea level fluctuations that can be resolved is determined by the length of the longest uninterrupted segment of continuous data points.

$$f_0 = 1/N\Delta t = 1/T$$

Although, cumulatively, all of the available data sets span a time period of at least 5 years from more or less 2010 to 2015 (recall **Figure 11**), the data is extremely interrupted and disjointed with gaps of varying length. In the case of storm surge related water level fluctuations which are expected to have periods of up to 3 days, an uninterrupted portion of data with a length of at least 3 days is required to perform a useful analysis.

For the purpose of identifying the most suitable data segments for use in the time series analysis, the start and end times of all continuous (uninterrupted) segments of data for all the data sets were recorded and are summarised in **Table 4**.

Table 4: Summary of gaps and continuous data segments in the water level data sets

Data Set	Ultrasound water level	Tide gauge water level
No. of gaps	1635	329
Ave. length of continuous data segments (hours)	8.4	47.6 (1.98 days)
Longest uninterrupted segment (hours)	146.83 (6.12 days)	1743.83 (72.66 days)
No. of segments > 3 days	11	31

It is noticeable here that all of the data sets contain at least one uninterrupted segment of data that is long enough to resolve a 3-day storm event. However, the longest uninterrupted segment in the

ultrasound data is 6 days. Although this is long enough to resolve a single large storm event, the likelihood of a significant event being present within that short data span is very low.

Furthermore, all gaps are at least 1 hour long and filling gaps of this length would likely result in erroneous values.

(c) Outliers

A search was done to locate outliers in the data. As a first approximation, an outlier was selected as any data point falling outside of 1.5 times the inter quartile range of the data set. Surprisingly no such individual outliers were present in the ultrasound water level dataset. The only occurrence of outlying data was a portion of data from March 2012 (roughly 9 days) that was shifted vertically by approximately 2m. This was corrected by shifting that portion of data down by the difference between its mean and the mean of the remainder of the dataset.

The weather data from Saldanha, particularly the pressure data, contained a few noticeable spikes. Individual erroneous points were simply deleted from the data set.

(d) Calibration

The ultrasound data was measured relative to LLD, and even so, was not calibrated to LLD exactly. It is understood that the height calibration of the measuring device was accurate to roughly 5cm (personal communication, CSIR 2015) and had to be shifted vertically to account for the datum change as well as the poor calibration. This was done as follows:

- i) The mean of the entire dataset was calculated, including all of the quality corrections applied prior to this step.
- ii) The mean of SANHO's measured tide gauge data was calculated.
- iii) The ultrasound data was adjusted vertically by the difference between i) and ii).

Furthermore, the timestamps for TNPA's weather data sets were calibrated to UTC and had to be converted to SAST. This was done by simply shifting all data points 2 hours back in time.

3.2.5 Preliminary Analysis of Residual Water Levels

Many of the analyses in this study are done on datasets of residual water levels. Residuals are calculated as the difference between the measured water levels and the predicted water levels. **Figure 12** below shows a plot of the full length of residual water level data that is attainable.

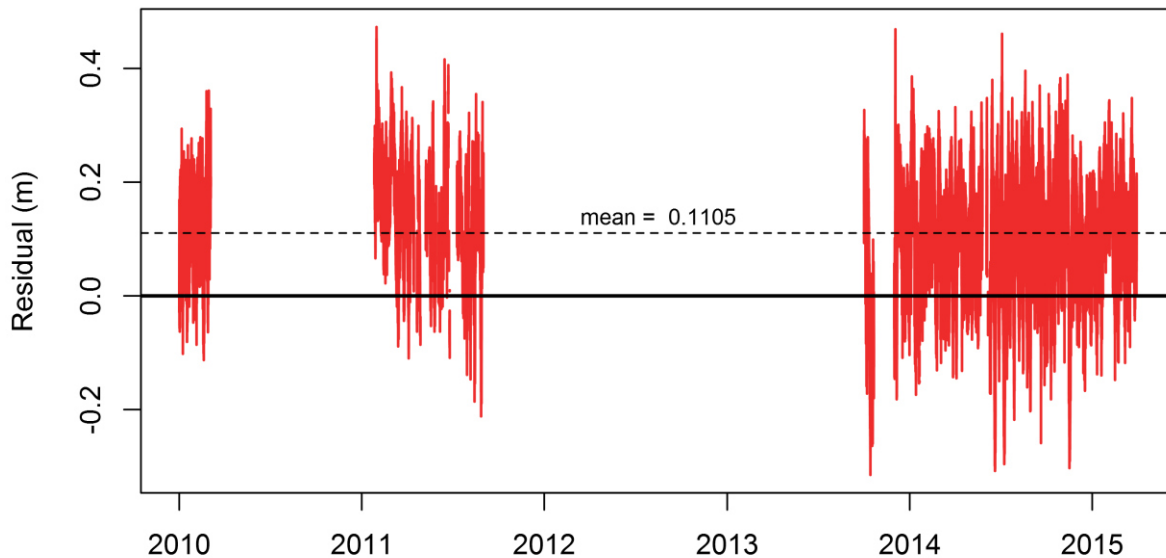


Figure 12: Complete residual data set for all available tide gauge data from January 2010 to March 2015

It is seen from the plot that the residuals are generally positive. The average height of the entire set of residuals (excluding gaps) amounts to 111mm. A mean residual level that is above zero suggests that water levels are, on average, higher than predicted/expected. This immediately raises the concern that there is a possible vertical datum error in the base data.

While it may be tempting to simply shift the base data downwards so as to end up with a residual set that averages around the zero line, this would not be wise. There is a possibility that the positive average of the residuals is in fact correct and that there are legitimate forcing mechanisms that account for this phenomenon. It could also be a combination of a vertical datum error and a coastal process of some sort.

In order to better understand the root cause behind the abovementioned positive residuals, a brief investigation was performed that focused upon the frequency of occurrence of positive residuals vs the frequency of occurrence of possible forcing mechanisms for positive residuals:

- A calculation was done to assess the split between positive and negative residuals. It was found that residuals are positive for 88% of the time.
- A similar calculation was done for the wind data corresponding to the times for which residuals were available. It was found that wind is onshore (southerly wind) for 75.85% of the time.
- Again, a similar calculation was done for the pressure data. It was found that pressure values were below the typical average sea level pressure for 63.51% of the time.

Knowing that low air pressure results in an increase in water-level (inverse barometer effect) and that onshore wind drives positive wind setup and considering that these two forcing mechanisms are acting

in favour of a rise in sea level for most of the time, it starts to seem acceptable that residuals are predominantly positive. With that being said, it is not possible to calculate exactly how much of the vertical shift is correct and how much of it is caused by possible errors in the base data. Therefore, at this point in time, the data will be accepted as it is. The impact that the predominantly positive residuals may have on subsequent results and outcomes will be assessed at a later stage.

3.3 SPECTRAL ANALYSIS OF RESIDUAL WATER LEVELS

3.3.1 Methodology

The Discrete Fourier Transform – more specifically, the FFT algorithm – was used to produce spectral energy density functions and plots for the water level time series data. The Fourier analysis theory had previously been discussed in the literature review. Other analysis techniques such as the wavelet transform were not considered because the FFT yielded satisfactory results, and also because the FFT algorithm is more commonly available on most analysis software packages. The “fft” function on R¹, as well as several supporting functions from the R package “signal”, was used for the computations as explained in this chapter.

The 3 longest available continuous water level data segments were analysed independently for dominant frequency oscillations. Due to the frequent gaps present in virtually all of the available data sets, it was not practical to analyse the frequency domain for the entire study period. However, care has been taken to ensure that for each site, segments representative of all dominant wind directions and storm seasons were included.

Furthermore, it was not considered wise to apply a single window FFT to the full lengths of the data sets. Instead, the data sets were divided up into windows of lengths varying between 3 days to a week. A Hanning window-function was applied to each window and consecutive windows were overlapped by 66%. Windowing the data as described above minimised frequency leakage and moreover also gave a better indication of variations present in the frequency domain over time. The spectra of all the individual windows were averaged so as to represent the general case for the entire period covered by the data set under consideration. In doing so, short duration spikes in unimportant frequency ranges were averaged out from the final spectrum. The theory and application of windowing and ensemble averaging as used here is documented in Thomson & Emery (2001).

The goal of the spectral analysis was ultimately to identify those waveforms that are relatively continuous throughout the recorded data. The identified waveforms would then be quantified and filtered out from the data series in order to approach the components of storm surge more closely. The process of filtering the recurring waveforms from the data is explained in more detail later.

3.3.2 Results

The 3 data sets that were selected for the spectral analysis are summarised in **Table 5**. For continuity, these same 3 data sets were also used repeatedly in the remainder of the analyses later in the study. For example, Numerical modelling was performed on data sets spanning the same time period as these 3

¹ R is an open source programming language and freeware software environment for statistical computing and graphics (R Core Team 2016).

sets. Analytical calculations, too, were performed using data from these 3 sets. It is important to note also, that for the remainder of this thesis, including subsequent chapters, the terms “data series No. 1”, “data series No. 2” and “data series No. 3” refer specifically to the 3 data sets as identified here.

Table 5: Summary of the 3 data sets that were selected for spectral analyses at Saldanha Bay

Summary\Data sets	Data series No. 1	Data series No. 2	Date series No. 3
Start date/time	2014-03-14 15:20	2010-01-01 00:00	2014-06-29 17:40
End date/time	2014-05-26 07:10	2010-03-05 00:00	2014-08-11 19:10
Duration	1743 hours	1512 hours	1033 hours
season	Late summer	Mid-summer	Mid-winter
Wind conditions	Predominantly S to SE winds, but includes strong N winds	Predominantly Southerly winds	Predominantly Northerly winds
<u>Summary statistics:</u>			
Wind (20 min average) – Mean	6.23 m/s	8.04 m/s	5.27 m/s
Wind (20 min average) – Max.	18.72 m/s	19.90 m/s	19.86 m/s
Pressure – Min.	1001 mbar	1003 mbar	999 mbar

Figure 13, **Figure 14** and **Figure 15** show the plotted data sets for data series 1 to 3 respectively. Ambient wind and pressure conditions are also included in these plots to illustrate the prevailing weather conditions that may have contributed to the final water levels.

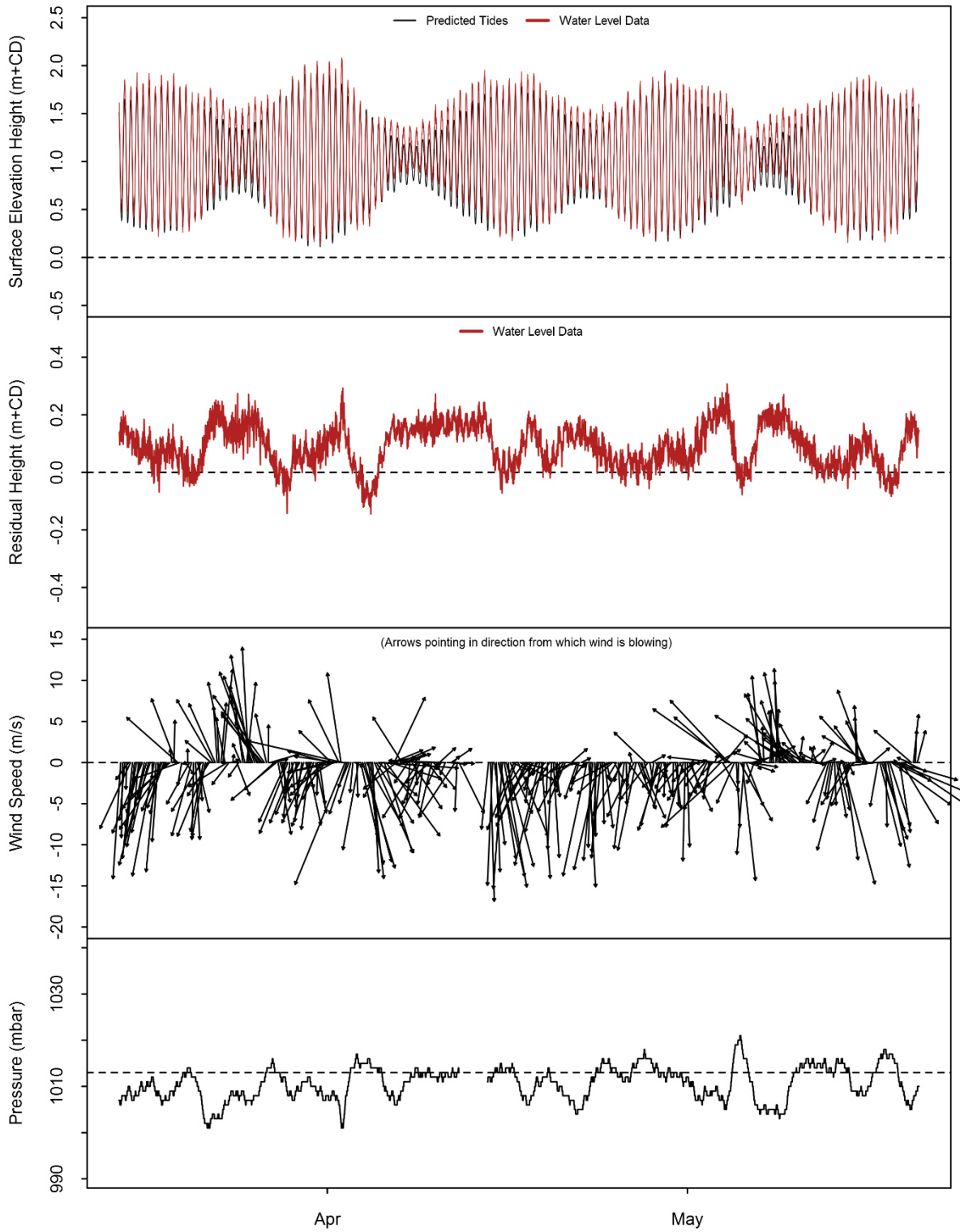


Figure 13: Summary plot of Data Series 1 showing water levels (measured, predicted and residuals) as well as ambient wind and pressure measurements. Start time is 2014-03-14 15:20 and end time is 2014-05-20 07:10

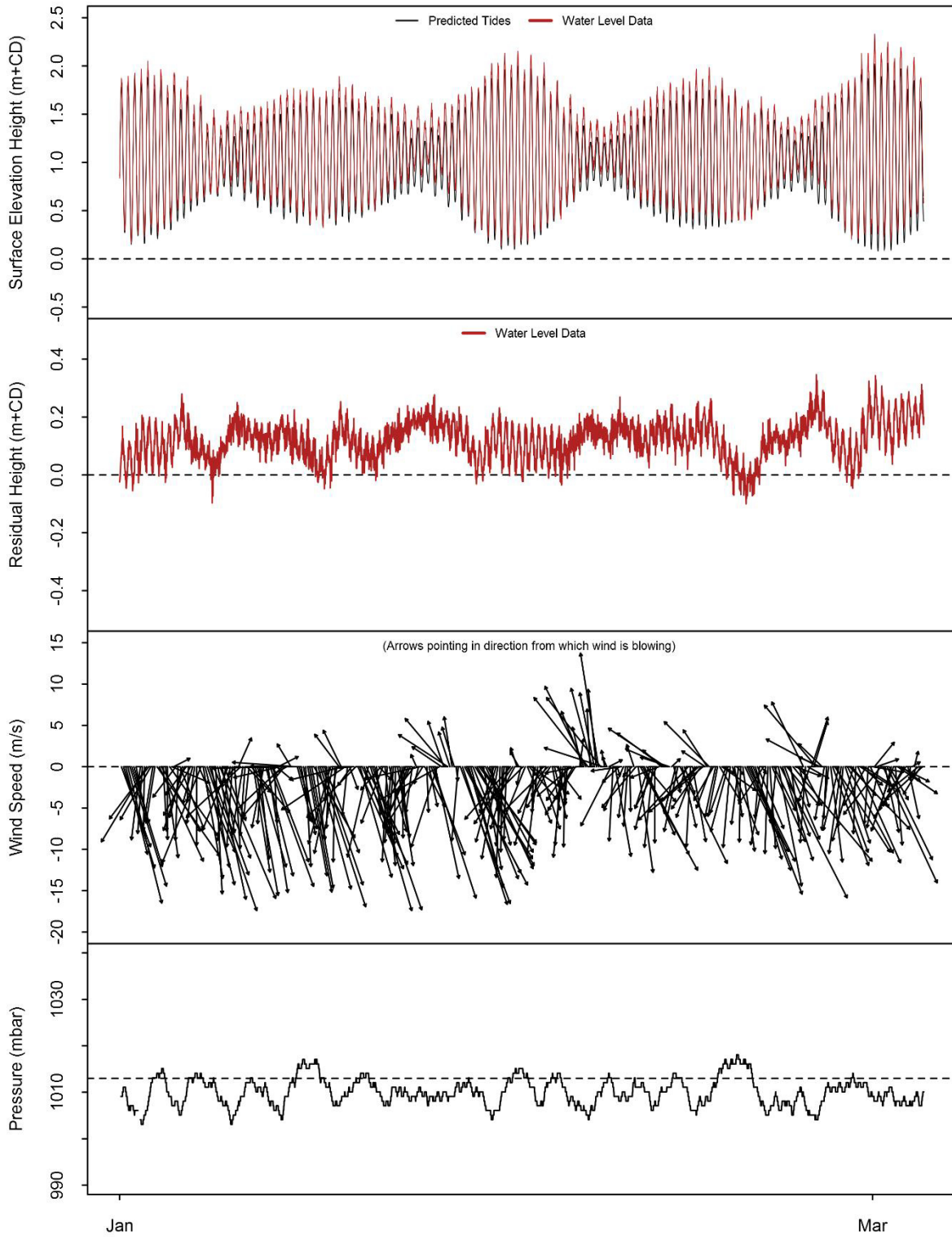


Figure 14: Summary plot of Data Series 2 showing water levels (measured, predicted and residuals) as well as ambient wind and pressure measurements. Start time is 2010-01-01 00:00 and end time is 2010-03-05 00:00

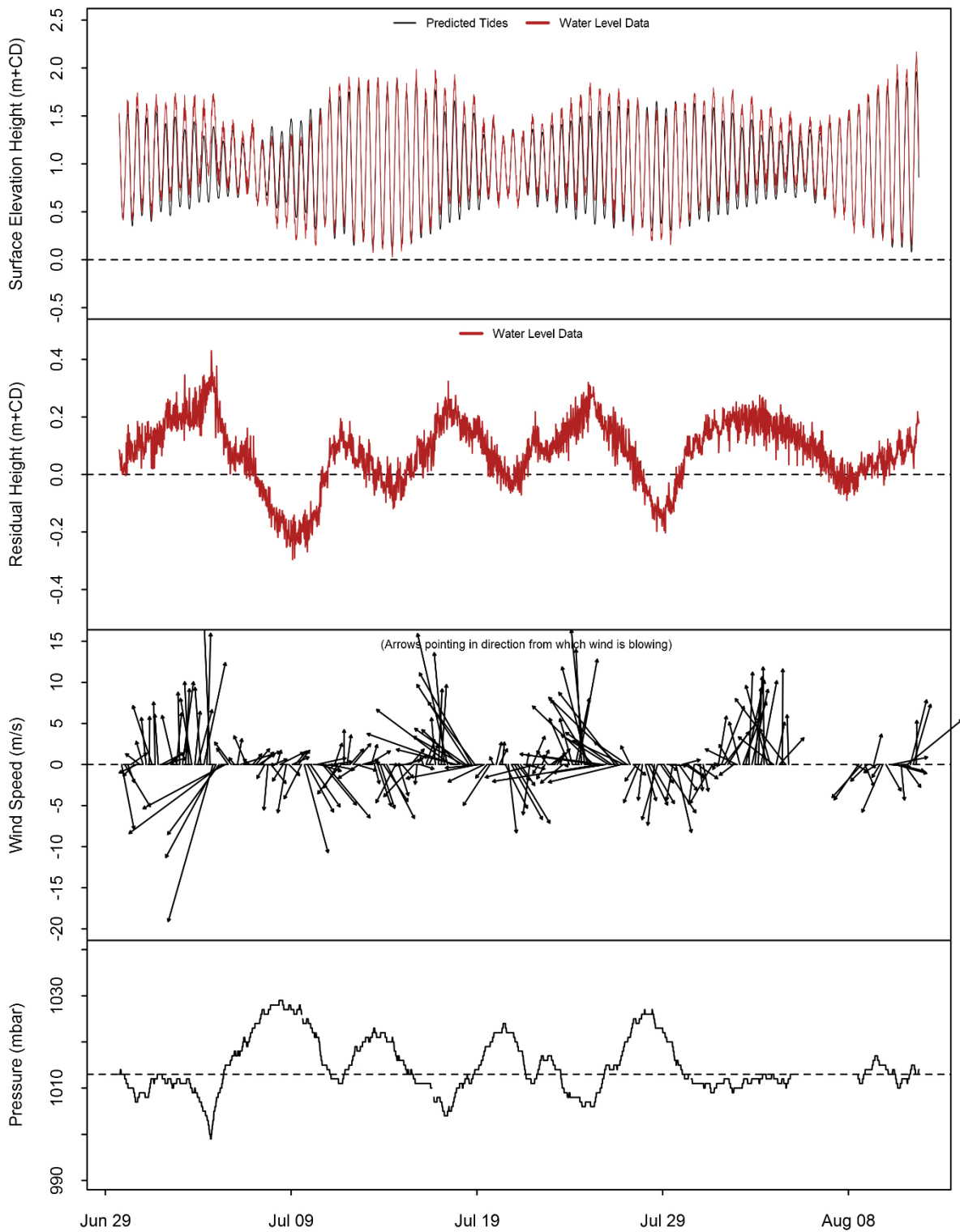


Figure 15: Summary plot of Data Series 3 showing water levels (measured, predicted and residuals) as well as ambient wind and pressure measurements. Start time is 2014-06-29 17:40 and end time is 2014-08-11 19:10

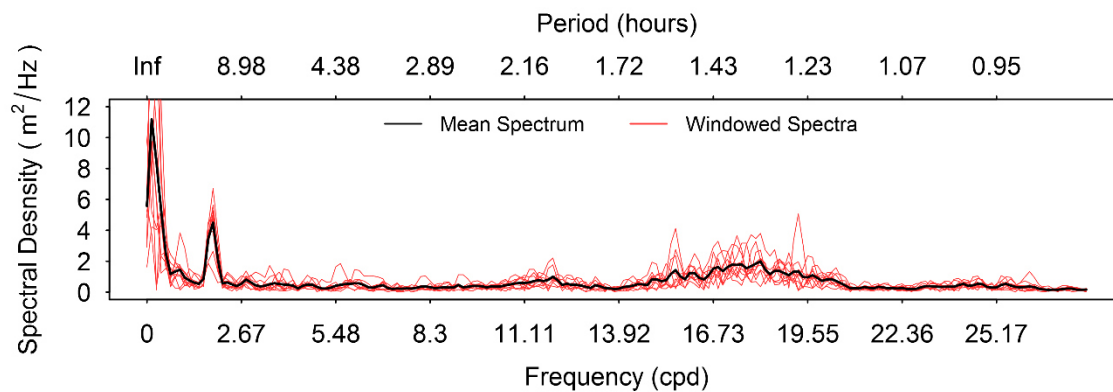


Figure 16: Spectrum plot of for residual water levels for Saldanha data series No. 1. Red lines indicate the spectra for each 1-week window. The black line is the average spectrum over 10 windows.

Analysis of data series 1 of 3

Data series no. 1 was divided into 10 equally sized windows with each window covering a time-span of roughly 1 week. The resulting spectra are shown in **Figure 16**. The average spectrum has 3 prominent features: A Large spike in the near-zero frequencies, a second large spike at frequency 1.97 cpd (that is a period of 12.19 hours) and a third widely-spread “hill” at roughly 17.90 cpd (1.3 hours). A fourth feature – one that is less prominent, but potentially important – is the small hill at around 12.20 cpd (2 hours).

The first of the abovementioned features, the large spike near the zero frequency, is the result of unresolved low frequencies. With a longer data record or with a higher resolution FFT it would perhaps be possible to resolve more of these frequencies. However, the period range of these oscillations lies in the order of 10 days, or more, and is thus not at all likely to be related to storm surge or anything else of interest for that matter. In fact, the presence of this large spike in the spectrum is in all likelihood attributed to relatively large residual values at the boundary points for each FFT window. On this basis, no further attention was given to the first large spike as described here.

The second large spike, with a period of 12.19 hours, was initially hypothesised as being associated with one of two phenomena namely:

Hypothesis (1) Standing long waves (seiches) in the bay

Hypothesis (2) a time lag between the predicted tides and the measured water levels

However, it was easy to prove that the spike was in fact a result of phase lag as per hypothesis (2), and it was thus not necessary to look into the possibility of hypothesis (1). Hypothesis (2) was accepted on the basis of the proof as follows:

An energy density spectrum, similar to that which has been considered up to now, was created, but for the predicted tides data set on its own. Here it was indeed found that the tidal spectrum contained a major energy component at that same frequency of 1.97cpd that was seen in the residual spectrum.

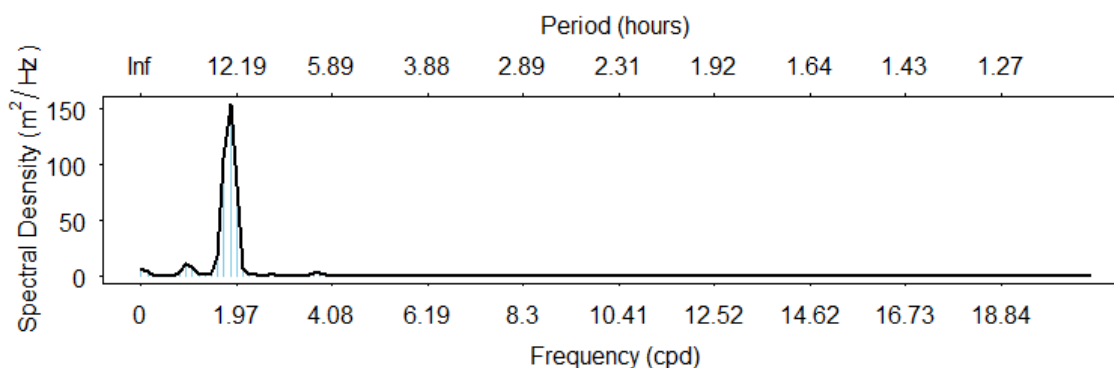


Figure 17: Spectrum plot of for predicted tides

Consider two exact sinusoidal waveforms with matching amplitudes and frequencies, but with slightly different phases. The difference between the two waveforms is also a sinusoidal signal with its amplitude equal to the maximum vertical displacement between the two input waveforms. That is essentially what is being observed in the residual data series under consideration here.

Focussing, again, on the residual spectrum and the second peak under consideration, it was thought possible to a recalculate the input data series with corrected time stamps. It was hypothesised that perhaps other important frequency components would become more apparent in the energy density spectrum of the residuals should the phase difference be corrected. An order of magnitude test was done initially to get a feel for the amount by which the input series would have to be shifted to correct the phase lag. Assuming average tidal heights and upper and lower limits for the phase lag, a required time shift of approximately 2 to 4 minutes was calculated. However, because the residual dataset was only available in 10min intervals, it was deemed impractical to shift the times as it would only have distorted the data even further. Therefore, it was concluded that the second large peak in the energy spectrum of data series No. 1 could simply be ignored.

The third feature in the spectrum, the widely-spread hill at roughly 17.90 cpd, was the interesting one. There are several aspects about this hill that are pointing towards possibly being caused by storm surge:

- i) It is in the frequency range where one would expect storm surge to manifest itself. The periods covered by the hill range roughly from 1.1hours to 1.7 hours.

- ii) The individual spikes in the windowed spectra (red lines on the graph) are varying in position along the frequency axis as well as in magnitude. This implies that whatever mechanism it was that caused these oscillations were present more frequently in some weeks than in other (similar to the normal pattern of wind) and also that it was more severe in some weeks than in others.
- ii) The upper limit of its frequency i.e. that corresponding to a period of roughly 1.7 hours is outside that which would be expected for shelf waves (which is expected to have periods of 10 to 60 minutes) thus eliminating that possibility.

The fourth and last feature, the small hill at 12.20 cpd, bears close resemblance to its more prominent sister-hill that was discussed in the previous paragraph. This one spans the frequencies approximately corresponding to a period range of 1.7 hours to 2.7 hours, but in all other respects its characteristics may be described as similar to the formerly discussed frequency hill.

In conclusion: The first two prominent spikes were deemed unimportant with regards to storm surge. The widely-spread components of spectral density along the 12.2 to 21.4 cpd range are likely to be representative of storm surge.

Analysis of data series 2 of 3

A similar approach was taken for the second selected data series as with the first series. The initial FFT plot is shown in **Figure 18**

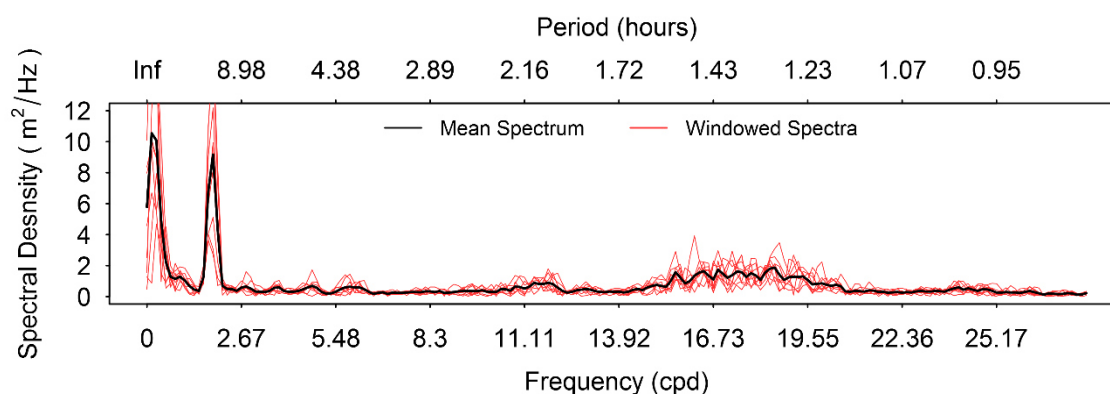


Figure 18: Spectrum plot of for residual water levels for Saldanha data series No. 2. Red lines indicate the spectra for each 1-week window. The black line is the average spectrum over 9 windows.

The result for the spectrum transform is virtually an exact match of that for the first data series. The distribution of spectral energy and even the magnitudes of spectral peaks match almost exactly that of the first data series. It is therefore assumed that similar conclusions may be drawn from this series than from the previous one. Similar to data series No.1, this one also had spectral density components of

possible storm surge origin along the frequency range of 14.4 to 21.42 cpd (1.1 hours to 1.7 hours). Other features on the spectrum were ignored.

Analysis of data series 3 of 3

Once again, a similar approach was taken for the third selected data series as with the previous two. The initial FFT plot is shown in **Figure 19**.

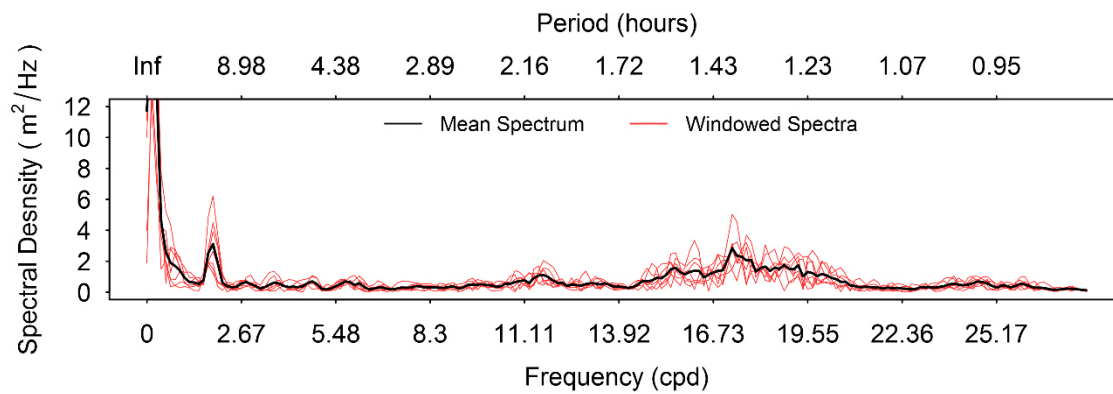


Figure 19: Spectrum plot of for residual water levels for Saldanha data series No. 3. Red lines indicate the spectra for each 1-week window. The black line is the average spectrum over 7 windows.

Here, again, the result for the spectrum transform is virtually an exact match of that for the previous two data series. Again, it is assumed that similar conclusions may be drawn from this series than from the previous two.

3.4 DATA FILTERING

In the previous section, 3 subsets from the residual data series were selected and analysed for meaningful frequencies. The next step in the time series analysis is to run the data through filters which would remove oscillations of unwanted frequencies while still maintaining those meaningful frequencies for further analysis. Recall, for example, that waveforms within the 1.1 to 2.7-hour period range were found to be meaningful. These oscillations had to remain present in the data series. **Table 6** provides a full summary of various identified frequency groups and their filtering requirements.

Table 6: Summary of frequency groups in Saldanha Bay residual water level data and their respective filtering requirements.

Frequency (Period) range	Associated phenomena	Filtering requirements
0-1.26 cpd (∞ - 19.0 hours)	Seasonal variations – unresolved low-frequency sea level fluctuations	None
01.83-2.11 cpd (13.1 – 11.4 hours)	An erroneous phase lag between the predicted and measured components of the tides (centred at 12.19 cpd)	Band-stop filtering
8.86 -21.38 cpd (2.7 – 1.1 hours)	Hypothesised as wind driven oscillations	Band-pass filter
21.39 – ∞ cpd (<1.0 hour)	Noise	Low-pass filter

A Butterworth filter was used for filtering operations. As before, the processing was done on R, using the built-in functions from the package “signal” (R Core Team 2016). A 1st order forward-reverse cascaded filter was used. There are many other filter types which may have been used instead and which may have produced equally satisfying results. For ease of use, and due to its availability on the R package, it was decided to opt for the Butterworth filter.

Figure 20 shows the results of the filtered data series no.1. Here, the effects of tidal lag at 1.97cpd, as well as all noise of frequency greater than 21.4 cpd were removed.

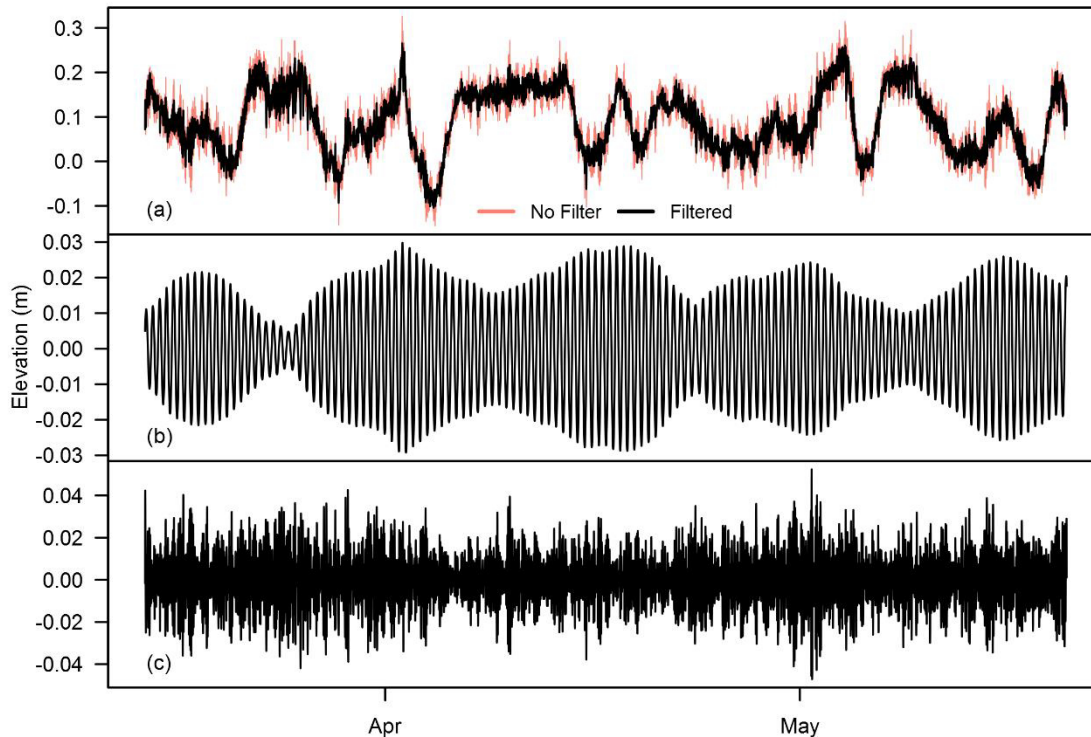


Figure 20: Results of preliminary filtering for Saldanha data set No.1 (a) *unfiltered (red) vs. filtered data (black)*
 (b) *isolated tide lag component 1.97 cpd* (c) *isolated noise of frequencies greater than 20.4 cpd*

By looking at the various filtered components in isolation, it may be seen that the effect of the tidal lag is small as expected – with a maximum contribution of 30mm during the period of observation.

The effect of those frequencies which were highlighted as meaningful with regard to wind response in Section 3.3, is seen here as also being small. These components reach a 95th percentile maximum of 24mm during the period of observation.

Similar filtering operations were performed on the other two residual data series and the results were almost exactly the same. For data series no. 2, the 95th percentile maximum “wind contribution” component was 23mm and for the third data set it was 28mm. The term “wind contribution” is used in inverted commas here because at this stage, the hypothesis that these waveforms are wind-related could not yet be supported sufficiently. It needed to be proven, first of all, that there was a substantial correlation between these waveforms and the measured wind. Section 3.5 deals with the statistical correlations between residual components and weather data, but here it was seen fit to first make a visual analysis of the wind-residual components. **Figure 21** shows plots of the wind and residual “wind contributions” for the 3 data series.

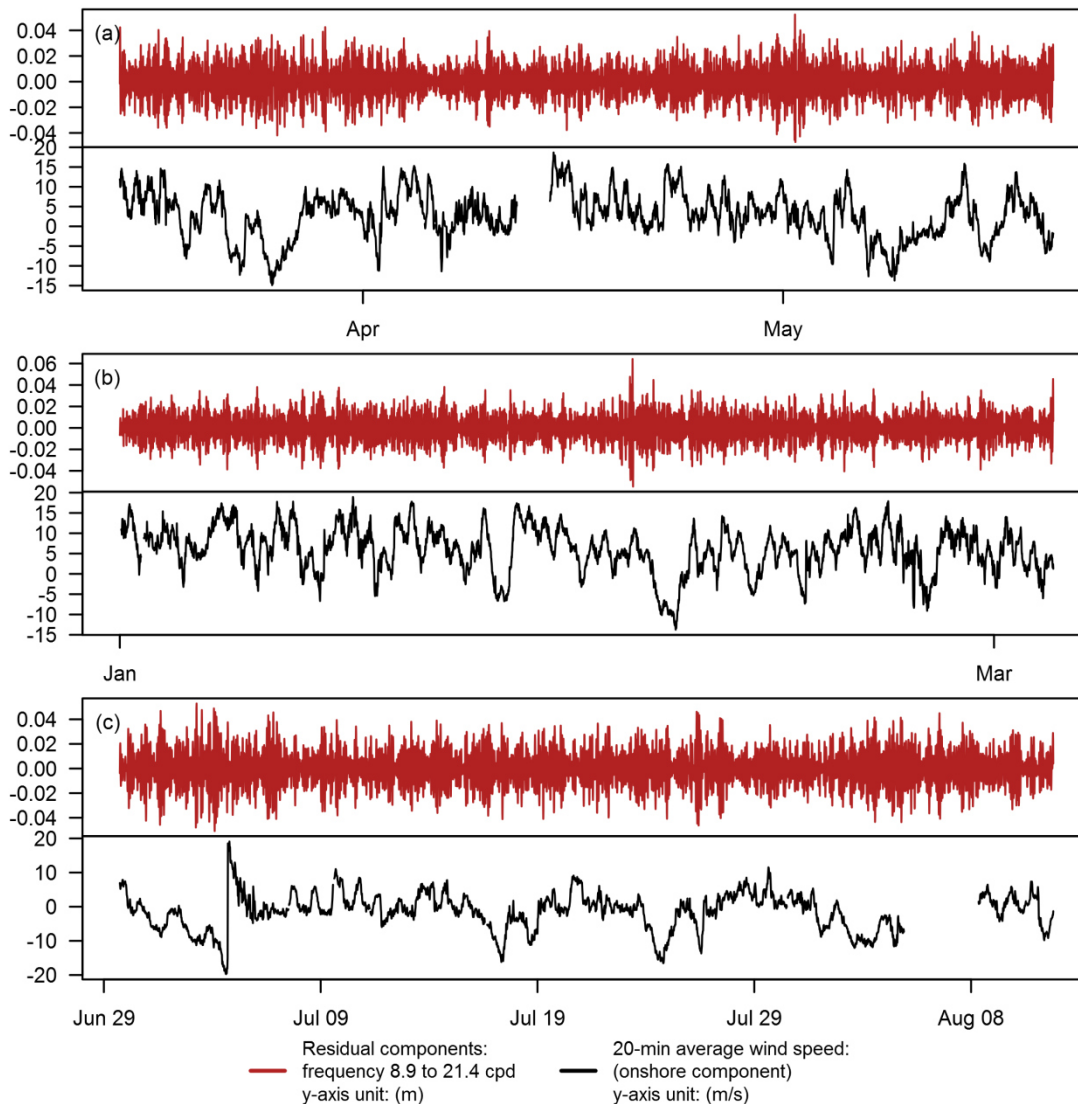


Figure 21: Comparison plots of residual components (frequencies 8.9 to 21.4 cpd) and onshore (south) wind speeds. (a), (b) and (c) represent data series 1, 2 and 3 respectively.

From **Figure 21**, it is clear that both the wind and the water level residuals are rapidly varying throughout all data sets and visual correlation is difficult to achieve and not immediately apparent.

In **Figure 22**, **Figure 23** and **Figure 24** the data series were smoothed using 0.5 day, 1 day and 2 day moving averages (centred). For data sets no.1 and no.2, the smoothing had little effect and it was still not possible to draw visual correlation between wind and the residual component of the 8.9 to 21.4 cpd frequency range. However, for data series no.3 the smoothed data does result in the revelation of a correlation that may be observed visually.

It is interesting that only data set no.3 resulted in a visually observable correlation and moreover that the correlation appears strongest in the presence of strong offshore (northerly) winds. A possible explanation for this may be as follows:

- Northerly winds blow over a shallow part of the bay (the northern bay) which intensifies the effects of wind setup.
- The Marcus island breakwater and the dry bulk terminal (and oil quay) partially act as a barrier to the south and the measured water levels are recorded up against these barriers.

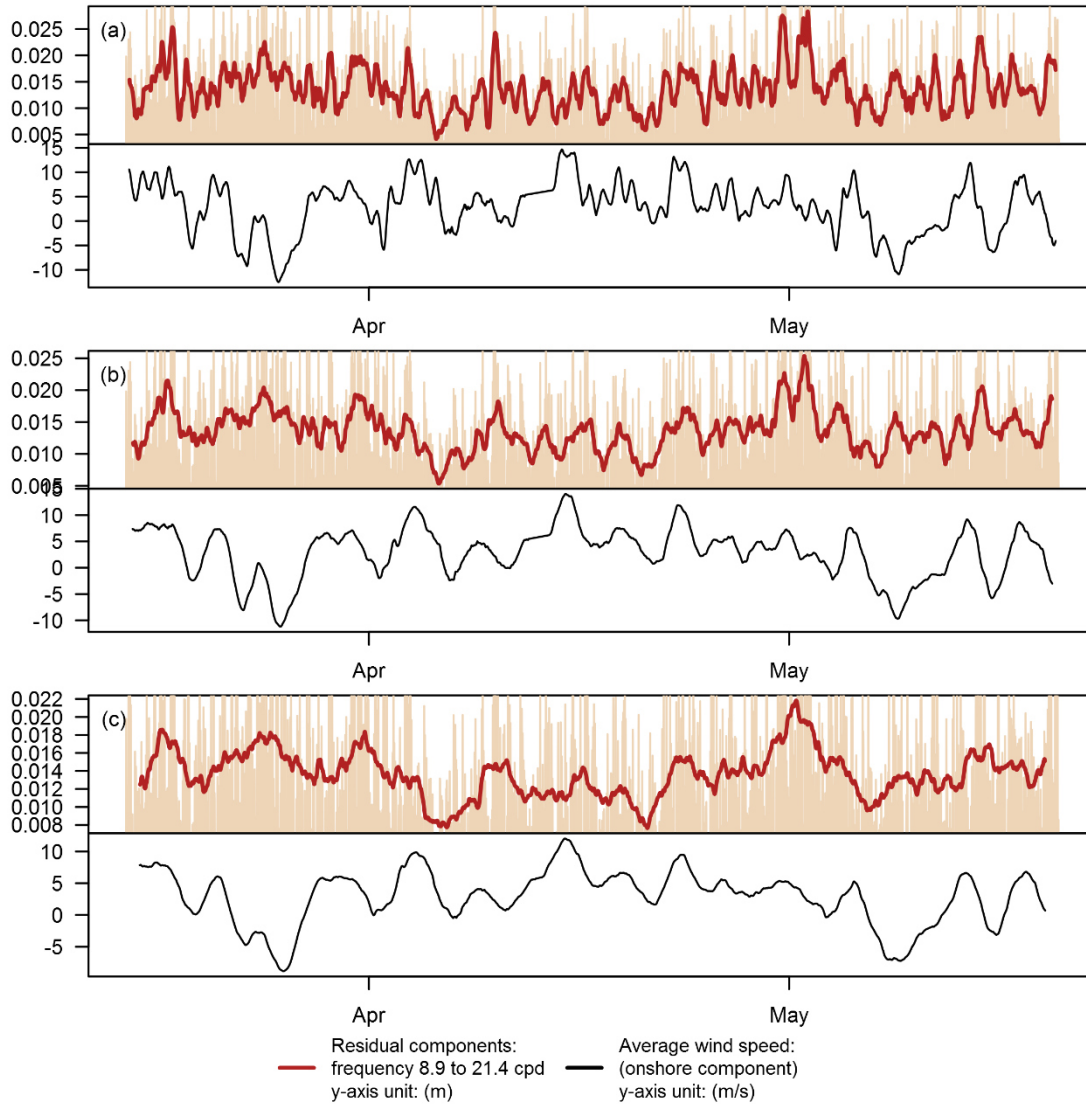


Figure 22: Comparison plots of smoothed residual components (frequencies 8.9 to 21.4 cpd) and onshore wind for data series No.1. (a) 12 hour moving average (b) 1 day moving average (c) 2 day moving average

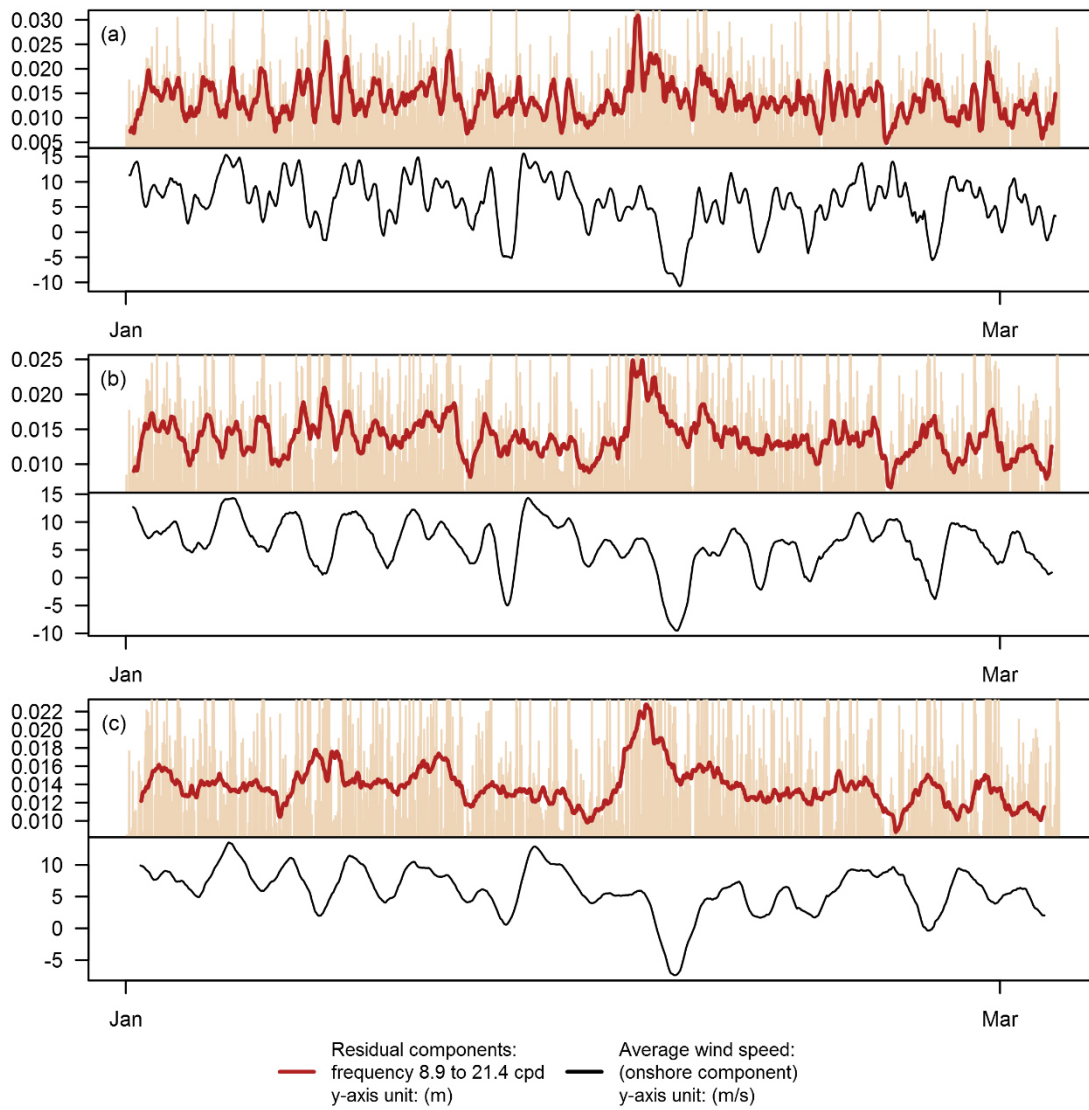


Figure 23: Comparison plots of smoothed residual components (frequencies 8.9 to 21.4 cpd) and onshore wind for data series No.2. (a) 12 hour moving average (b) 1 day moving average (c) 2 day moving average

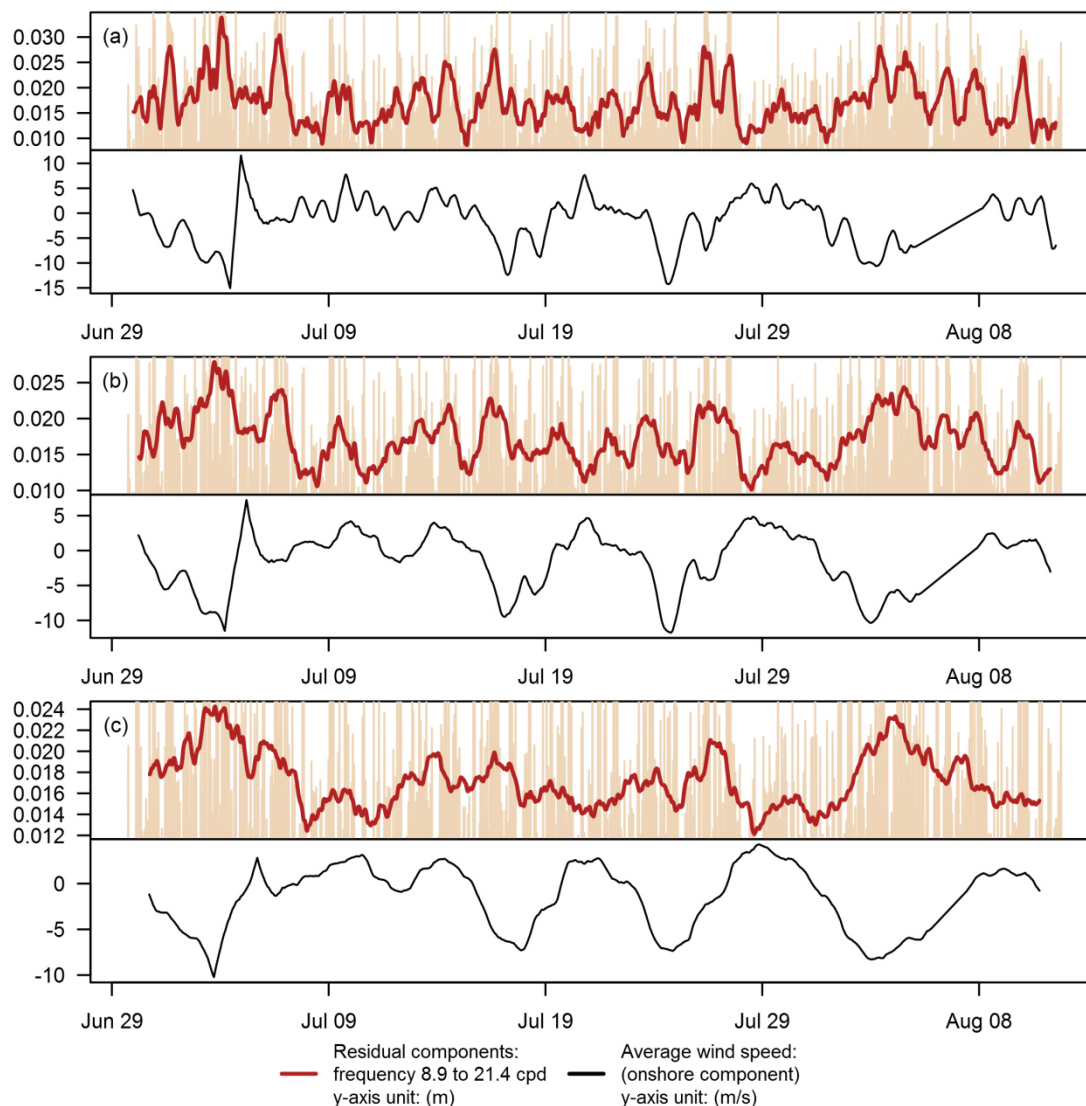


Figure 24: Comparison plots of smoothed residual components (frequencies 8.9 to 21.4 cpd) and onshore wind for data series No.3. (a) 12 hour moving average (b) 1 day moving average (c) 2 day moving average.

From these results it was concluded that from a high-level visual approach as taken here, the oscillations in the frequency range of 8.9 to 21.4 cpd – that which was earlier hypothesised as being wind-generated – indeed appears to be wind related. While the heights of these oscillations are small, the visually observed correlation (in one of the data sets at least) remains an important factor to take into account for the purpose of this study.

With regards to the height of these oscillations, it should be noted that the 10th percentile minimum height is 7mm (and 5mm, 6mm for data series 1 and 2). It is therefore accepted that although wind is a contributing force, the full magnitude of these frequency components is not caused by wind only. At least some of the components were most likely caused by unresolved noise in the data.

3.5 COMPARITIVE ANALYSIS

3.5.1 Methodology

A cross correlation analysis was performed between different pairs of data. This was done, in order to test for the lag, between two series, at which the greatest correlation exists.

Consider two identical time series consisting of white noise only and with the one series at an arbitrary phase shift in relation to the other. If one is to test for correlation between these two series it would surely result in a very weak correlation (zero), because there is inherently no serial correlation in a white noise signal. However, if the correlation between these two series is tested after lagging the one series relative to the other at a lag that is exactly equal to the length of the phase shift, the correlation will equal unity, which is expected because the values are perfectly correlated with themselves.

Similarly, for example, wind and water levels may be strongly correlated, but if the water level response lags the wind force significantly, a normal correlation test will indicate an erroneously weak correlation. A cross correlation analysis will indicate by how long the water level response is lagging the wind force. It will also indicate how strong such correlation may be at that lag and what the statistical significance of the correlation result is.

The expression for the cross correlation function, as documented in Thomson & Emery (2001) is as follows:

$$R_{xy}(\tau) = \frac{1}{N-k} \sum_{i=1}^{N-k} y_i x_{i+k} \quad (10)$$

Where R is the cross-correlation function for data series x and y ; τ is the lag time, $\tau = \tau_k = k\Delta t$ ($k = 0, \dots, M$), for k sampling increments, Δt , and $M \ll N$.

The normalised cross correlation function is given by

$$\rho_{xy} = \frac{R_{xy}(\tau)}{\sigma_x \sigma_y} \quad (11)$$

The statistical significance of a correlation result is tested against the t-distribution with $n_{eff} - 2$ degrees of freedom and to a desired significance level of $(1-\alpha)$ where α is typically taken as 0.05. The t-test parameter, \hat{t} , is calculated as

$$\hat{t} = |R_{xy}| \sqrt{\frac{n_{eff} - 2}{1 - R_{xy}^2}} \quad (12)$$

A correlation is thus accepted as statistically significant by a significance of $(1-\alpha)$ if $\hat{t} \geq t_{n,\alpha}$.

In ocean time series, the effective number of degrees of freedom, n_{eff} , is related to the number of independent variables in a time series and is not equal to the number of sample points, N (i.e. not all N samples are independent of each other). Thomson & Emery (2001) gives the effective number of degrees of freedom as

$$n_{eff} = \frac{T}{T_{int}} \quad (13)$$

Where T is the total time duration of a series and T_{int} is the integral time scale of an observed variable.

T_{int} , in a cross correlation analysis, is the time integral of the product to the two data sets' autocorrelation functions, given by

$$\sum_{k=-\infty}^{\infty} R_{yy}(k\Delta t)R_{xx}(k\Delta t) \Delta t \quad (14)$$

Where the autocorrelation function is similar to the cross correlation function (equation XX), but calculates the correlation of a variable with itself at time lag τ . The expression for the autocorrelation function is given by

$$R_{yy}(\tau) = \frac{1}{N-k} \sum_{i=1}^{N-k} y_i y_{i+k} \quad (15)$$

And normalised as

$$\rho_{yy} = \frac{R_{yy}(\tau)}{\sigma^2} \quad (16)$$

The time integral of variable's autocorrelations would therefore be a cumulative summation of autocorrelation products for consecutive lags over the total number of lags present. The time integral typically reaches a maximum at a particular lag. This time integral value which is taken where the curve reaches a maximum height is selected as the integral time scale of the correlation, T_{int} , that is to be used in Equation (13).

An example is shown here of the typical process followed for the cross correlation analysis: Consider the cross correlation analysis between the maximum predicted tidal heights¹ and the filtered residual water levels² at Saldanha Bay. The cross correlation function, as seen in **Figure 25 (a)** reaches an absolute maximum correlation at a time lag of 10.2 hours. The correlation coefficient associated with this lag is -0.42. It can therefore be said that a higher than usual tidal cycle is often followed, roughly 10.2 hours later, by drop in residual water levels. However, the correlation coefficient of -0.42 suggests

¹ A time series consisting of only the maximum heights predicted to be reached during each tidal cycle.

² Residuals from which noise and other erroneous oscillations have been filtered out. See Section 3.4.

a weak correlation. In order to estimate the statistical significance of the correlation result, it was required to determine the effective degrees of freedom to be used in the t-test. Here the autocorrelation functions are shown in **Figure 25 (b)** and the time integral function in **Figure 25 (c)**. The time integral function reaches a peak of 163.5 time steps. From this result, the t-test was performed and the significant threshold values determined. Significance lines are indicated in **Figure 25 (a)** in blue (dashed).

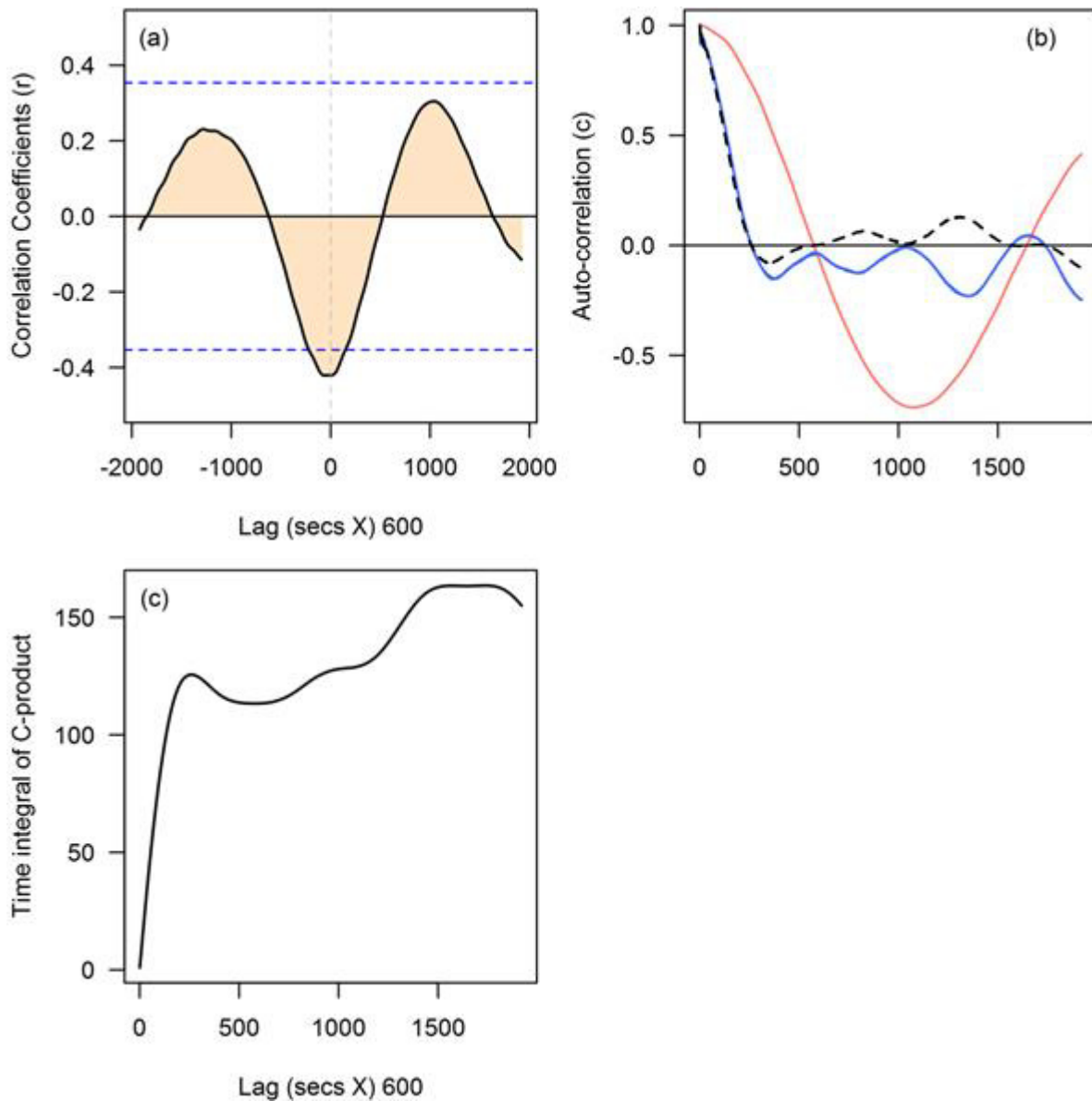


Figure 25: Cross correlation between maximum tidal heights and filtered residual water levels. (a) Cross Correlation (b) Auto correlation for maximum tidal height (red), filtered residuals (blue) and their product (black dash) (c) Time integral of autocorrelation functions

3.5.2 Results

Cross correlation analyses were performed between the following pairs of data series (**Table 7**):

Table 7: List of data series pairs on which cross correlation analysis were performed

Test No.	Independent variable		Dependent variable	
1	Tidal height	(T)	Filtered residual	(FR)
2	Onshore wind speed component	(OSW)	Wind-frequency residual components	(FR _{wf})
3	Longshore wind speed component	(LSW)	Wind-frequency residual components	(FR _{wf})
4 ¹	Surface level pressure	(P)	Filtered residual	(FR)
5	Onshore wind speed component	(OSW)	Adjusted Filtered residual	(AFR)
6	Longshore wind speed component	(LSW)	Adjusted Filtered residual	(AFR)

Results of the cross correlation analyses are shown in **Table 8** but a more detailed description follows here below:

Correlation Test (1): Tidal height (T) vs. Filtered residuals (FR)

Data sets of the maximum predicted height reached during each high tide cycle were produced to test for correlation with filtered residuals. (Note: This is the same correlation test that was used as an example in Section 3.5.1) The results show weak correlations for all three data sets as well as unrealistic lag times. It is concluded, therefore, that a higher than usual or lower than usual tidal cycle thus has no impact on the filtered water level residuals.

Correlation Tests (2) and (3): Wind speed components (onshore and cross shore) vs. Wind-frequency residual components (FR_{wf})

Filtered oscillations within the frequency range of 8.9 to 21.4 cpd – as discussed in Section 3.3 – were analysed against wind speed² (onshore as well as cross shore). It was found that the data sets, for onshore wind and before smoothing, showed no real correlation. After the data was smoothed with 12-hour, 1-day and 2-day centred moving averages, the water level response to onshore winds showed improved correlation, especially in the winter when offshore winds prevail. Here, a correlation coefficient of 0.64

¹ After Test no. 4 was completed, linear regression was used to produce adjusted filtered residuals

² It should be kept in mind that this particular correlation test was already done visually between these same two data series in Section 3.4

was achieved. This is in agreement with that which was concluded from the visual correlation test in Section 3.4.

There was no correlation between longshore wind components even after the data was smoothed.

It is concluded that wind, over short periods, have little impact on water levels, but over periods of up to two days, set up (or set down depending on wind direction) becomes evident in the water level response. This is the case for on/offshore winds and for the water level response of oscillations within the 8.9 to 21.4 cpd frequency range.

Correlation Test (4): Filtered residual (P) vs. Filtered residual (FR)

The surface level air pressure shows strong correlation with the filtered residuals. In summer less so than in winter (0.63 and 0.88), nevertheless, a relatively strong correlation is seen throughout the year. The water level response lags pressure changes, on average, by 9.4 hours.

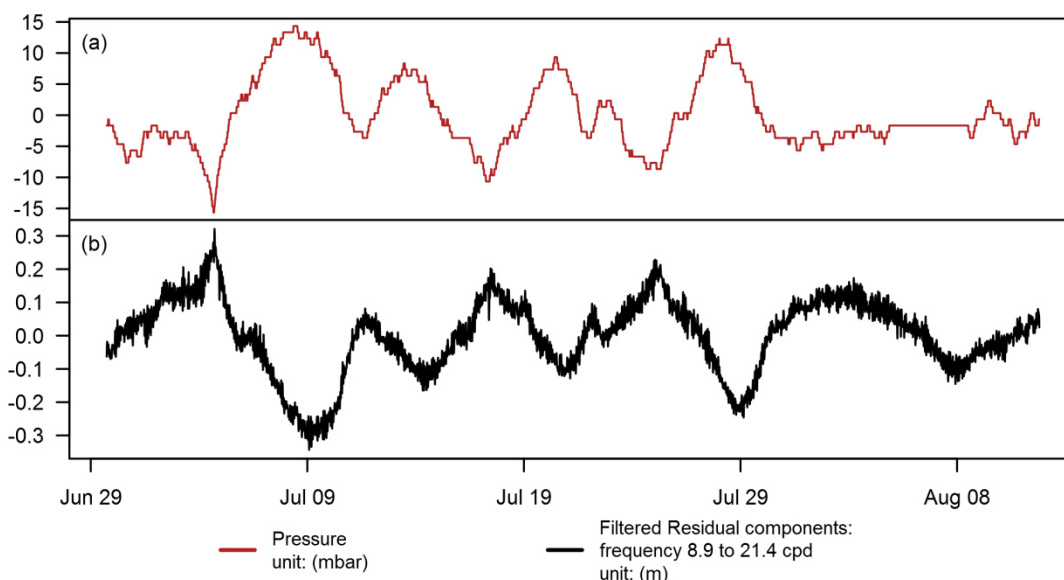


Figure 26: Pressure (a) and Filtered residuals (b) for data set No.3 (2014-06-29 to 2014-08-11)

To quantify the magnitude of the barometer effect as observed, simple linear regression analyses were performed on each of the data sets. An example of the data scatter and the estimated linear model is shown in **Figure 26** for data set No. 3.

Whereas theory suggests that a change in pressure of 1mbar would result in an inverse 1cm change in water level, the results of the linear regression analyses performed here suggests otherwise. The inverse barometer effect for data sets No.1, 2 and 3 were calculated as 1.3cm, 1.1cm and 1.7cm of surface elevation change respectively for each mbar deviation in pressure from the average. The barometer effect is thus observed as higher than expected.

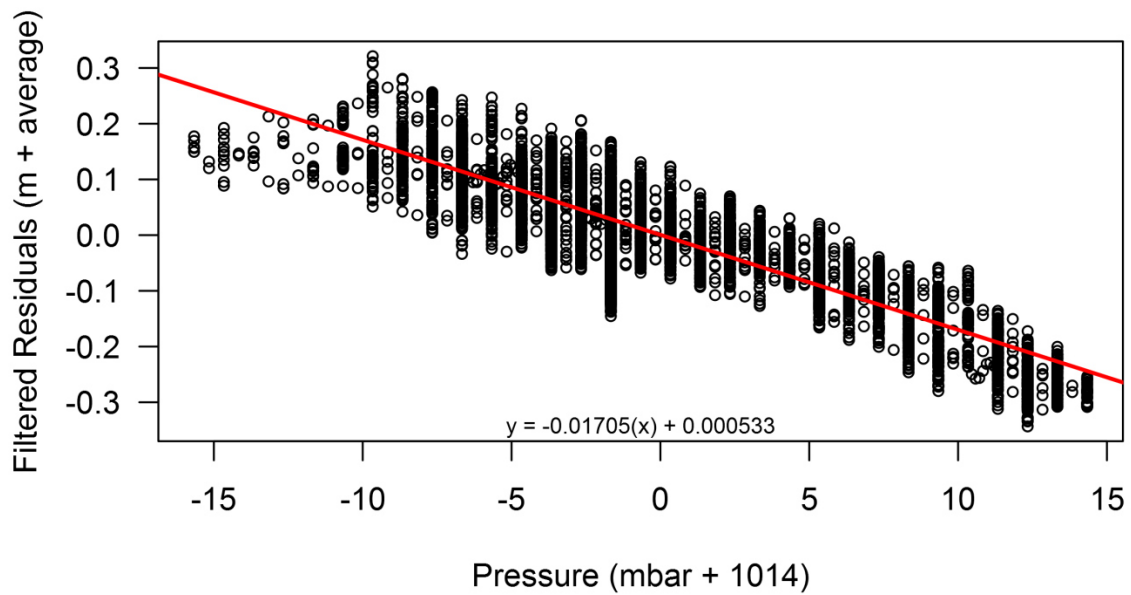


Figure 27: Scatter plot of filtered residual water levels against pressure at Saldanha Bay for data set No. 1

De Cuevas (1985) carried out a similar exercise for Lamberts Bay (approximately 140km north of Saldanha) and reported similar results. For example, De Cuavas' study also reported larger than isostatic predictions (i.e higher than the theoretical response) and ranging from 1.57 to 2.04 cm/mbar.

Returning to the regressions as estimated here, the linear models were applied to estimate (or model) the pressure induced components of the residuals for all 3 data sets. These estimated pressure component series were then subtracted from the filtered residual series to produce adjusted residual series. The adjusted residual series for the three data sets are shown in **Figure 28**.

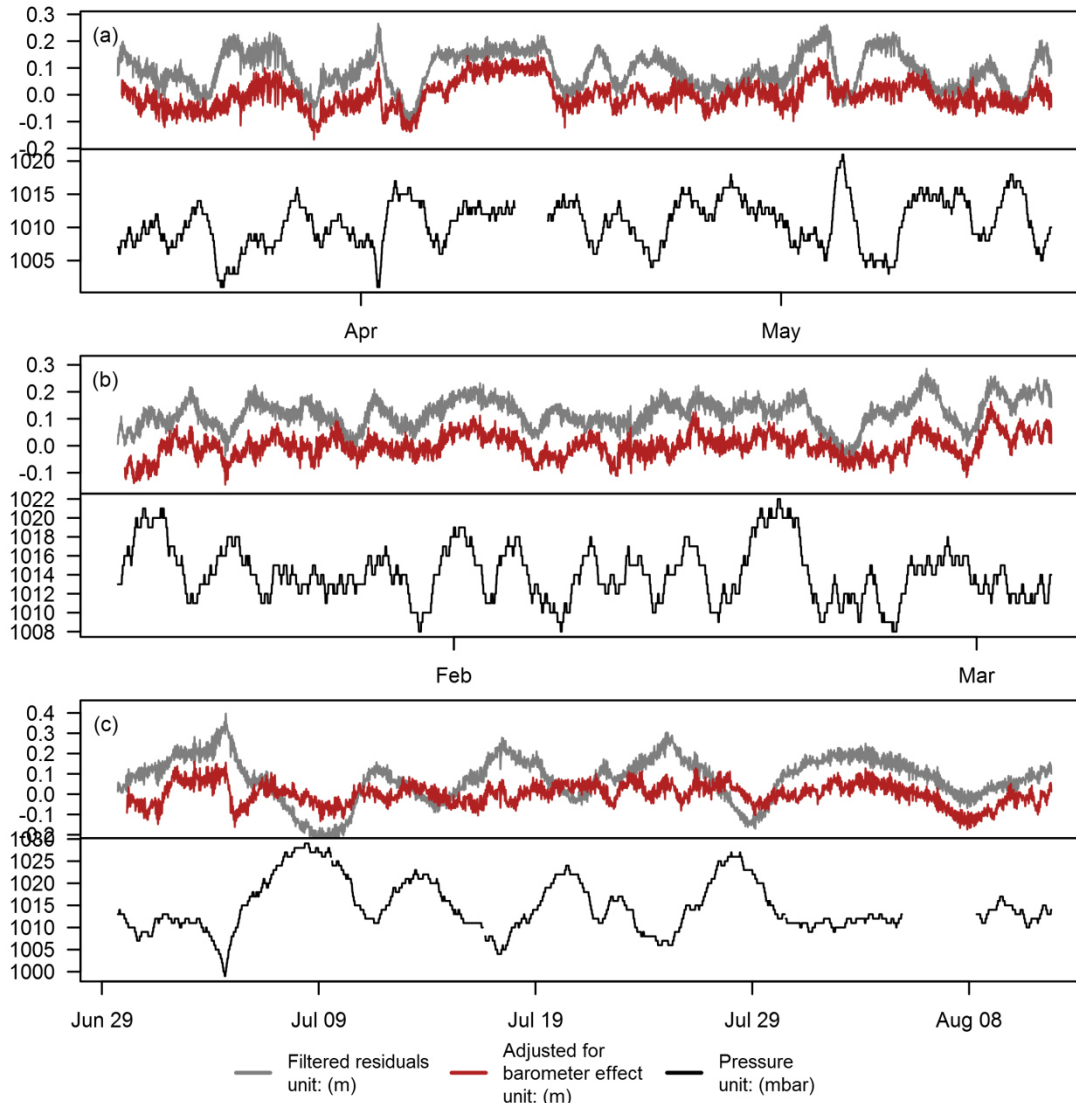


Figure 28: Comparison plots of Filtered residual water levels with and without adjustment for inverse barometer effect. (a) Data series No.1 (2014) (b) Data series No.2 (2010) (c) Data series No.3 (2014)

The adjusted residuals still showed significant fluctuations remaining, indicating, as expected, that only a portion (albeit a large portion) of the residuals are made up of pressure response components.

Subsequent iterations of cross-correlation analyses were performed on these adjusted residuals in an attempt to allocate the remaining fluctuations to wind:

(5) OSW vs. AFR

Correlations between the adjusted residuals and onshore winds proved weak and showed little consistency with the expected response for wind setup or set-down. Even after smoothing the data, correlations remained weak and inconsistent. It can therefore not be deduced, on the basis of the cross-

correlation tests performed here, that there exists any significant relationship between the levels of the adjusted residuals and onshore wind.

(6) LSW vs. AFR

Cross-correlation results for longshore wind and adjusted residuals yielded similar results to (5) above, but with even weaker and more inconsistent correlations. Similarly, here, there exists no significant relationship between longshore wind and the levels of the adjusted residual data sets.

Table 8: Results of cross correlation analysis

Test No.	Variables	Correlation (r)			Lag Time (hours)		
		(1)	(2)	(3)	(1)	(2)	(3)
1	T -FR	-0.42	+0.43	-0.55	10.2	-133	-67.7
2.1	OSW - FR _{wf}	-0.17	-0.12	-0.19	-199.0	139.8	-1.5
2.2	1 day run. mean	-0.38	+0.32	-0.50	-193.8	136	6.2
2.3	2 day run. mean	-0.50	+0.49	-0.64	-185.7	146.7	15.2
3.1	LSW - FR _{wf}	0.13	0.17	0.14	-177.7	86.2	193.5
3.2	2 day run. mean	0.38	0.42	0.44	-190.2	85.5	206.8
4	P - FR	-0.66	-0.59	-0.88	6.8	11.3	10.2
5	OSW - AFR	-0.26	-0.35	-0.36	6.0	13.0	8.0
5.1	2 day run. mean	-0.30	-0.47	-0.46	7.0	11.6	0.8
6	LSW -AFR	-0.29	+0.23	+0.25	55.5	31.3	29.8
6.1	2 day run. mean	-0.45	0.29	0.40	65.2	16.0	197.5

***All correlations listed are significant to at least 95%**

****A negative lag means that the independent variable lags the dependent variable**

T = Tidal height; FR = Filtered residuals; OSW = Onshore wind; FR_{wf} = Wind frequency component of filtered residuals; LSW = Longshore (cross shore) wind; P = Surface level pressure; AFR = Adjusted filtered residuals

3.6 DISCUSSION OF RESULTS

3.6.1 Component breakdown

From the results of the analyses performed, five components were identified as contributing to the residual water levels of the three selected data sets. The five components are:

- (1) Sampling errors
- (2) High frequency noise
- (3) Wind components
- (4) Pressure components
- (5) Dynamic effects

It was of interest to calculate and to summarise, for each of these components, its magnitude as well as its percentage contribution to the total residual water elevations. Only positive elevation components were considered.

(1) Sampling Errors – These were identified from the spectral analysis as the oscillations falling within the 11.4 to 13.1-hour period range and are caused by a phase shift in the measured water levels relative to the predicted tides. The heights that were measured in datasets no.1 and no.3 are fairly similar. The heights measured in data set no.2, however, is considerably higher. The reason for the higher heights measured in dataset no.2 is owing to the fact that astronomical tides reached heights near to the HAT during this period. The heights as determined for this component for the three selected data series are shown in **Table 9**. The contribution of this component to the total measured positive residuals is small and, on average, amounts to 8.4%.

Table 9: Summary of sampling error components in residual water levels at Saldanha Bay

Height (m)	AVERAGE	Data set No.1	Data set No.2	Data set No.3
Mean	15.8mm	12mm	25mm	10mm
Maximum	53.3mm	30mm	81mm	49mm
% of total	8.4%	7.2%	12.1%	6.0%

(2) High Frequency Noise – This component is made up of oscillations which, in the spectral analysis, were identified as noise having periods of less than 1 hour. It is expected that contained within this component of the observed residuals, are the effects of phenomena and actions including trapped waves,

wind waves, ship waves and edge waves. However, the sampling rate of the raw data did not allow for a more detailed breakdown so as to prove the occurrence of these phenomena as mentioned.

The contribution of the noise component is also small and on average, makes up 7.0% of the total positive height of the residual water levels in the three selected data series. A summary of the heights determined is shown in **Table 10**.

Table 10: Summary of high frequency noise components in residual water levels at Saldanha Bay

Height (m)	AVERAGE	Data set No.1	Data set No.2	Data set No.3
Mean	11.0mm	10mm	10mm	13mm
Maximum	81.7mm	71mm	82mm	92mm
% of total	7.0%	7.0%	5.5%	8.6%

(3) Wind Components – The correlation analysis showed that the regularly present oscillations of the 8.9-21.4 cpd frequency range, as identified in the spectral analysis, are somewhat linked to onshore wind. However, correlations were relatively weak and could only be reasonably confirmed after the data had been smoothed to 2 day moving averages (reasonable confirmation was not possible on the raw data). It is therefore deduced that merely a portion of this data component can be related to wind setup and that an unknown portion still represents higher frequency noise. It can also be assumed that some unknown portion of actual wind generated oscillations is missing from this output.

Although the above discussion suggests that only a portion of the data in this frequency may be confirmed as wind components, it was not possible, within the constraints of this study, to resolve the matter any further. Therefore, the assumption was made, for quantification purposes, that the dataset under consideration here, is consisting entirely of wind setup.

Table 11 below shows a summary of the heights as determined. The heights are small and make up, on average, but 6.4% of the total observed positive residual water levels for the three selected data series. Note that the 95th and 99th percentile maximum heights are also given in the table. The reason for including both these parameters is the fact that the wind component output series is rapidly varying. Also the significant departure of the absolute maximum values from the means suggest that the data is skewed. There is also the possibility that noise, which is thought to be present in the output series, could be the cause of spikes which are skewing the data. The 95th and 99th percentile maximum heights are thus considered more suitable parameters for presenting the maximum wind setups. From the analyses that have been performed thus far, it is not possible to know exactly how much the maximum heights are skewed by noise. Therefore, providing both the 95th and 99th percentile maximum values makes

provision for two scenarios; one assuming a greater degree of distortion of the maximum values due to noise than the other.

Table 11: Summary of wind components in residual water levels at Saldanha Bay

Height (m)	AVERAGE	Data set No.1	Data set No.2	Data set No.3
Mean	<i>10mm</i>	9mm	9mm	11mm
95th percentile max.	<i>25mm</i>	24mm	23mm	28mm
99th percentile max.	<i>34mm</i>	32mm	31mm	38mm
Maximum	<i>56mm</i>	52mm	64mm	53mm
% of total	<i>6.4%</i>	6.6%	5.3%	7.4%

(4) Pressure Components – A strong correlation was found between measured surface level pressure and residual water levels. Based on the strongest respective correlation for each of the three data series, linear regression was used to estimate the pressure components. The pressure components heights are relatively large and make up, on average, 24.8% of the total observed positive residuals.

Table 12: Summary of pressure components in residual water levels at Saldanha Bay

Height (m)	AVERAGE	Data set No.1	Data set No.2	Data set No.3
Mean	46.7mm	42mm	34mm	64mm
Maximum	161.7mm	126mm	91mm	268mm
% of total	24.8%	25.3%	17.7%	31.3%

(5) Dynamic Effects – For the previous two components, as discussed above, it was possible to link the outputs directly to the locally measured wind and pressure. In other words, a direct correlation could be drawn, in a direct or inverse proportion, between the water levels and weather data that was recorded within close proximity of the water level measurements. These components are thus categorised as static effects and for continuity, will be referred to as static effects for the remainder of this study. However, there still remains a relatively large portion of the water level residuals to which no direct correlation could be drawn with the available weather data. In trying to correctly allocate these large remaining components the following should be considered:

- Storm surge is known to behave dynamically with respect to complex response to varying water depths (Gonnert et al. 2001)
- The weather data measurements available for this study (the wind data in particular) is data that was measured locally, i.e. measured within close proximity of the location where the water levels were measured. It is common for wind measured at coastal stations to be influenced by

local effects. In other words, the magnitude and/or direction of winds are influenced by sea breezes, topography, buildings, vegetation etc.

- Since storm surge can propagate along a continental shelf (Sebastian et al. 2014) the wind measured locally may not be representative of the distant wind which may have forced propagating surge towards Saldanha Bay.
- Second order storm surge effects may result from the interaction between storm surge and tides (Bretschneider 1967).

At this stage it has to be accepted that within the limitations of the available data, the large unknown components cannot be linked to storm surge with any certainty. However, the possibility still exists that these components are in fact linked to storm surge dynamically in one or more ways as discussed in the bullet points above. At this stage it is hypothesised that these components may be better resolved in the numerical models that follow in a later chapter. In the absence of a better definition, these large components are labelled “dynamic effects components”. For continuity, these components will be referred to as dynamic effects components throughout the remainder of this thesis.

As mentioned, the heights of these dynamic effects components are relatively large and make up 53.4% of the total positive residual heights. **Table 13** provides a more detailed summary of the heights of these components.

Table 13: Summary of dynamic effects components in residual water levels at Saldanha Bay

Height (m)	AVERAGE	Data set No.1	Data set No.2	Data set No.3
Mean	100.0mm	94mm	121mm	85mm
Maximum	227.7mm	222mm	264mm	197mm
% of total	53.4%	53.9%	59.4%	46.8%

3.6.2 Summary of Residual Components: Saldanha Bay

Table 14 shows a summary of the component make-up for the three selected sets of residual water level data.

Table 14: Summary of percentage contributions from storm surge components. Saldanha Bay

Component	AVERAGE	Data set No.1	Data set No.2	Data set No.3
Sampling Errors	8.4%	7.2%	12.1%	6.0%
High Frequency Noise	7.0%	7.0%	5.5%	8.6%
Wind Set-up	6.4%	6.6%	5.3%	7.4%
Pressure Effects	24.8%	25.3%	17.7%	31.3%
Dynamic Effects	53.4%	53.9%	59.4%	46.8%

A series of plots were produced that serve to illustrate, visually, the findings of the time series analysis. **Figure 29**, **Figure 30** and **Figure 31** are summary plots of the component make-up for data series No.1, 2 and 3 respectively.

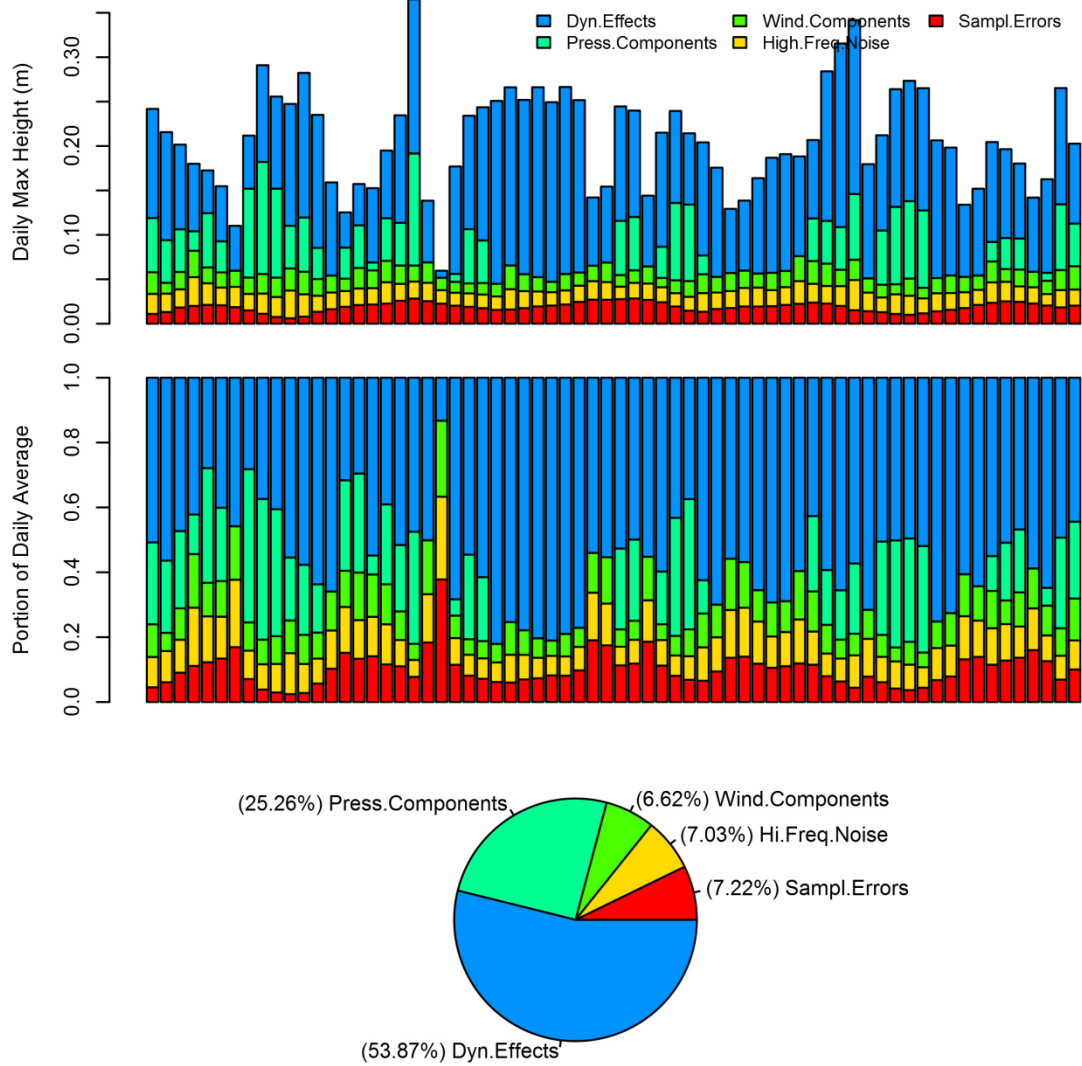


Figure 29: Summary plot of storm surge components in Saldanha Bay data series No. 1

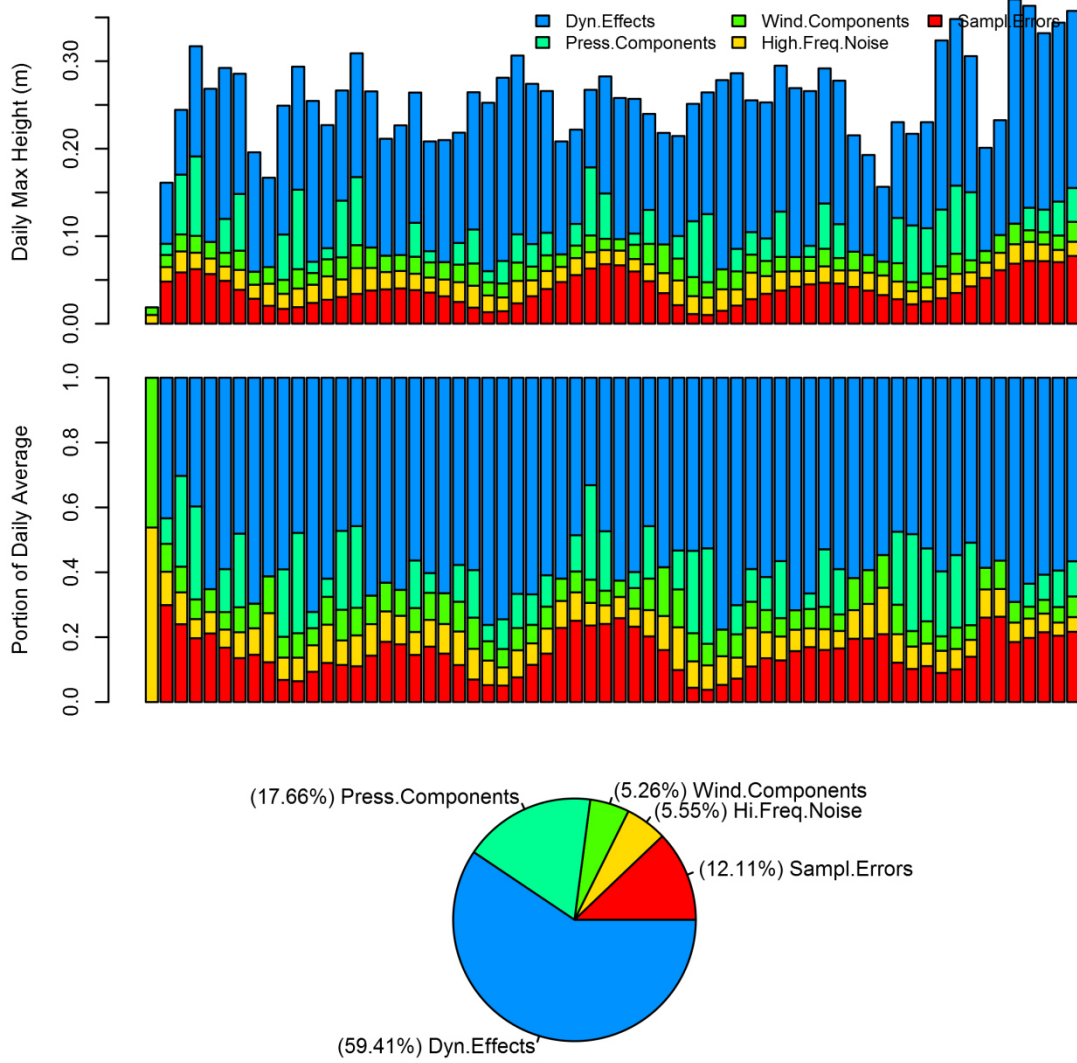


Figure 30: Summary plot of storm surge components in Saldanha Bay data series No. 2

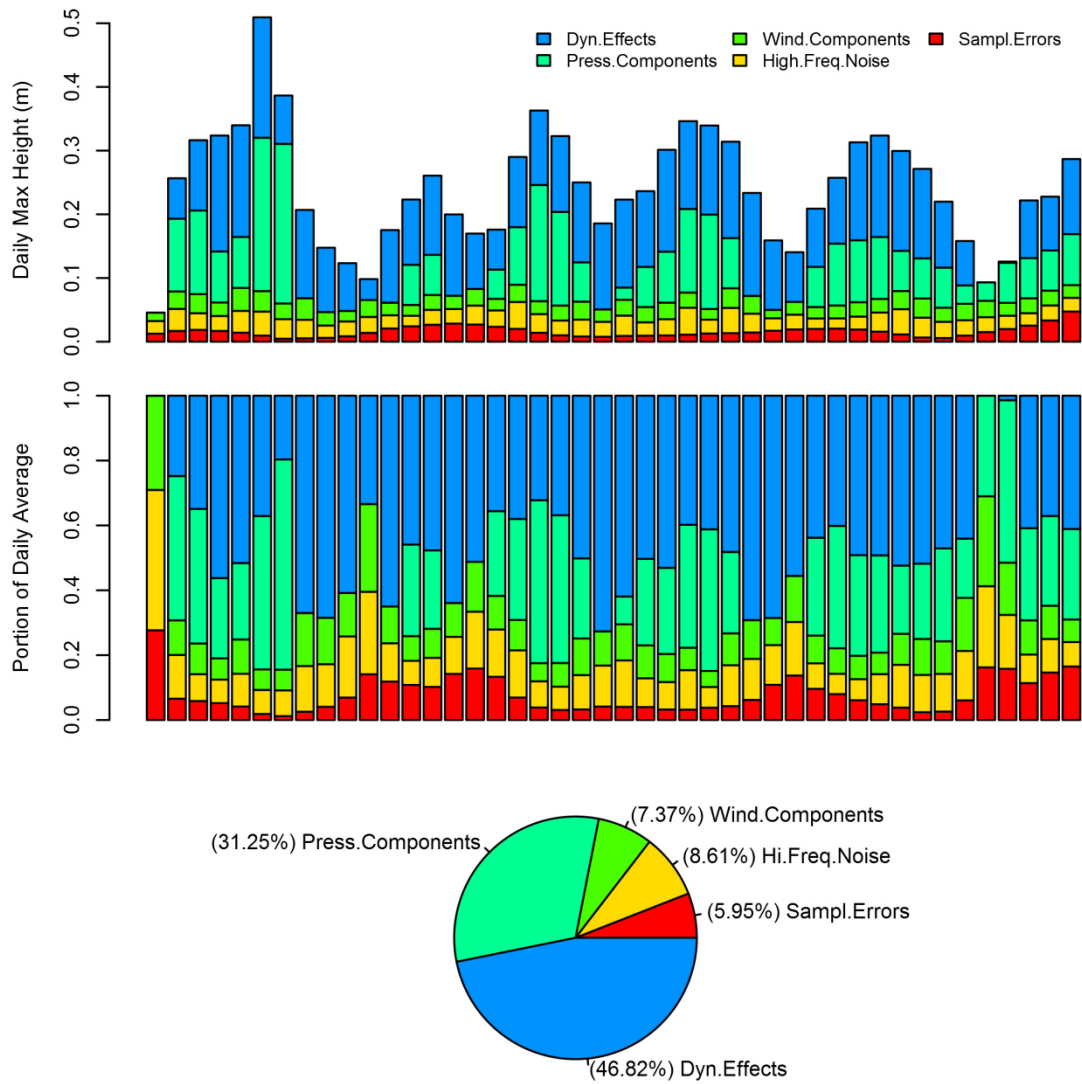


Figure 31: Summary plot of storm surge components in Saldanha Bay data series No. 3

In section 3.2.5, where the available data was scrutinised for quality control purposes it was noted that there appears to be a possible datum shift error in the measured water level data. The remark was made then that this datum shift error may possibly result in erroneous, predominately positive residuals. If this be the case, then it would imply that the magnitude of the dynamic effects component is exaggerated, because the dynamic effects component is calculated as the total residual minus all other known components.

At this point in time, although it is not ideal, it may be accepted that the magnitude of the dynamic effects contains the error of the datum shift in the water level data. The objective of the study is to quantify storm surge components and until this dynamic effects component can be proven to relate to storm surge, the exact accuracy to which its magnitude is determined is not critical. It is comforting to know, at least, that the magnitudes of the other set of components, the static components, are not affected by the possible datum shift.

3.6.3 Storm Surge: Saldanha Bay

Of the five components of residual water levels identified and discussed in this chapter, the high frequency noise and the sampling error components are considered as **not** contributing to storm surge. The remaining three components as discussed (static wind and pressure effects and dynamic effects) are considered to make up the **total storm surge** contribution within the measured data.

Figure 32 shows plots of the total determined storm surge levels for the three selected data sets. Sampling errors- and noise-components had been removed from these data plots.

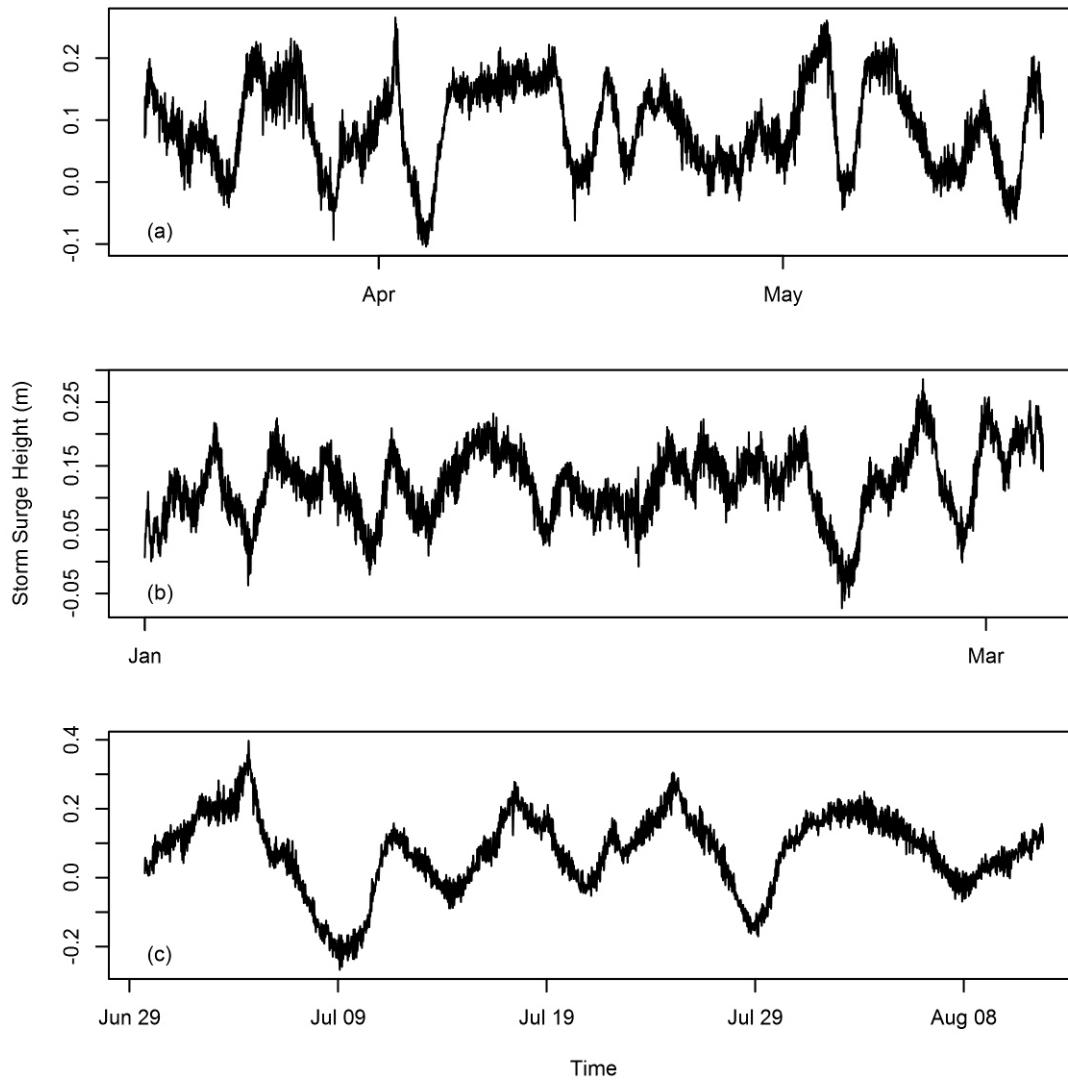


Figure 32: Total storm surge components at Saldanha Bay for (a) Data series no.1 (b) No.2 and (c)No. 3 as determined in the time series analysis

CHAPTER 4

4 Extreme Water Levels Based on NCEP Data

4.1 GENERAL

In the previous chapter, analyses of water levels were performed on relatively short-duration data sets. While it was useful for breaking the residual water levels down to its various components, 5 years' worth of data is hardly sufficient for determining extreme surge estimates or trends.

Later (Section 4.3), the focus will be on determining extreme values for storm surges. For such purposes, there is a need for data of longer duration in order to better estimate extreme values. One such data set that was considered extensively is the data as obtained from the NCEP/DOE Reanalysis II project.

The NCEP/DOE Reanalysis II project is the successor of the NCEP/NCAR Reanalysis project commonly used in earlier years. Both these projects are collaboration projects by the US National Centre for Environmental Protection and National Centre for Atmospheric research. Essentially, the Reanalysis projects provide data sets of various atmospheric parameters, at grid points across the globe, which have been reproduced and modelled from past data. Data sets date back to 1979 and are given at time intervals of 6 hours on a global grid of 2.5 degrees by 2.5 degrees. Data is also given at different atmospheric levels i.e at different elevations (NOAA 2016). For the remainder of this study the Reanalysis II data will simply be referred to as the NCEP data.

Of interest for this study, were the wind velocity and pressure data sets given at 10m above mean sea level – both of which are included in the NCEP database. Data was obtained from NOAA's web page in NetCDF format. The R packages "ncdf" and "RNetCDF" were used to convert the encrypted data to formats which could be read in the MIKE Zero software interface (R Core Team 2016).

NCEP data was first validated against measured data. It was subsequently used as input to the numerical models for the purposes of determining extreme storm surge heights.

4.2 VALIDATION OF NCEP DATA

4.2.1 Validation of NCEP Wind Data

In order to validate and to assess the quality of the NCEP data, cross correlation analyses were performed (according to the same methodology used in Section 3.5) between samples of NCEP data and measured data. The entire length of the available measured wind and pressure data sets (2010 – 2015) was compared to an equivalent NCEP data set spanning the same period. For validation of the wind data set specifically, the measured data was also visually compared with the NCEP data for correlation with wind direction. This was done by means of wind roses.

At Saldanha Bay, the 2 nearest grid points of available NCEP data is (1) at -33.333S 16.875E which is 100km out to sea from the port and (2) at -33.333S 18.750E which is 80km inland from the port. It was found after looking at the data from both these grid points in some detail, that the data from grid point number (1) resembled the measured data more closely. The data from grid point 1 was thus selected for further use.

Figure 33 shows a plot of the NCEP wind speed data verses the measured wind speeds.

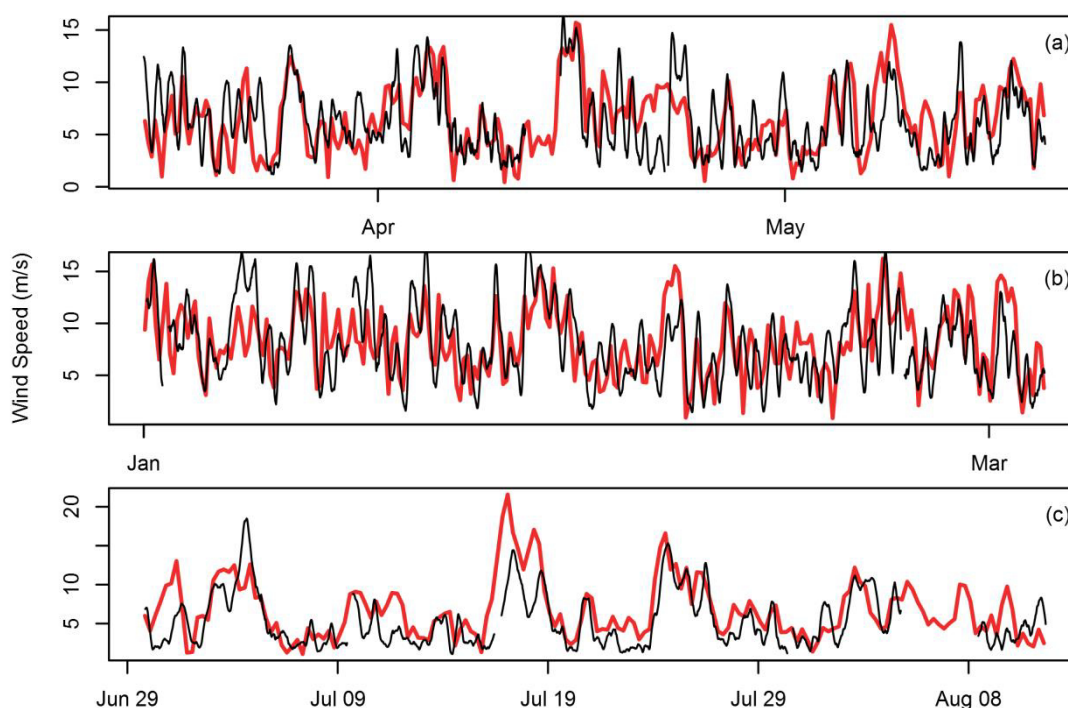


Figure 33: NCEP (Red) and measured (Black) wind speed at Saldanha Bay. (a) Data set No.1 (b) No.2 (c) No.3

The results of a cross correlation analyses show a fairly strong correlation between measured wind speed and modelled (NCEP) **wind speed**. The calculated correlation coefficient is 0.59 for 6 hourly data and improves to 0.7 for 1-day averaged data. The average lag is less than 6 hours.

For **wind direction**, on the other hand, the visual correlation showed poor results. There is a significant difference between the dominant wind direction of the NCEP data and that of the measured data. The dominant wind measured in Saldanha Bay is from a south to southwesterly direction (over the 5 years of available measured data). The reanalyses data, however, shows the dominant wind direction as southwest and shows a strong component from a northeasterly direction whereas north east winds were rarely measured in Saldanha Bay. **Figure 34** and **Figure 35** show the wind rose plots for the measured wind and the NCEP wind data sets respectively.

It was concluded that the NCEP data represents the trends in **wind speed** in Saldanha Bay reasonably accurately, but that the **wind direction** is not represented to an acceptable level of accuracy.

However, the **NCEP wind data was not rejected**. Despite the wind direction not accurately matching that of the measured data, it was decided to nevertheless still make use of this data for subsequent analyses. This was done, bearing in mind that the intention of the numerical models (later) and moreover the intention of this study, as a whole, is not merely to compute realistic water levels in Saldanha Bay, but also, and especially, to be able to comment on storm surge components along the South African coast in general. Should the NCEP data be used as input to the computations which follow in subsequent chapters, it would not necessarily be a realistic portrayal of the storm surges with respect to spatial aspects (i.e the exact position within the bay where maximum water heights would occur), but in terms of magnitude and frequency of occurrence of extreme events, the results may be acceptable.

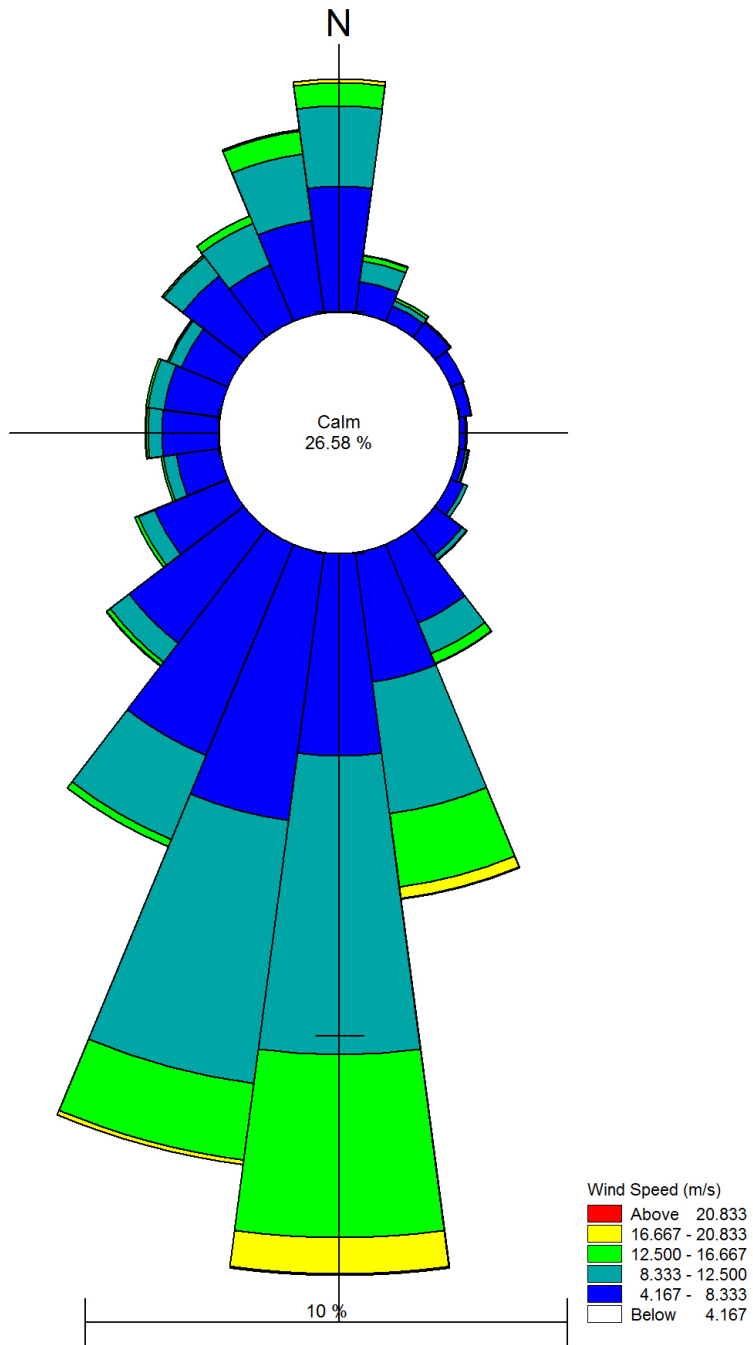


Figure 34: Rose Plot of measured wind (20 minute average at 10 aMSL) for the full duration of measured data (from Jan 2010 to Jan 2015)

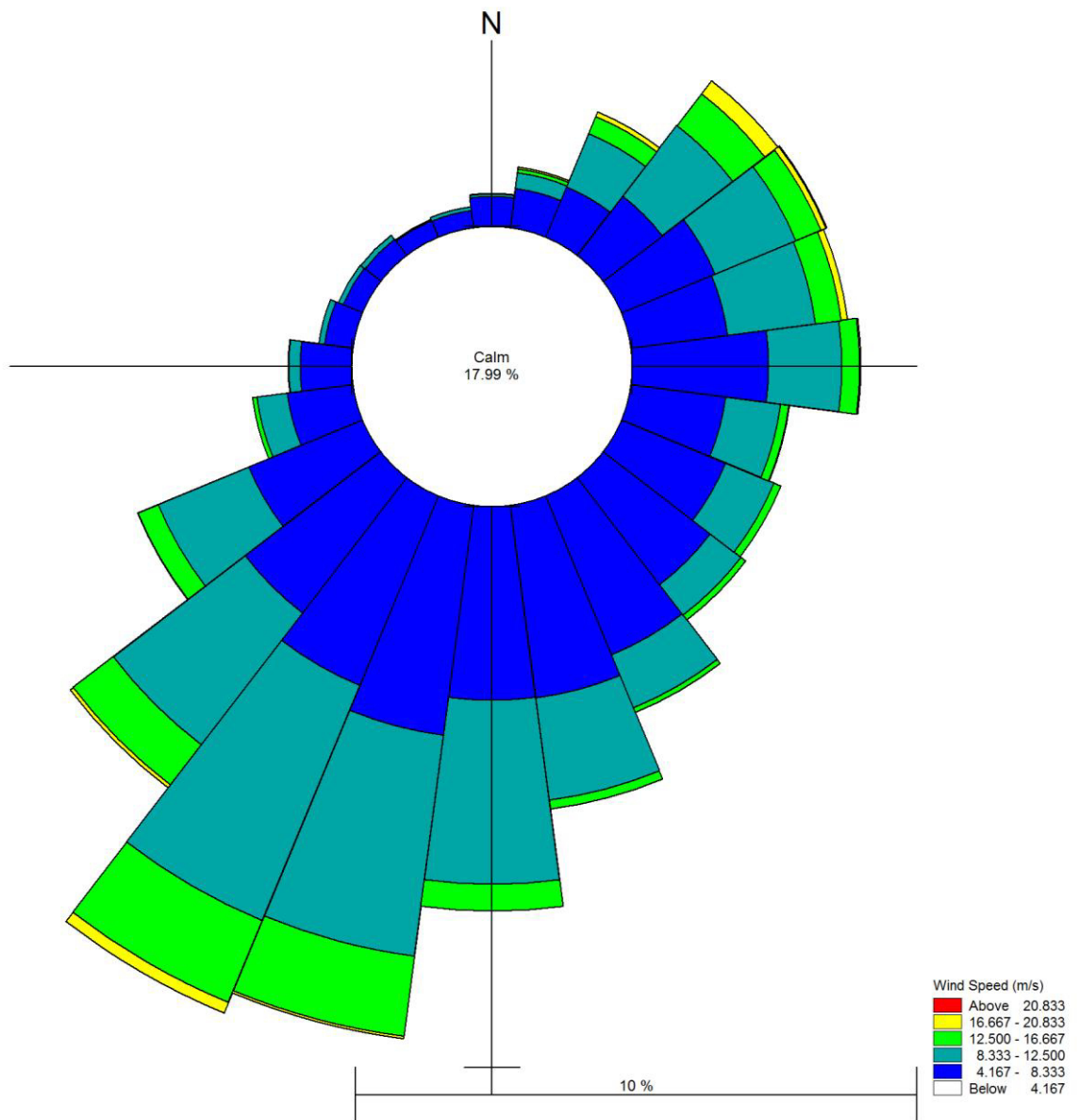


Figure 35: Rose Plot of NCEP wind (6 hour average at 10 aMSL). Data subset is from Jan 2010 to Jan 2015

4.2.2 Validation of NCEP Pressure Data

As for pressure, the NCEP data sets are an almost exact match of the measured data. Visual comparisons showed satisfactory results from which to conclude the validation of the NCEP pressure data without the need for further validation analysis through cross correlation. **Figure 36** below shows a plot of the NCEP and measured pressure data for the three selected data sets and **Figure 37** shows the same data over the entire time span of the measure data (2010 to 2015).

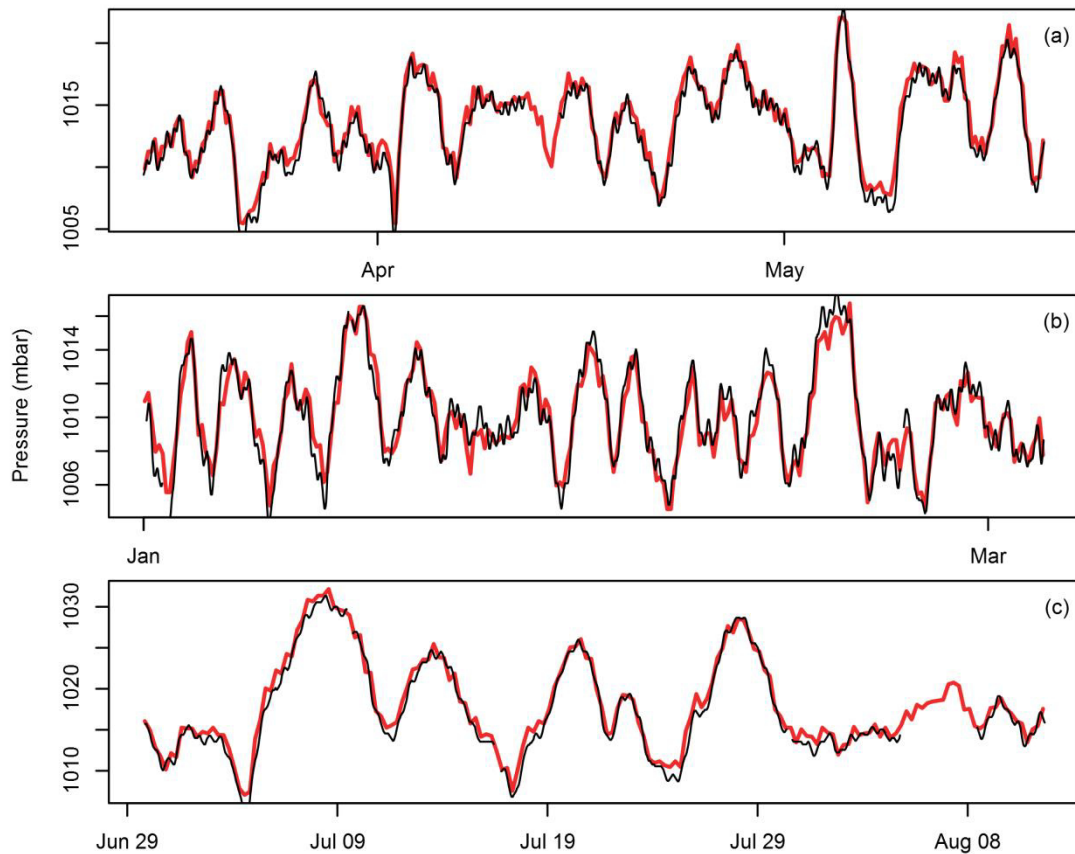


Figure 36: Visual comparison of NCEP pressure data (red) vs measured pressure data (black) for (a) Data set No.1, (b) Data set No. 2 and (c) Data set No. 3.

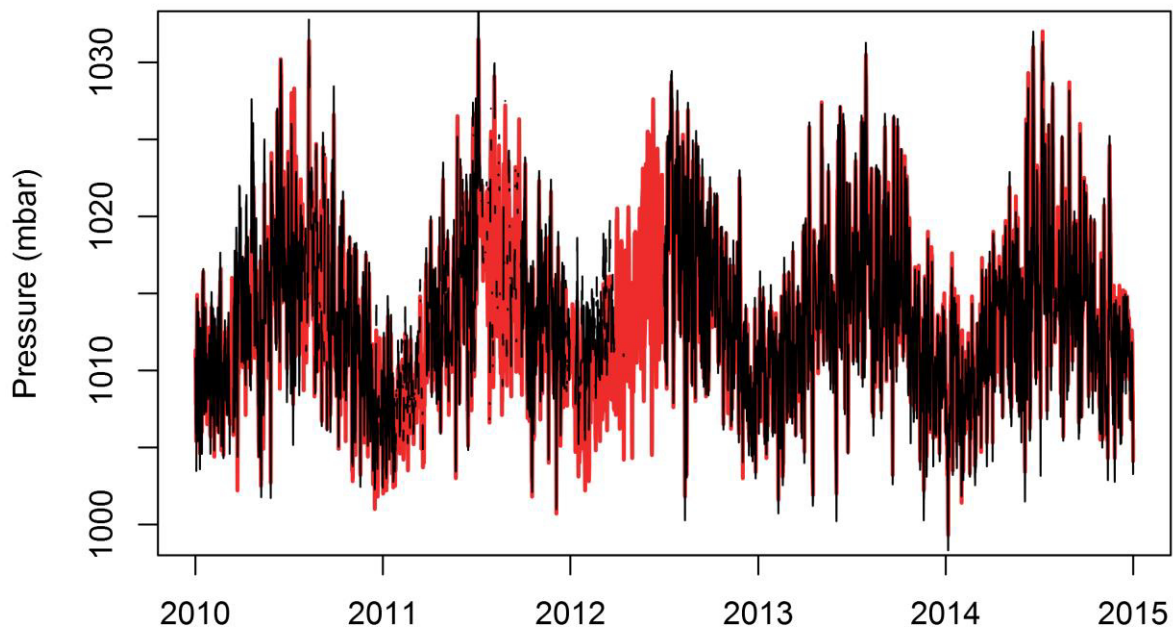


Figure 37: Visual comparison of NCEP pressure data (red) vs measured pressure data (black) for data spanning Jan 2010 to Jan 2015

4.3 EXTREME VALUE ANALYSIS OF NCEP DATA

An extreme value analysis was performed on the full set of available NCEP data for wind and pressure. From the analysis, it is possible to allocate extreme wind and pressure values to selected return periods.

4.3.1 EVA Theory and methodology

The extreme value analysis was done by the use of the EVA toolbox on the MIKE zero software developed by DHI. The statistical theory used in this toolkit is described in some detail in the software support documentation (DHI, 2013). The key statistical considerations are highlighted here:

- An annual maximum series (AMS) is extracted from the available 36 years of available NCEP data. The AMS contains one value for each year, with each value representing the maximum value on record for that particular year. The remainder of the EVA analysis is done on this AMS only.
- A theoretical probability distribution is fitted to the AMS – A Weibull and a Generalized extreme value distribution was fitted to the wind AMS and pressure AMS respectively.
- A Method of Moments (MOM) approach was taken to best estimate the parameters of the probability distributions.
- Probability plots with return periods were generated.

4.3.2 Results

Positive wind speeds in all directions were considered for the analysis. The results of the analysis may be seen in **Figure 38** and **Table 15**

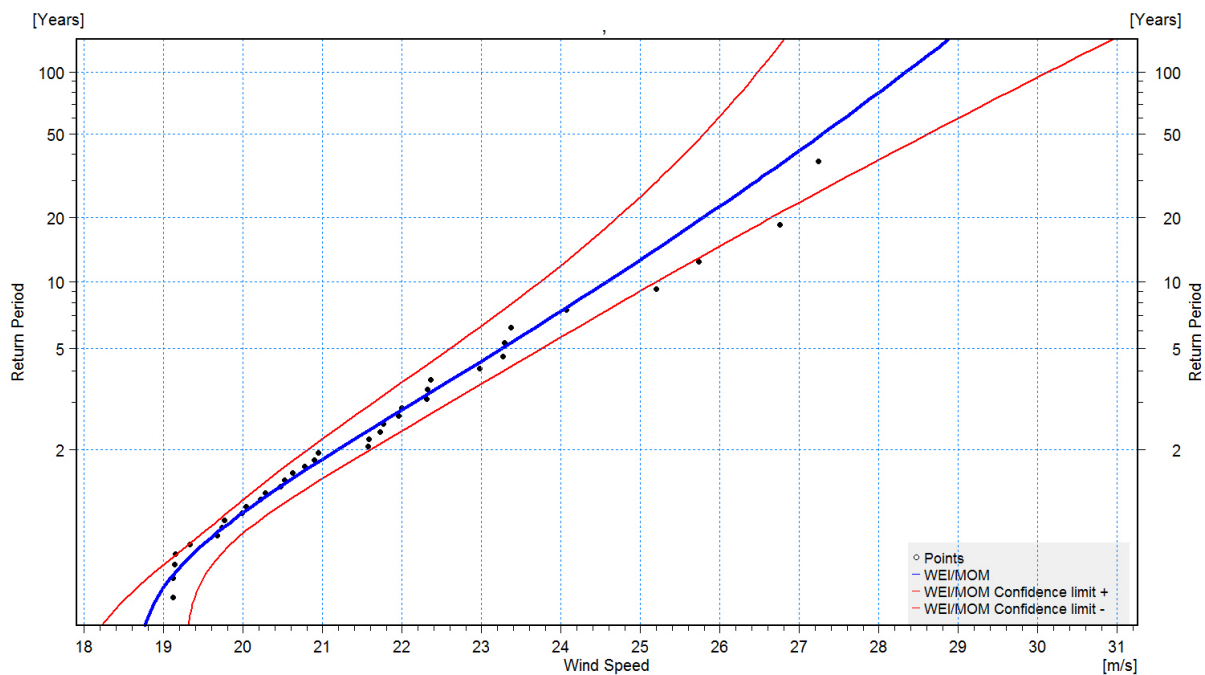


Figure 38: Probability plot for Extreme Value analysis of NCEP Wind speeds

Table 15: Tabulated results of Extreme Value Analysis of NCEP Wind speeds (in m/s)

Return Period (T)	Lower 95% confidence limit	Upper 95% confidence limit	Best Estimate
2	20.81	21.6	21.20
5	22.60	23.75	23.25
10	23.67	25.2	24.49
20	24.66	26.63	25.80
50	25.69	28.61	27.24
100	26.42	30.06	28.27

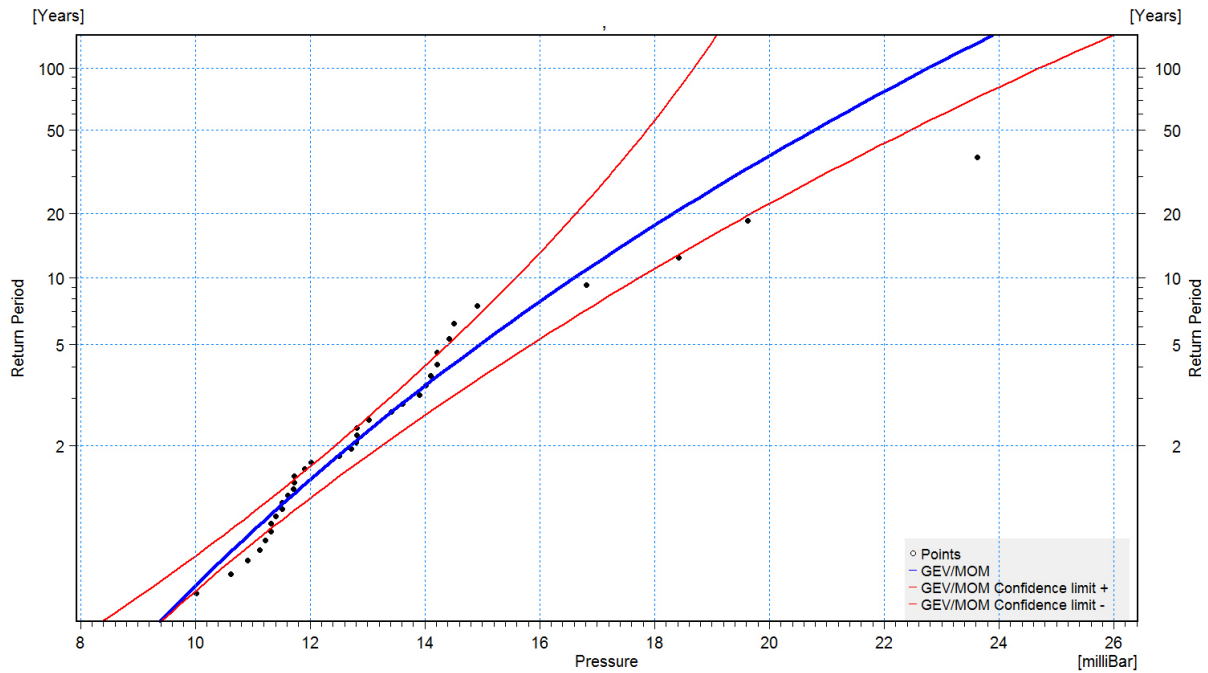


Figure 39: Probability plot for Extreme Value analysis of NCEP Pressure data

For the pressure data, the annual minimum values were of interest rather than the annual maximum as positive storm surge is brought about by a drop in pressure from normal and not a rise. In this case, therefore, the input time series was manipulated so that the values as indicated on the graph (**Figure 39: Probability plot for Extreme Value analysis of NCEP Pressure data**) are not the actual extreme value pressure estimates, but rather the negative deviation from the mean of the input data set. The mean of the input data set was calculated as 1013.53 mbar. Therefore, for example, a reading on the graph of, say, 16mbar, must be interpreted as 997.53mbar ($1013.53 - 16 = 997.53$).

Table 16: Tabulated results of Extreme Value Analysis of NCEP Pressure data (in mbar). Values are as read off from the probability plot (followed by actual corrected values in brackets)

Return Period (T)	Lower 95% confidence limit	Upper 95% confidence limit	Best Estimate
2	12.44 (1001.09)	13.24 (1000.29)	12.7 (1000.83)
5	14.4 (999.13)	15.85 (997.68)	14.95 (998.58)
10	15.59 (997.94)	17.82 (995.71)	16.61 (996.92)
20	16.63 (996.9)	19.72 (993.81)	18.33 (995.2)
50	17.86 (995.67)	22.45 (991.08)	20.77 (992.76)
100	18.64 (994.89)	24.66 (988.87)	22.68 (990.85)

CHAPTER 5

5 Analytical Computations of Storm Surge

5.1 GENERAL

Here, the formulae, as discussed in the literature review, are used to analytically calculate the wind setup and pressure components of storm surge. The analytical methods are expected to give simplified solutions, especially for the calculation of wind setup where neither bottom- nor surface friction coefficients are accurately known. Moreover, insufficient field data is available from which to determine these friction coefficients correctly. However, the results are expected to give a good order of magnitude estimate which would later be compared with the results from the time series analysis and the numerical modelling.

In the literature review it became clear that the calculation of wind setup is known to be a complex procedure and is thus mostly solved through numerical modelling. It was seen, also, that the majority of popular texts would either provide only the basic differential equation (without providing a solution) or, alternatively, an analytical formula that is only applicable to enclosed rectangular basins of constant water depth. However, Kamphuis (2000) gives a handy method by which to approximate wind setup at an open coast and varying water depth. This method makes use of a variation of the basic differential equation

$$\frac{dS}{dx} = \frac{k(V \cdot \cos \varphi)^2}{gD} \quad (17)$$

Where:

S is wind setup height

k is a constant (takes into account surface stresses).

V is the wind velocity at 10m above mean seal level.

φ is wind angle (deviation from normal to the shoreline).

D is the water depth calculated as $D = d + S$. Where d is the still water depth and S is the wind setup as calculated at the end of the previous dx increment. d is assumed constant along each dx increment

In Kamphuis' equation (17), the surface stress parameters of the original differential equation are being accounted for by the dimensionless constant, k , multiplied by wind speed. Kamphuis recommends

solving for wind setup, S , incrementally at intervals of length, dx . The depth at the end of the first increment is assumed $D = d + S$. This value of D is then used to calculate S for the next section and so forth. An example of the application of this method was introduced in Chapter 2.

Another suitable equation that may be used is from one of the older studies by Bretschneider (1967). Here, a solution to the differential equation has been approximated for the special case of an open coastline and where the sea bed has a constant slope.

$$S = \frac{kV^2F \cos \varphi}{g[D_0 - D_c - S]} \ln \frac{D_0}{(D_c + S)} \quad (18)$$

Where:

F is the total fetch along which wind setup is generated.

D_c is the depth near the coastline.

D_0 is the depth some distance, F , offshore from the position of D_c .

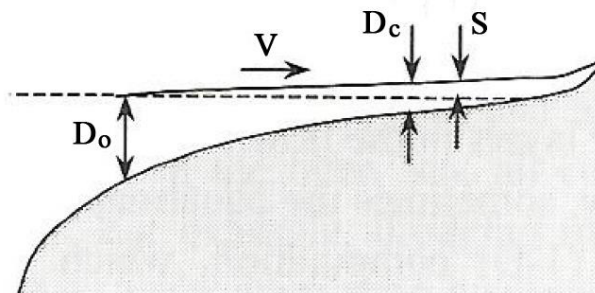


Figure 40: Schematic of wind setup parameters for the open coast

The main difference between Equations (17) and (18) is that (18), Bretschneider's equation, assumes a constant slope between two points whereas (17) takes into account the changing slope of the seabed. It is expected therefore, that Equation (17) would yield more accurate results. Nevertheless, both of the equations as discussed above were used for the calculation of wind setup.

Bretschneider, in his formulation of Equation (18), warns that the approximation is best suited for gently sloping continental shelves. The bathymetry of Saldanha Bay, as applicable in some of the calculations considered here, is fairly steep in places. Therefore, it was uncertain, from the start, whether Equation (18) would yield satisfactory results – an interesting experiment none the less.

5.2 CALCULATION OF WIND SETUP

First, it was necessary to select appropriate **wind velocities** and **test positions** which would be used in calculations. The selection of these parameters was made based on the requirement to obtain results that are most suitable for comparison with results from the time series as well from numerical models. It was necessary to identify lines along which setup would be calculated, the average slope of the seabed along these lines, and the start- and end-depths on the aforementioned slopes. In the case of Equation (17), a detailed long section of the bathymetry was required along those lines as mentioned above.

5.2.1 Selecting Suitable Test Positions for Calculating Wind Setup

Wind set-up components were calculated analytically at 3 points within the Saldanha Bay, corresponding roughly with points that were selected for the outputs of the numerical model in a subsequent chapter. Additional to the 3 points that were selected for analysis, multiple fetch orientations were selected based on prevailing wind speeds so as to make up 5 scenarios as shown on **Figure 41**.



Figure 41: Test scenarios for analytical wind setup calculations

Table 17 corresponds to the figure above and shows a summary of the test positions that were selected. The table also includes all of the parameters needed for application of Equation (18) including start depths, end depths and fetch lengths. For the application of Equation (17), detailed longitudinal sections were extracted from TNPA's bathymetry data. **Figure 42** shows an overview of the bathymetry profiles that were extracted.

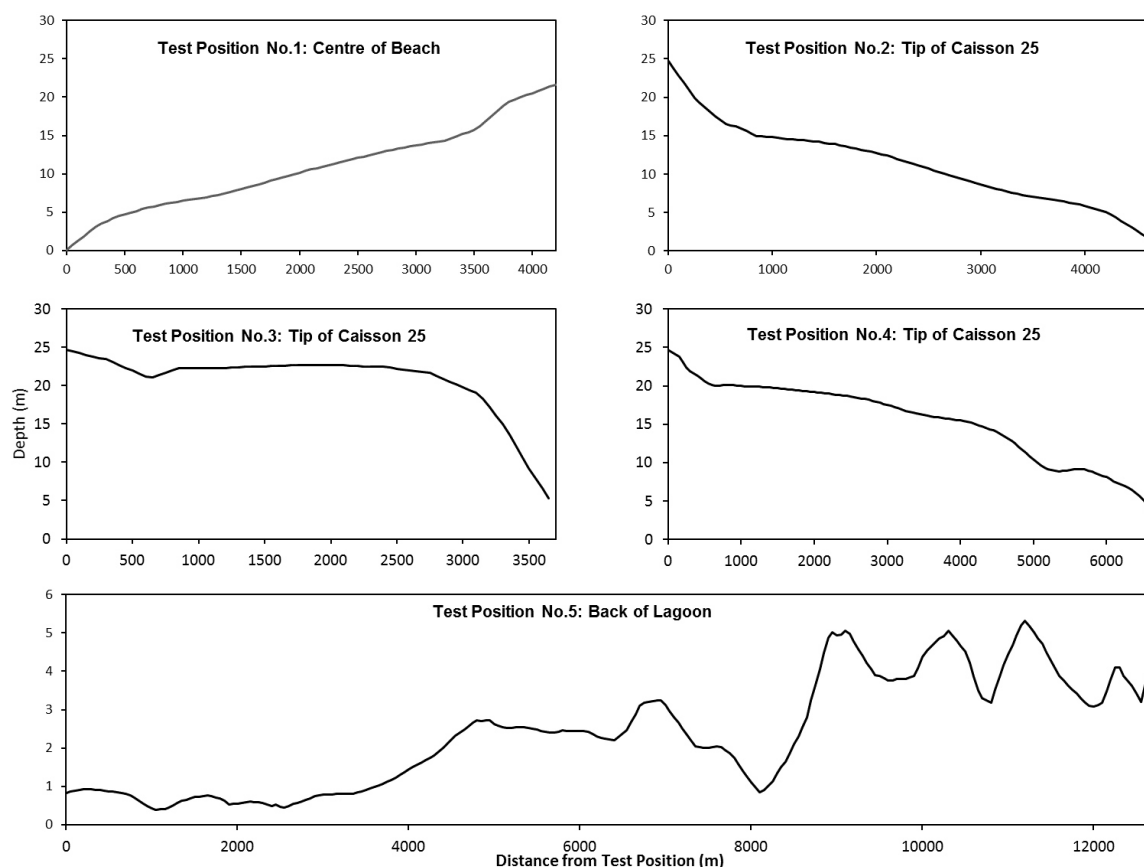


Figure 42: Bathymetry cross sections for test lines used in analytical calculations

Table 17: Description of test point positions selected for analytical wind setup calculations

Scenario No.	Description	*Wind direction	Fetch length (Approx.)	Offshore depth	In-shore depth
1	Centre of beach: Kleinbaai	SSE	4.2 km	21.5 m	1.5 m
2	Tip of Caisson 25	NW	4.7 km	2.5 m	19.5 m
3	Tip of Caisson 25	S	3.7 km	15.5 m	25.5 m
4	Tip of Caisson 25	SE	6.7 km	8.0 m	24.0 m
5	Langebaan lagoon	NW	12.7 km	4.0 m	0.25 m

**The direction is selected based on the longest possible fetch*

5.2.2 Selecting Wind Velocities for use in calculations

For each of the two equations used, two sets of calculations were done – one using the short data subsets and another using a long duration data set.

In the first set, wind velocities were selected from short data subsets corresponding exactly to that of data sets 1 to 3 as defined in Section 3.3. Each of the three data subsets were analysed for the maximum (20min average) wind velocities in various wind directions. From these maximum wind speeds, a selection was made (based on wind direction) of values to be used as input parameters in calculating wind setup for each of the 5 test scenarios. These computations of wind setup, because they are calculated at similar positions, may be used as order of magnitude tests for the results of the numerical models performed in Chapter 6 .

The selected maximum wind speeds, as determined for the short data sets (Data sets 1 to 3), are summarised in **Table 18**.

Table 18: Wind speed in m/s. Wind speeds are maximum measured wind speeds (20min average at 10m) for data sets 1 to 3.

DIRECTION	DAT SET	No.1	No.2	No.3
N		14.93	13.9	19.76
NE		11.6	9.3	8.63
E		12.59	6.8	6.66
SE		13.79	19.9	10.35
S		18.72	19.7	19.86
SW		16.97	11.6	14.17
W		13.6	11.5	13.28
NW		12.43	12.2	16.02

The wind speeds selected for the second set of calculations are from the extreme value wind speeds as determined from the NCEP data (refer to Section 4.3). Wind speeds were selected at different return periods. These extreme wind speeds were then used in calculations to determine long term predicted maximum wind setup heights for different return periods.

For the short data-set wind speeds as shown in **Table 18** above, it was possible to determine maximum wind speeds for a given wind direction of interest, specifically. However, for the extreme value NCEP wind speeds that are shown in **Table 19** below, the wind speeds are given independent of the wind direction. It is simply assumed, conservatively so, that the wind speeds are in an arbitrary direction, meaning that for calculation purposes, any direction may be assumed without altering the wind speed

magnitude. These maximum NCEP wind speeds are, as determined in Section 4.3, summarised in the table below (note that only the “best fit” estimates of the extreme value analysis are used).

Table 19: Summary of maximum NCEP wind speeds (m/s at 10m) as determined using the MIKE Zero EVA tool (best fit estimates)

Return Period (T)	Best Estimate
2	21.20
5	23.25
10	24.49
20	25.80
50	27.24
100	30.06

Results for calculations which make use of the selected wind speeds as discussed above are shown and summarised later.

5.3 CALCULATION OF PRESSURE EFFECTS

The calculation of pressure setup is a simple calculation. As seen from the literature study, every 1 mbar change in pressure from the normal simply results in an inverse 1cm change water surface level. In the time series analysis, it has already been established, however, that the sea level at Saldanha actually responds to pressure changes by more than what is suggested by the theory. Measured sea level responses, in actual fact, varied from 1.1cm to 1.7cm per 1 mbar pressure change.

Considering the above, an upper limit and a lower limit was calculated for pressure effects. The upper limit is based on a 1.7cm response to each 1mbar of pressure change and the lower limit is based on the theoretical 1cm change for each 1mbar in air pressure. Pressure input values for the calculations were taken from the best estimate values as calculated in the extreme value analysis.

5.4 RESULTS

All wind setup calculations, for all the different wind speed conditions concerned, were resolved for scenarios 1 through to 5 as identified in Section 5.2.2 above using both Equation (17) and Equation (18). These results are illustrated on **Figure 43** to **Figure 47** below. A summary of the results is also given in **Table 20** to **Table 23**.

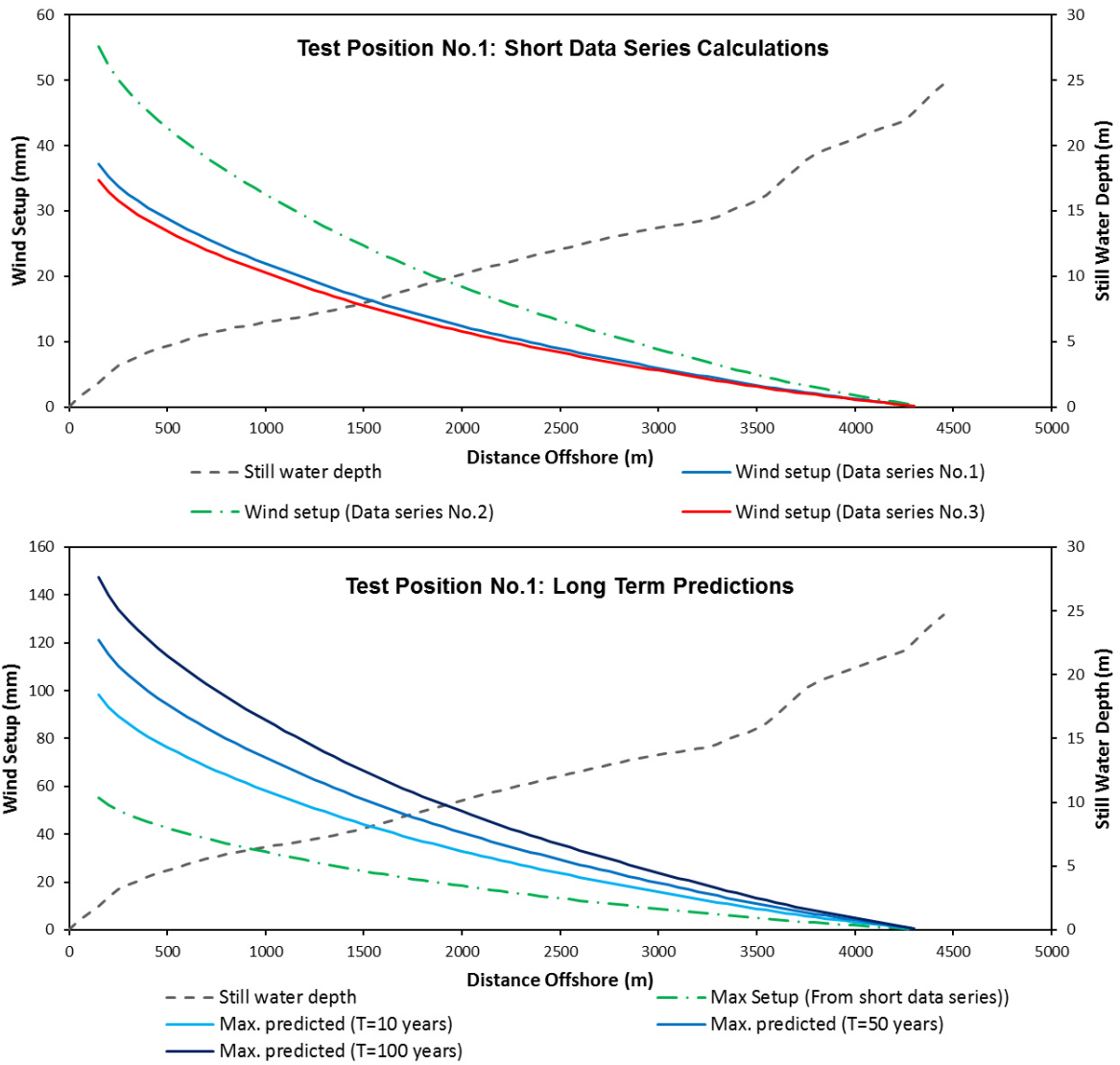


Figure 43: Results of analytical calculations for wind setup at test position no.1 using the Kamphuis equation (Equation (17))

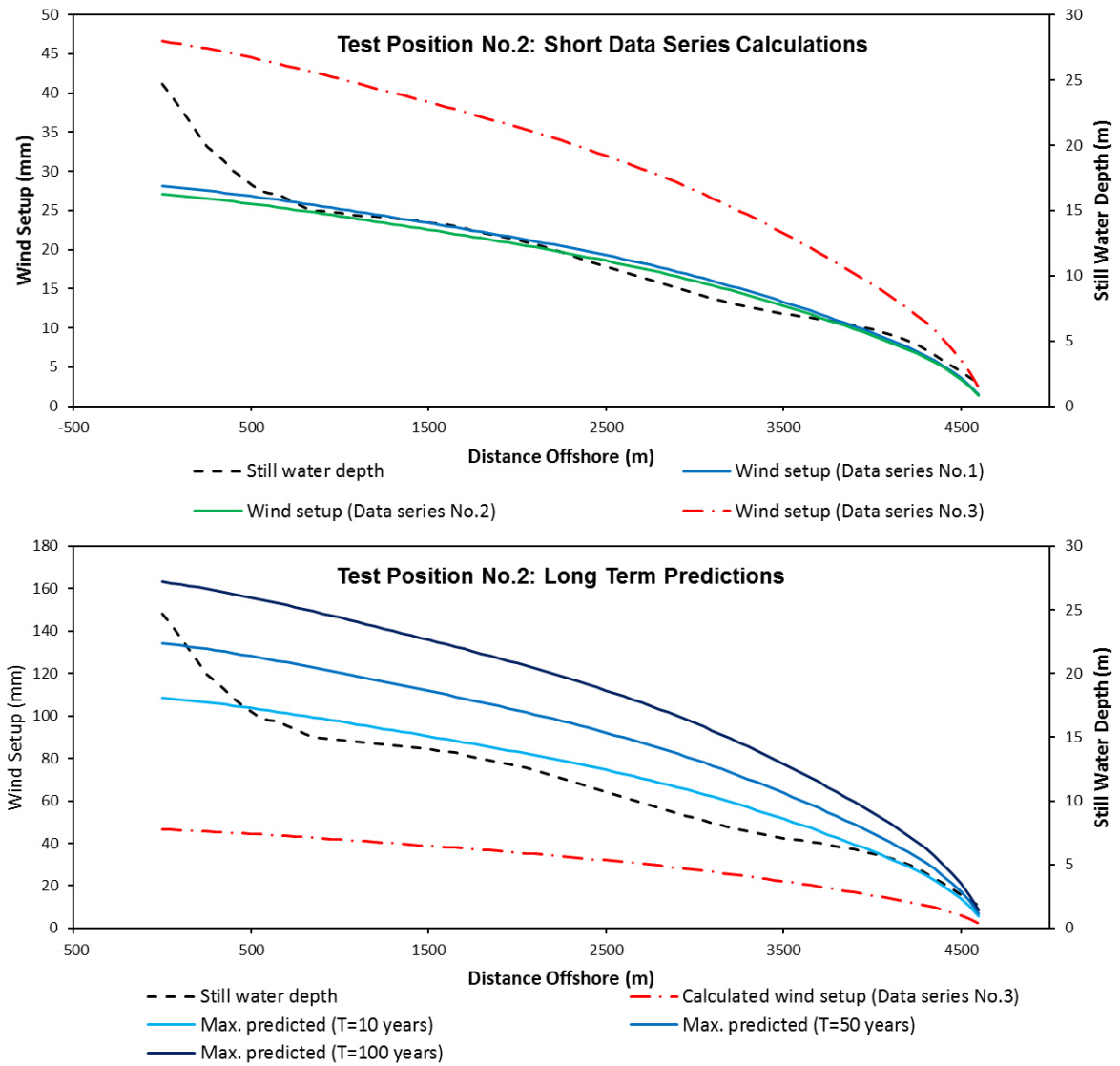


Figure 44: Results of analytical calculations for wind setup at test position no.2 using the Kamphuis equation (Equation(17))

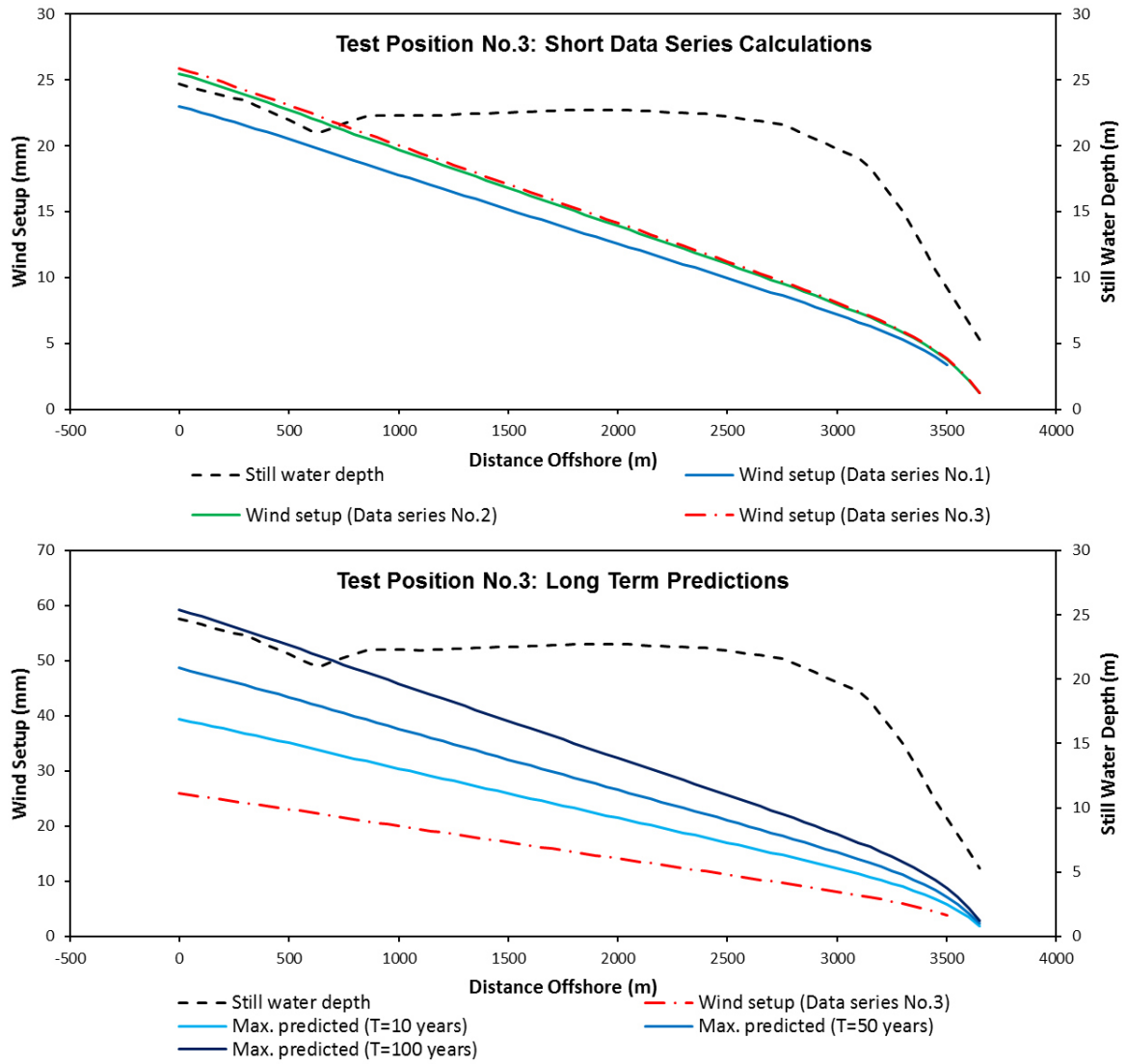


Figure 45: Results of analytical calculations for wind setup at test position no.3 using the Kamphuis equation (Equation (17))

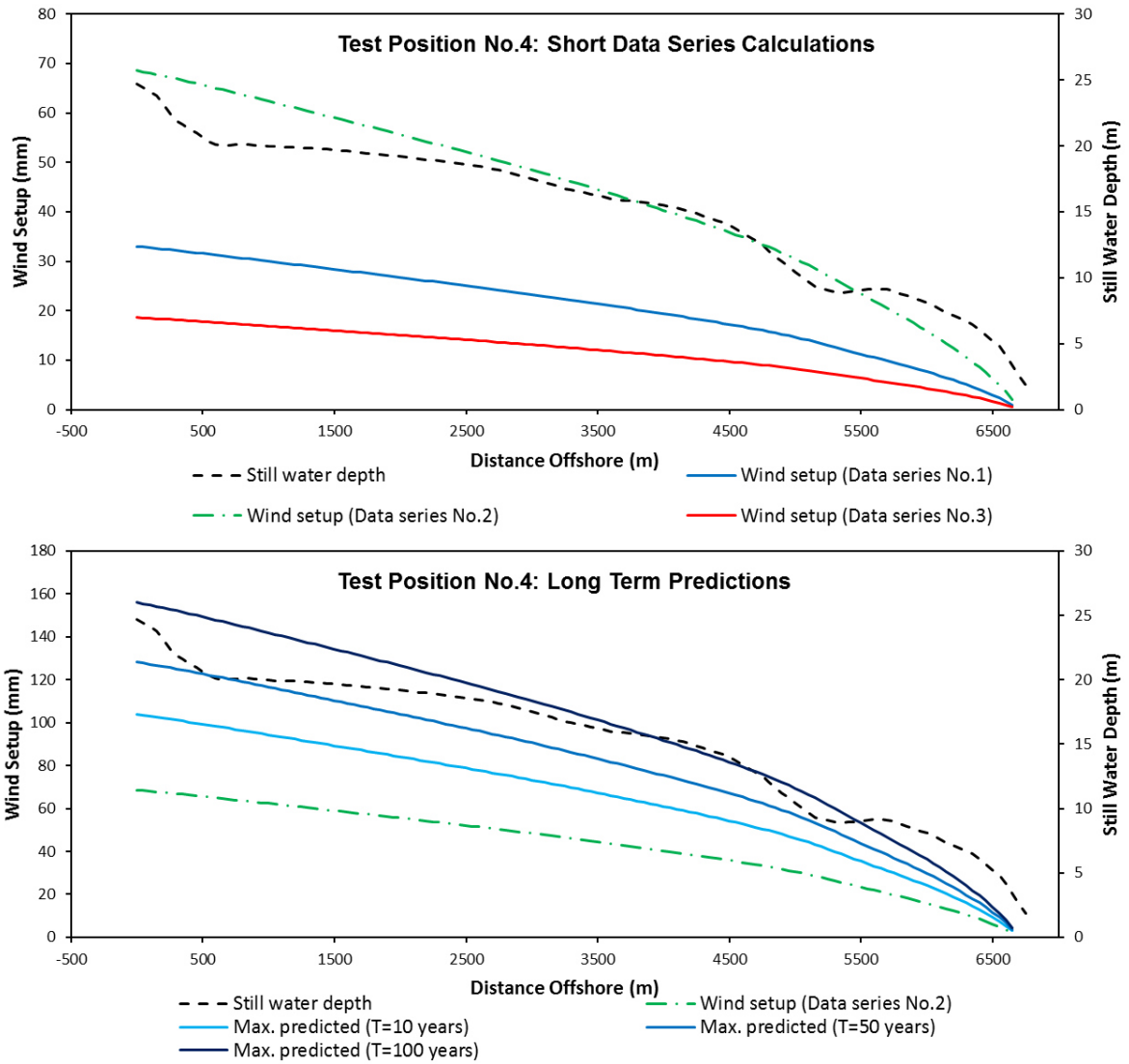


Figure 46: Results of analytical calculations for wind setup at test position no.4 using the Kamphuis equation (Equation (17))

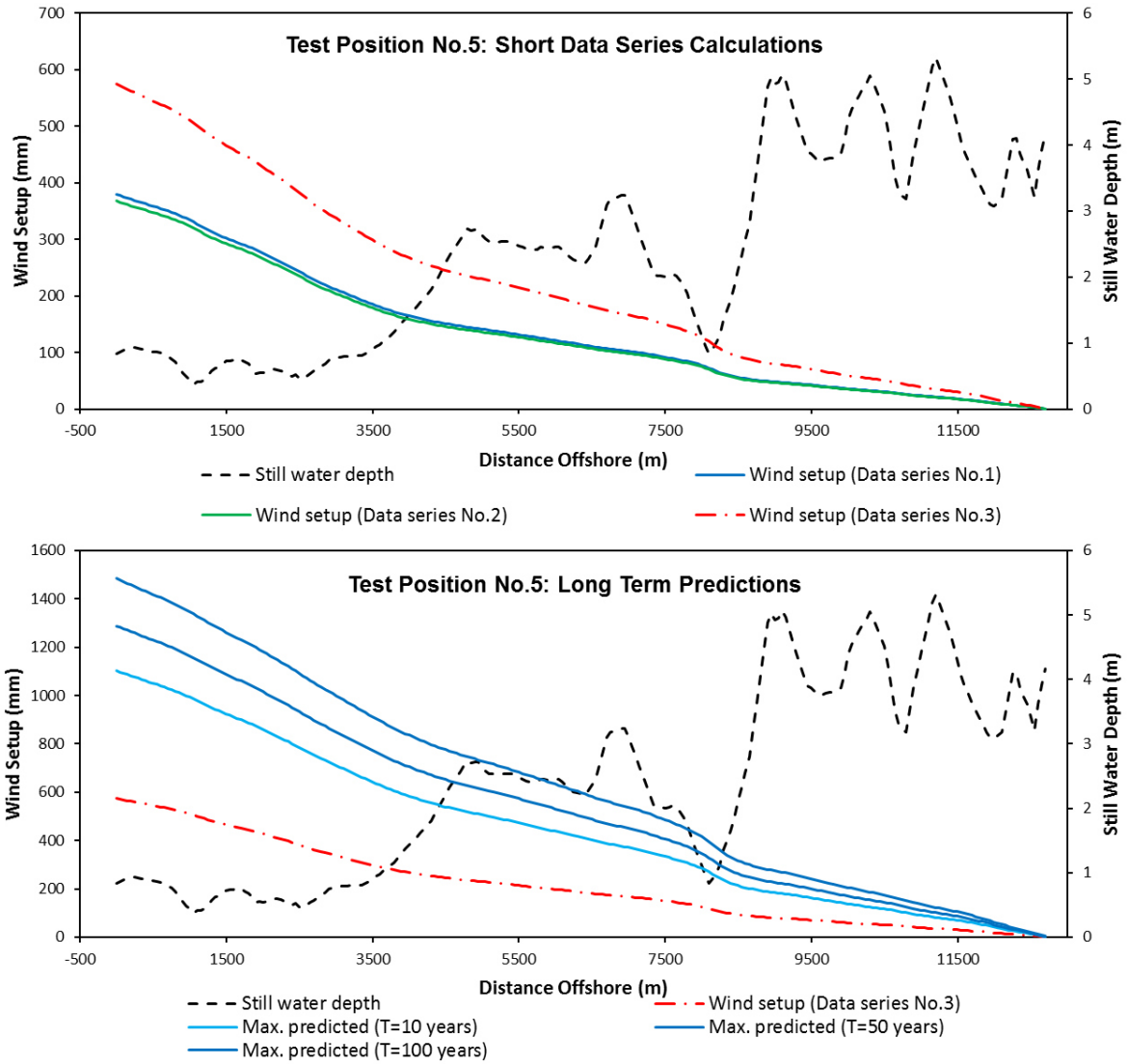


Figure 47: Results of analytical calculations for wind setup at test position no.5 using the Kamphuis equation (Equation (17))

Table 20: Wind set-up (in mm) calculated from maximum wind speeds in data set 1 to 3 using the Kamphuis equation (Equation (17))

No.	Description	Wind direction	Maximum Calculated Wind Set-up (mm)		
			Data Set No.1	Data Set No.2	Data Set No.3
1	Centre of beach	SSE	37	55	34
2	Tip of Caisson 25	NW	28	27	46
3	Tip of Caisson 25	S	23	25	26
4	Tip of Caisson 25	SE	32	69	19
5	Langebaan lagoon	NW	379	367	574

Table 21: Wind set-up (in mm) calculated from maximum wind speeds in data set 1 to 3 using the Bretschneider equation (Equation(18))

No.	Description	Wind direction	Maximum Calculated Wind Set-up (mm)		
			Data Set No.1	Data Set No.2	Data Set No.3
1	Centre of beach	SSE	46	68	40
2	Tip of Caisson 25	NW	30	28	49
3	Tip of Caisson 25	S	22	24	24
4	Tip of Caisson 25	SE	29	61	17
5	Langebaan lagoon	NW	452	436	720

Table 22: Wind set-up (in mm) calculated for selected return periods using the Kamphuis equation (Equation (17))

Point No.	Maximum Calculated Wind Set-up for Return Period (T) (mm)					
	2 years	5 years	10 years	20 years	50 years	100 years
1	74	89	98	109	121	147
2	82	98	109	120	134	163
3	30	35	39	44	49	59
4	78	93	104	115	128	156
5	888	1021	1102	1190	1288	1484

Table 23: Wind set-up (in mm) calculated for selected return periods using the Bretschneider equation
(Equation (18))

Point No.	Maximum Calculated Wind Set-up for Return Period (T) (mm)					
	2 years	5 years	10 years	20 years	50 years	100 years
1	85	102	113	125	140	170
2	86	103	115	127	142	173
3	28	33	37	41	46	56
4	70	84	93	103	115	140
5	1180	1381	1507	1643	1797	2106

The calculated pressure setup predictions for selected return periods is summarised in **Table 24** below:

Table 24: Pressure setup (in mm) calculated for selected return periods as determined from 36 years of NCEP data

Return Period (T)	(-) Pressure deviation from mean	Calculated water level increase –Lower Limit	Calculated water level increase –Upper Limit
2	12.7 mbar	127mm	216mm
5	14.95 mbar	150mm	254mm
10	16.61 mbar	166mm	282mm
20	18.33 mbar	183mm	312mm
50	20.77 mbar	208mm	353mm
100	22.68 mbar	227mm	386mm

5.5 DISCUSSION OF RESULTS

5.5.1 Results Comparison: Different Analytical Equations

The results from Kamphuis' equation (Equation (18)) were compared with the results from Bretschneider's equation (Equation (17)). This comparison is illustrated **Figure 48**. It is clear, from the figure, that for values calculated inside of Saldanha Bay, the two equations yield remarkably similar results. It may therefore be concluded that Bretschneider's equation is a very good approximation for wind setup with respect to the more detailed approach followed using Kamphuis' method. However, it is noted that for wind setup calculated in the Langebaan lagoon, although there is a strong correlation, the relationship is skewed. The straight line regression equation indicates that, for values calculated in the

lagoon, the wind setup is some 124mm higher on average. This implies, as expected, that Bretschneider's equation is not suited for use in a scenario such as this.

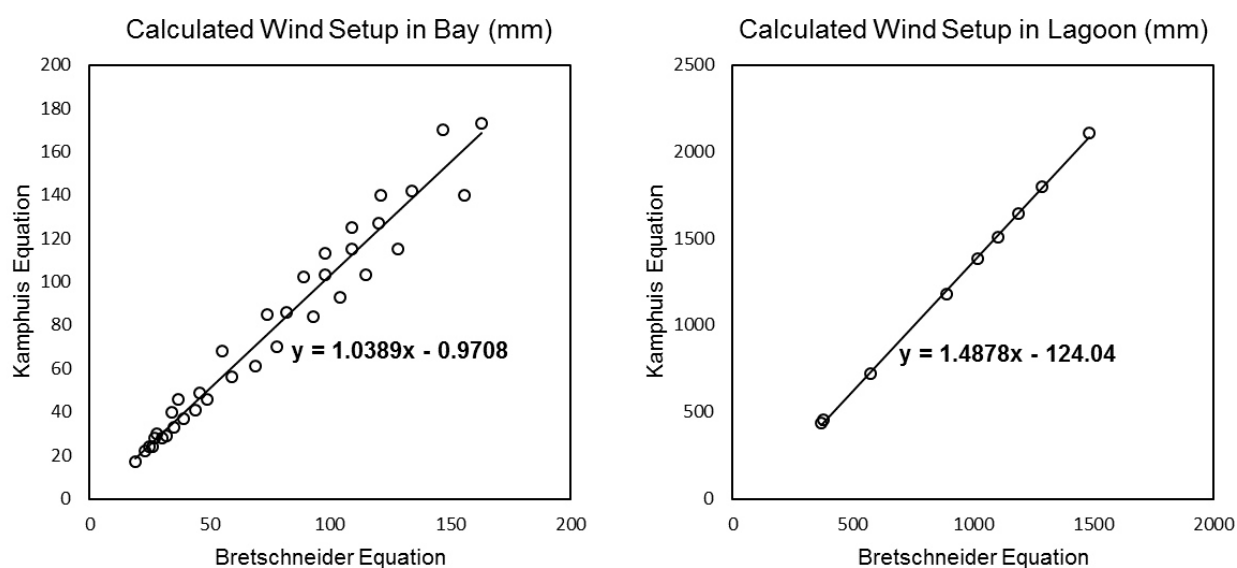


Figure 48: Comparison of calculated wind setup heights

5.5.2 Results Comparison: Analytical Equations vs Time Series Analysis

The results of the analytical calculations for wind setup were also compared with the setup as determined in the time series analysis.

Remembering that wind setup was calculated at the tip of Caisson 25 for 3 different wind scenarios, the results for these three sets of calculations are shown in **Table 25** below:

Table 25: Summary of calculated wind setup: Tip of Caisson 25 (Extract from Table 20)

Description	Wind direction	Maximum Calculated Wind Set-up (mm)		
		Data Set No.1	Data Set No.2	Data Set No.3
Tip of Caisson 25	NW	28	27	46
Tip of Caisson 25	S	23	25	26
Tip of Caisson 25	SE	32	69	19
	Max.	32mm	69mm	46mm

For each data set, the maximum wind setup was selected out of the values concerned. These maximum values are carried over to **Table 26** below where it is brought into comparison with the wind setup values as determined in the time series analysis of Chapter 3.

Three data sets were analysed in Chapter 3, and therefore, in this instance, only three values are available from which to assess the comparison. In hindsight here, it would have been useful to have analysed more than the three data series in the time series analysis, but the quality of the time series data did not allow for much more. Nevertheless, based on these three test cases, the overall comparison, one that would seem to be inconclusive at first glance (refer to **Table 26**), is discussed in more detail below:

*Table 26: Comparison of wind setup results as calculated analytically and as determined from the time series analysis (Time series analysis results extracted from **Table 11**)*

Data series	Calculated (A)	99% TS Anal. (B)	A/B
1	32mm	32mm	100%
2	69mm	31mm	222%
3	46mm	38mm	121%
Average	36.5mm	33.5mm	147%

Although for data set no.1, the calculated wind setup is an exact match of the analysed wind component, the comparison of the remaining two sets show significantly differing results. From this, one may conclude, at most, that the calculated wind setup is on average roughly 1.5 times larger than the equivalently determined wind setup component from the time series analysis.

With that being said, there are two thoughts, additionally, that may be considered:

- Firstly, wind components, as determined in the time series analysis, are highly variable, as is the wind that drove those components. For the analytical calculations however, the assumption is made that wind is both uniform and steady, meaning that wind fields are constant in space and in time and accordingly, the wind setup calculated is assumed to be fully developed and in a state of equilibrium – very much unlike the highly variable wind component of the time series analysis which had just been described.
- Secondly, all of the values as summarised in **Table 26** are relatively small – the overall highest value under consideration is 69mm. Now whether it is a calculated value or a measured value, the fact remains that for practical purposes, and design considerations, 69mm is rather insignificant. Depending on the application, an engineer or designer may well write these values off all together on the basis of being negligibly small. In this regard, one may satisfy oneself in concluding that the two calculated results are in fact similar to the measured values. Although the calculated setup varies greatly in terms of proportional similarity (up to 222%), the amount by which it varies is no more than 38mm. This 38mm may be considered as an acceptable error, depending on the application. When put into context of the total combined water level

fluctuations, which could be in the order of 2000mm, then a 38mm error constitutes merely 1.9% of the total sea level – a small value that may very well be ignored.

In conclusion, it remains true that, on the basis of the mere three comparisons that were made, the calculated wind setup, on average, is 1.5 times higher than the measured wind components. However, it remains at the discretion of the engineer or designer to accept the reliability of these results as there exists serious suggestions towards improved reliability of the results.

CHAPTER 6

6 Numerical Modelling of Storm Surge

6.1 GENERAL

In Chapter 3, the components of storm surge for three relatively short data segments were determined through the analysis of measured time series data. Subsequently, in Chapter 5, wind setup and pressure setup components were calculated analytically for those same three short data segments as well as for predicted extreme events. This chapter deals with developing a numerical model with two objectives in mind: (1) To create a validated model that can reproduce the measured storm surges in Saldanha Bay and which can then ultimately be used to predict extreme storm surges. (2) To serve, over and above analytical calculations, as an alternative computation method so that the performance of these two methods may be compared. Ultimately, it is of interest to recommend the preferred method (a playoff between modelling and analytical calculations) for future use and application at other sites around South Africa.

In the time series analysis, it was found that approximately half of the total height of the residual water levels was still unresolved for with respect to locally measured wind and pressure. This unresolved component was referred to, in the absence of a better explanation at the time, as dynamic effects. The numerical model which is developed here covers a large geographical area beyond that of the study area and its immediate surrounds. It was thus anticipated that the model could capture the dynamic effects of storm surge and its interaction with currents and the ocean bottom in such a way as to resolve for the so called dynamic components as mentioned above.

6.2 MODEL DESCRIPTION

The Flow Model from DHI's MIKE 21 package was used for modelling wind-induced flows and its resultant surface elevation fluctuations. Models were set up to take into account wind related surface drag forces as well as bottom friction of the sea bed. Tides, waves, air pressure, precipitation and sources (river inflow) were excluded from the model so that, essentially, only the effect of wind set-up would be present in the model results.

The model was calibrated against the three storm surge data series (excluding pressure components) for each site as determined in Section 3.6.

6.2.1 Model Setup

The bathymetry data available for the construction of the model mesh was described in Chapter 3.

A flexible mesh was used – meaning mesh elements are triangular and have the benefit of easily making up any irregular shape. The computational intricacies related to the use of flexible meshes are summarised in DHI (2013). In the MIKE 21 Flow Model, the mesh element properties have a significant impact on the modelling time. The modelling time interval is selected by the software so that the value of the Courant number, for any given mesh element in the model, does not exceed ¹1. The Courant number is defined as

$$C_r = \frac{\Delta t \sqrt{gh}}{\Delta x} \leq 1 \quad (19)$$

Where h is the total water depth; Δt is the time interval or model time step; and Δx is the size of the mesh element.

Depth is a function of the bathymetry and so in order to limit the Courant number, the designer must make a trade-off decision between accepting small time steps (which results in prolonged modelling time) or accepting large grid cells (which affects the accuracy of the model).

Bearing in mind the optimisation of modelling run-time as well striving for reasonable results, the mesh was set up and constrained as follows:

- The land-boundary arcs were constrained to a minimum length of 100m – this limits triangle size in the shallow water
- The smallest allowable angle on flexible mesh elements was set to 26 degrees.
- Element vertex z-values were interpolated linearly from the available bathymetry points.
- Mesh elements size vary linearly from the largest cells in the deepest water to the smallest cells in the shallowest water. The shallow areas, where wind stress affects the greatest flows, are modelled in detail as required.

An image of the completed mesh (zoomed to the port and lagoon area) for the Saldanha Bay model is shown in **Figure 49**. (The extent of the mesh was later reduced in order to reduce modelling time. This is discussed in Section 6.3.2)

¹ Mathematically, for model stability, a Courant number of less than 1 is required. The MIKE 21 Flow Model uses 0.8 as a maximum allowable Courant number. This is considered as conservative and guarantees greater model stability.

Model boundary conditions are also specified in the mesh. Two boundary conditions were used:

- A zero normal velocity land boundary along the full length of the coast line and islands; and
- Open water boundaries at ocean-bound extremities.

The extents of these boundaries are shown in **Figure 50**.

Wind setup (or wind forcing, as it is referred to in the MIKE package) is solved in the MIKE model. The model is based on the solution of the three dimensional incompressible Reynolds averaged Navier-Stokes equations (DHI 2013). The user may input a value for the drag coefficient of air, c_D , as well as a bottom stress drag coefficient, c_f , for calibration purposes. (The selection of these coefficients as calibration parameters will be discussed in more detail later on.) Furthermore, it should be noted that wind was fed into the model as varying in time but constant across the domain.

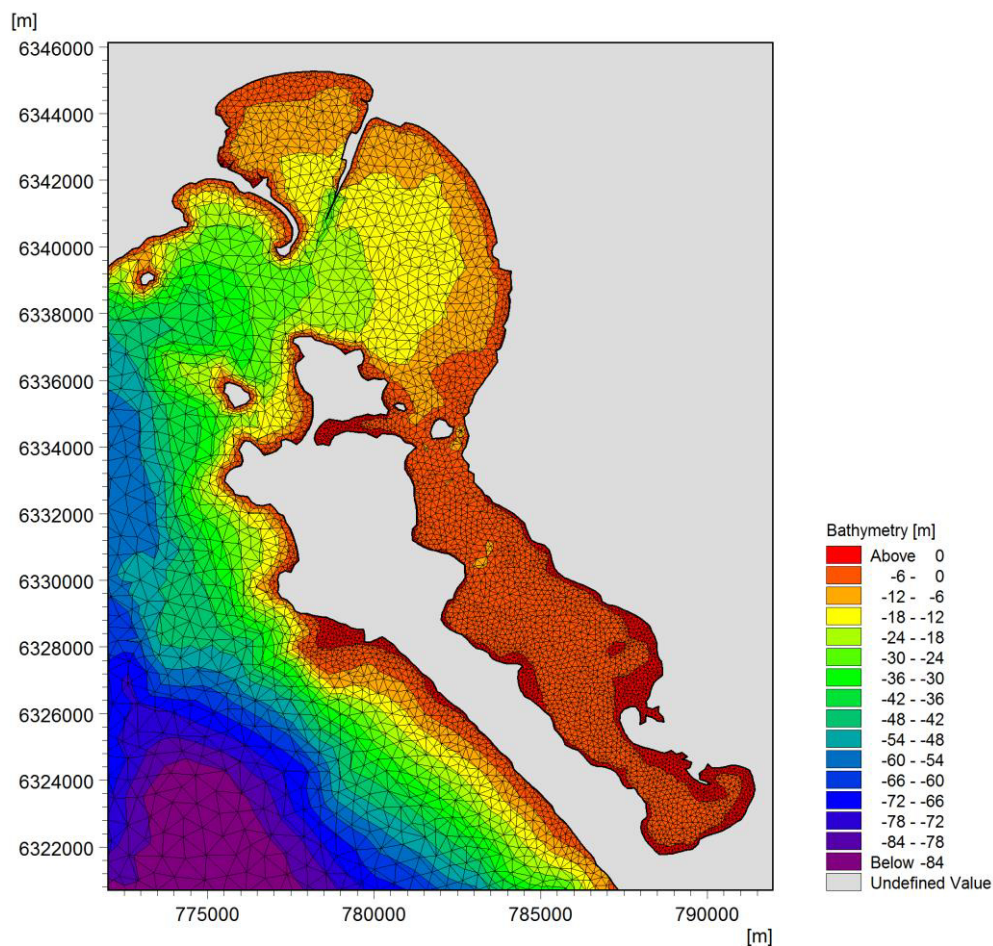


Figure 49: Saldanha bay numerical model mesh (magnification of port and lagoon area)

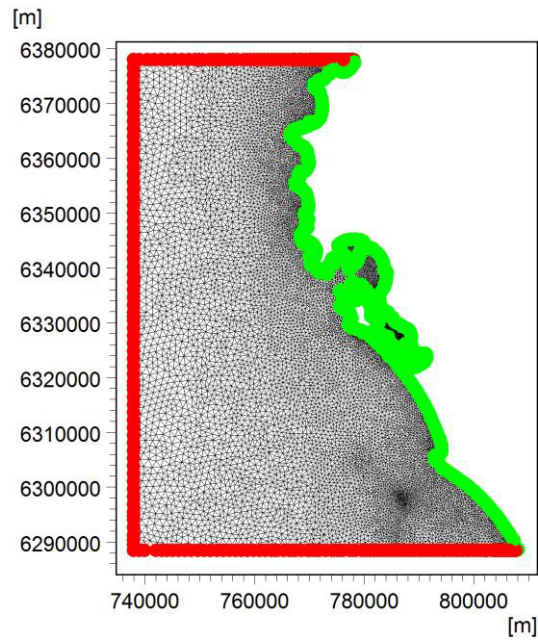


Figure 50: Saldanha Bay numerical model boundary conditions: (red) open boundary (gree) zero normal velocity land boundary

6.2.2 Model Outputs

Two types of model outputs were generated: (a) Time series at selected points and (b) area series for the complete domain.

The time series outputs were generated for the 6 individual points¹ as shown on **Figure 51**. These points are identified as follows:

- (1) Tip of Caisson 25
- (2) Small Craft Harbour
- (3) Beach (western side)
- (4) Beach (centre)
- (5) Beach (eastern side)
- (6) Back of lagoon (Langebaan)

Data output for the time series points are generated in intervals of 1 minute and the area-data is generated in intervals of 1hour.

¹ Note that points 1, 4 and 6 correspond exactly to points 1-3, 4 and 5 of Chapter 5.

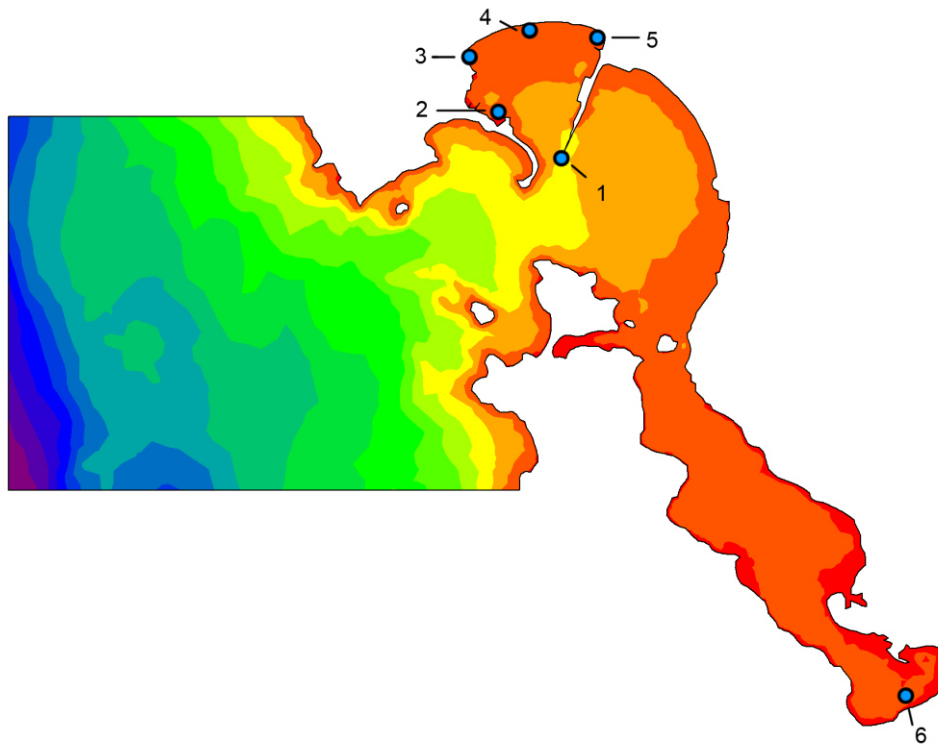


Figure 51: Selected points for time series model outputs

6.3 MODEL CALIBRATION

6.3.1 Discussion

Calibration of the model was not achieved in the manner as anticipated or wanted. This seemingly disappointing outcome is considered as an important topic of discussion. But before discussing the outcomes, it would be sensible here, as a starting point, to reiterate first, what the expected outcomes were for the calibration of the model to start off with:

In the time series analysis (Chapter 3) the local effects of pressure were clearly identifiable and were fairly significant relative to other components identified. Similarly, the local effects of wind were identifiable albeit less significant. A third, and very significant, component that was identified was one that showed no correlation with locally measured wind or pressure. It was assumed at that stage, that this unknown component could have resulted from distant pressure or wind set-ups that had propagated towards the study area and as such this component was labelled “dynamic effects”. The hypothesis had then been made that the numerical model (which is considered in this chapter) would be capable of resolving this “dynamic effects component”. The motivation for this hypothesis being that the large geographical area covered by the model would enable the simulation of the propagation of offshore surge disturbances towards the study area and that these propagated surge disturbances would become more prominent in the shallower waters of the study area.

With the above hypothesis in mind, results of the initial model runs were compared with the “total storm surge contribution” data series as derived from the time series analysis (Chapter 3) for calibration testing. It should be kept in mind that this so called “total storm surge contribution” data series consists of a summation of the local wind effects, local pressure effects and, importantly, the so called dynamic effects (refer to Section 6.3.2 to Section 6.3.7 below). Here it was found, in contrary to the hypothesis, that model results showed extremely poor correlation to the comparison series and furthermore, that the fluctuations in the modelled series were of several orders of magnitude smaller than the fluctuations in the comparison series.

Various different scenarios were considered for the calibration test as described, but for as long as the dynamic effects component was included in the comparison series, satisfactory calibration could not be achieved for any of the test cases.

6.3.2 Calibration Scenarios: Domain Size Sensitivity

Initially, the model domain was set up to include the full extents of the available bathymetry data. As a result, these initial model runs had long modelling times. A sensitivity test was performed to evaluate the effects that smaller domain sizes would have on the model results with the intention of reducing modelling time. It was expected that by reducing the extents of the domain (in the deep water), the results of the model would not be affected significantly but that model times would become shorter. This seemed plausible as it is known that wind set-up is inversely proportional to water depth and that including large areas of deep water in the model domain is redundant.

Three similar model runs with varying domain sizes were performed as follows:

- (1) the maximum possible model domain size was used;
- (2) a reduced domain which included all of the inner bay plus an additional area stretching to roughly 15km offshore of the extremities of the bay and;
- (3) a reduced domain including the inner bay only.

Plots of these domains and their respective model outputs are shown in **Figure 52** and **Figure 53**.

Model outputs from scenario (1) and (2) as described above were found to be very similar. On average, scenario (2) shows all of 70% of the total fluctuations¹ that are shown in (1). It was thus decided that by reducing the domain as per scenario (2), that model results still show an acceptable degree of detail and that the reduction in fluctuation heights may easily be corrected by adjusting other calibration parameters.

¹ This was calculated as the ratio of the average height of positive surface elevations of the scenario (1) outputs to that of the scenario (2) outputs.

Model outputs from scenario (3) however, contained only a small portion of the detail relative to the other two scenarios. On average, only 22% of the components of (1) were successfully preserved in (3). On this basis, the use of such a small domain was rejected.

In conclusion, based on the sensitivity test as described above, a reduced domain as per scenario (2) was accepted for further use. In this manner, model run time for subsequent model runs was reduced by some 85%.

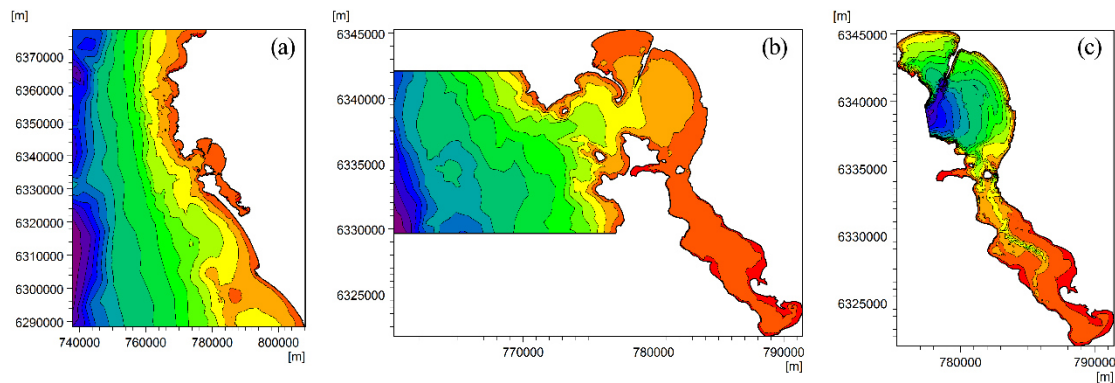


Figure 52: Extents of different domains used in sensitivity analysis. (a) Maximum available domain (b) Inner bay and 15 of offshore bathymetry (c) Inner bay only

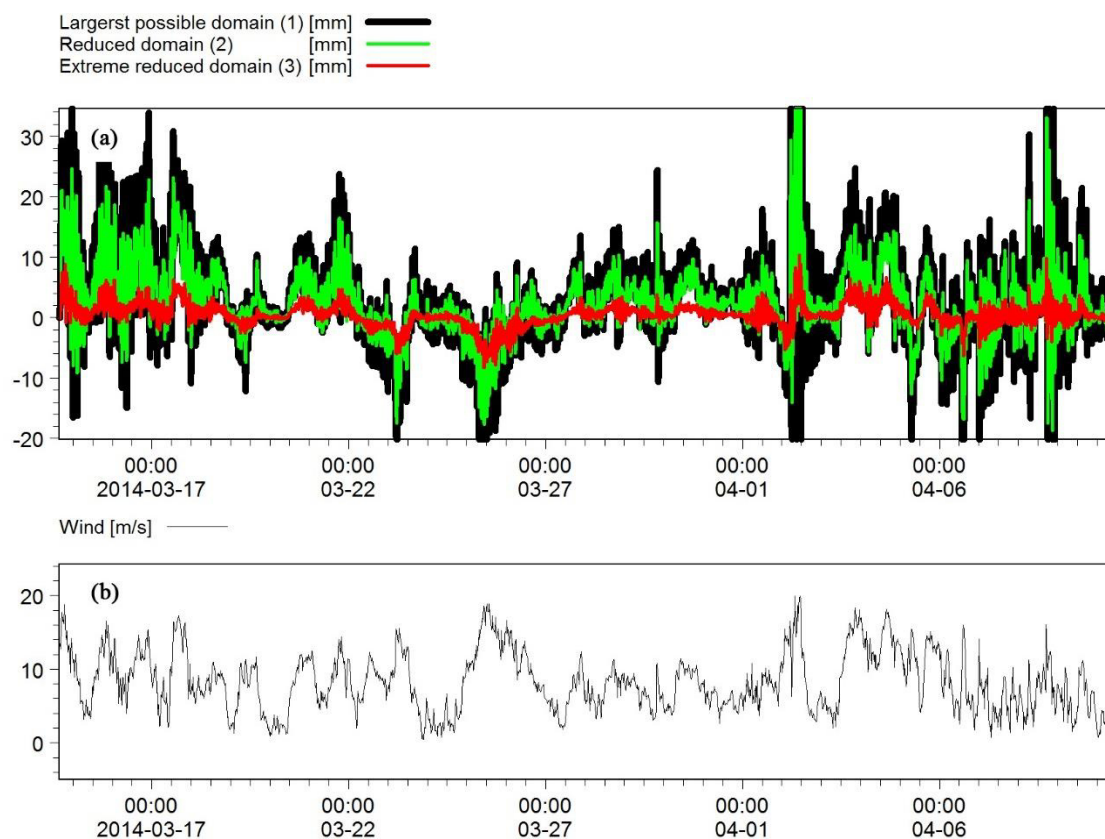


Figure 53: Modelled wind set-up results for 3 test runs of varying domain sizes. (a) Wind setup heights for different domain sizes (b) Wind input data set

6.3.3 Calibration Scenarios: Wind Drag Coefficient Sensitivity

The MIKE model calculates wind stress as follows:

$$\bar{\tau}_s = \rho_a c_d |u_w| \bar{u}_w \quad (20)$$

Where τ_s is wind stress; ρ_a is air pressure; u_w is wind velocity at 10m above mean seal level; and c_d is the empirically determined wind drag coefficient.

The suggested values for c_d range from 1.255×10^{-3} for low wind speeds (up to 7m/s) and up to 2.424×10^{-3} for strong wind speed (25m/s and greater) (DHI 2013)

Three modelling scenarios were selected to test for calibration; each with different values for c_d :

- (1) Constant c_d of 1.255×10^{-3} for all wind speeds;
- (2) the recommended values, namely 1.255×10^{-3} for low wind speeds and linearly increasing to 2.424×10^{-3} for high wind speeds and;
- (3) an exaggerated 3.595×10^{-3} for low wind speeds and linearly increasing to 5.0×10^{-3} for high wind speeds.

Figure 54 shows the effects of the wind drag coefficient on the surface water level fluctuation heights for three different model runs.

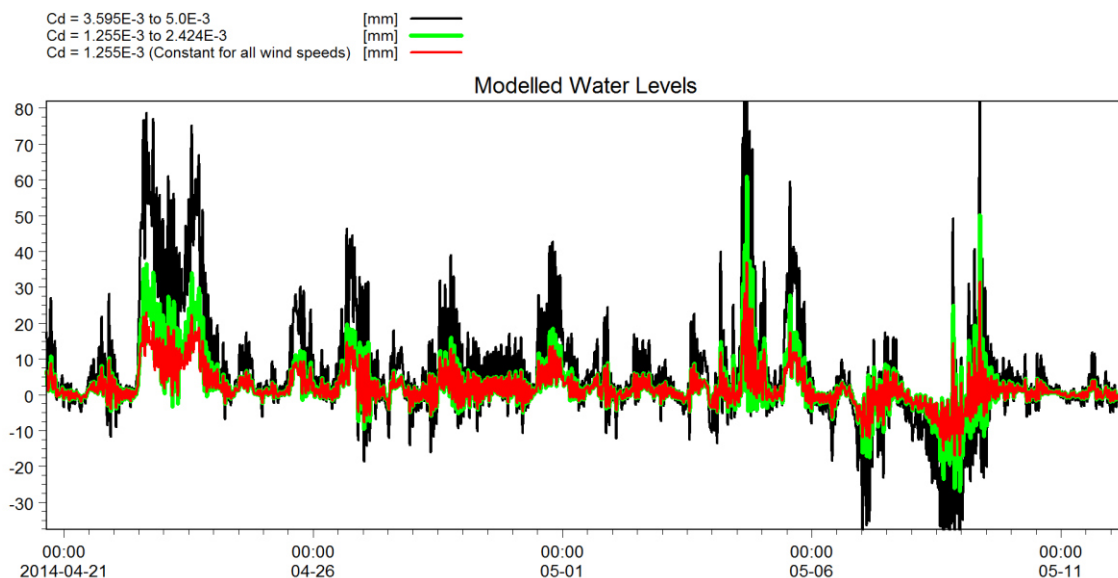


Figure 54: Modelled results for wind setup (Y-axis shows height in mm) for 3 different test runs whereby varying only the wind drag coefficient in each run

It is clear that increasing the wind drag coefficient resulted, as expected, in more exaggerated surface elevation fluctuations. However, even for the most extreme of these three scenarios, where coefficients

were selected much higher than recommended values, the results are still far from within the range of the comparison series. To illustrate this, **Figure 55** shows a comparison plot between the modelled water levels for scenario (3) and the comparison series.

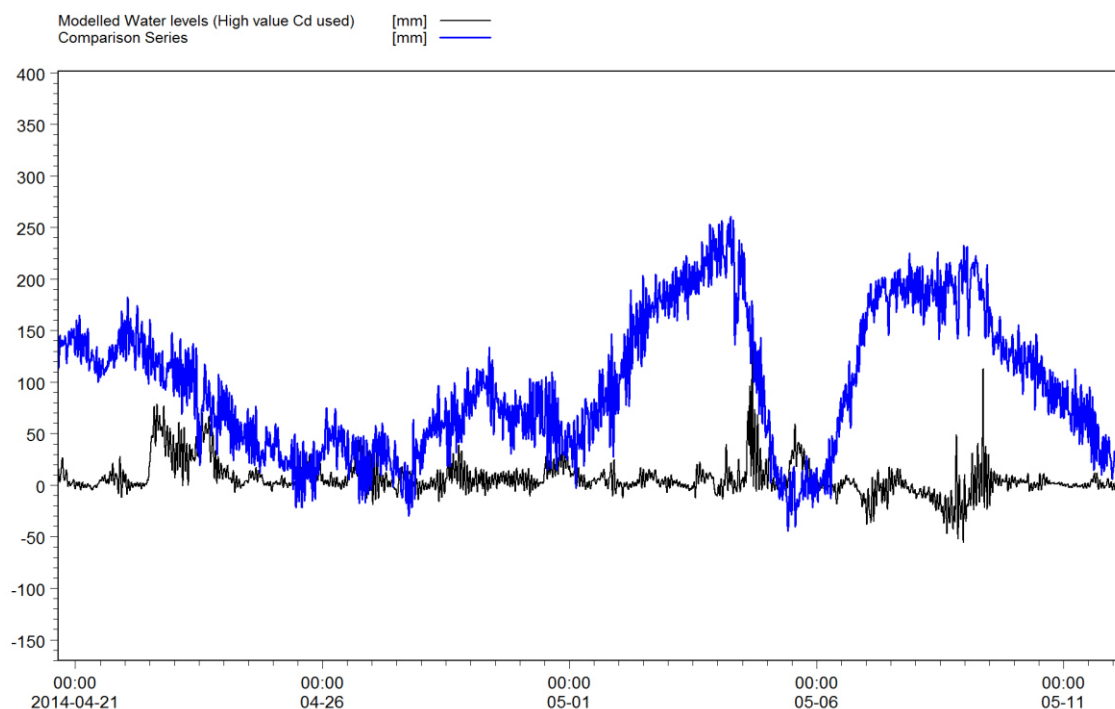


Figure 55: Modelled wind setup height (in mm) compared with storm surge as determined in the data analysis of Chapter 3 (dynamic effects included)

On average, the positive maximum water level of the modelled series is only 24.3% as high as that of the comparison series¹. Furthermore, there is no clear temporal correlation between the two series.

It becomes clear, at this stage, that calibration is unlikely to be achieved between locally wind-driven surface level fluctuations (the modelled series) and measured components of wind setup and dynamic effects (the comparison series).

6.3.4 Calibration Scenarios: Bottom Friction Coefficient Sensitivity

Bottom friction (or bed resistance) is calculated in the MIKE 21 model as

$$\tau_b = c_f u_b^2 \rho_0 \quad (21)$$

Where c_f is the drag coefficient; u_b is the flow velocity; and ρ_0 is the water density.

¹ The **comparison series** as referred to here, comprises of the dynamic effects- and wind components as determined in Chapter 3.

The recommended range of values to use for c_f is 20 to 40 $m^{1/3}/s$ with 32 $m^{1/3}/s$ typically selected in the absence of data to suggest otherwise (DHI 2013)

Three similar model runs were executed, changing the value of the drag coefficient alternatively to:

- (1) 20 $m^{1/3}/s$;
- (2) 32 $m^{1/3}/s$;
- (3) 40 $m^{1/3}/s$.

The model outputs for the above scenarios are plotted in **Figure 56**

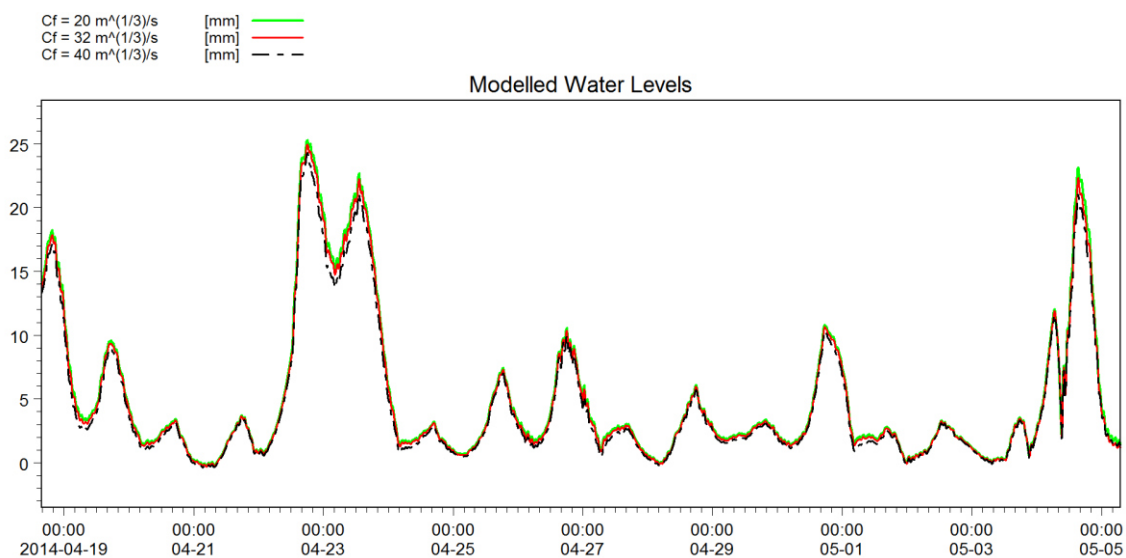


Figure 56: Modelled wind set up (Height in mm) for 3 different test runs whereby varying only the bottom friction coefficient

It may be seen that by decreasing the bottom stress, the water level fluctuations increase marginally but even so, and once again, these changes are small in relation to the fluctuations of the comparison series. In fact, the changes in water levels brought about by changing the bottom friction coefficient to extreme low- or high values are in the order of 1 to 2mm and is therefore considered negligible. The likelihood that calibration is achievable on this basis is therefore rejected.

From this point onwards all subsequent models were set up assuming the default value for c_f of 32 $m^{1/3}/s$.

6.3.5 Calibration Scenarios: Wind Data Time-step Size Sensitivity

At this point in time, it had already been shown that neither wind- nor bottom friction coefficients would serve as a means to successfully attain calibration of the model under consideration. With this in mind it was considered that perhaps, the modelled water level fluctuations were small because the wind input

series is varying too rapidly, and as such, there is insufficient time available for water level response to come to equilibrium within the constraints of the model time steps.

An attempt was therefore made to use, as input, wind series for which the velocity was averaged over (1) 6 hours, and (2) one day, so as to be varying less rapidly. The model outputs were compared with that of a similar model where the usual 20 minute measured wind data was used as input. The results are shown **Figure 57**.

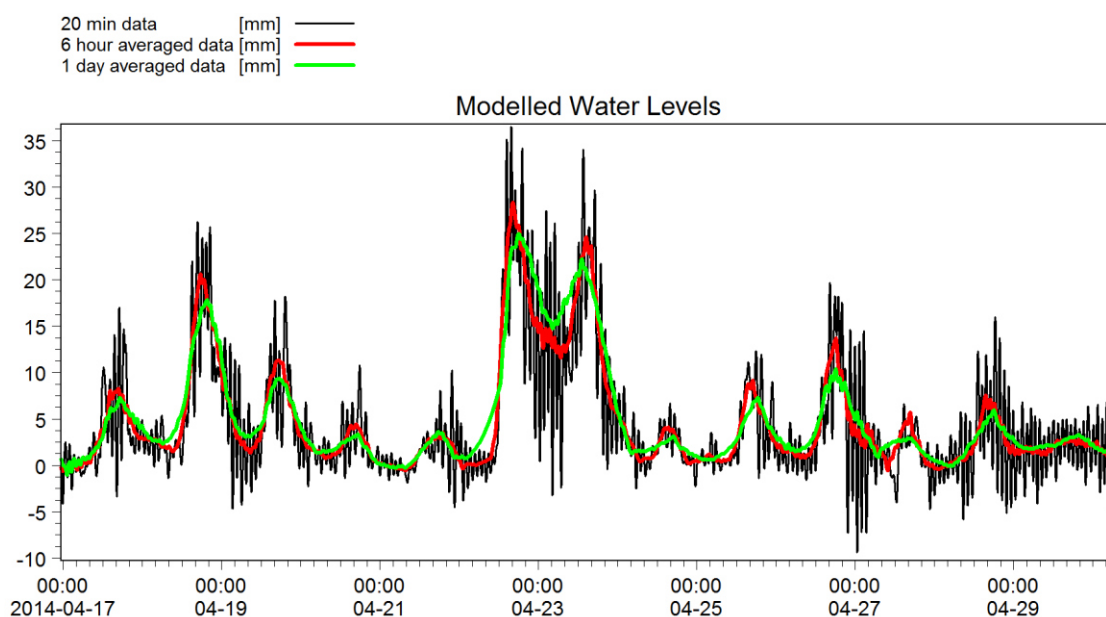


Figure 57: Modelled wind set up (Height in mm) for 3 different test runs whereby the wind input series are averaged over varying times

Here, too, calibration to the comparison series appears unlikely as averaging the wind input series merely resulted in smoothed output results and not in increased water level fluctuation heights as anticipated.

6.3.6 Calibration Scenarios: Pressure

Up until this point, the attempted calibration models have taken into account wind forcing and bottom friction only – and not pressure. An interesting way to incorporate pressure here would have been to see how pressure disturbances from some distance offshore would propagate towards the study area. However, in order to achieve such results, time- and spatially varying pressure data is required. Bearing in mind that only pressure data measured at a single point is available for this study, it is impossible to realistically model the effects of dynamic pressure systems offshore of the study area.

A rudimentary attempt was made at applying the available pressure data to the model as varying in time but constant across the whole domain. This was done by assigning, as boundary conditions, equal time-varying water level fluctuations to all of the open boundaries. These assigned water level fluctuations

were selected as equal to pressure components of measured residuals as determined in Chapter 3. Essentially it is applying the inverse barometer effect to all open boundaries.

The results of this test model as described above are shown in **Figure 58**.

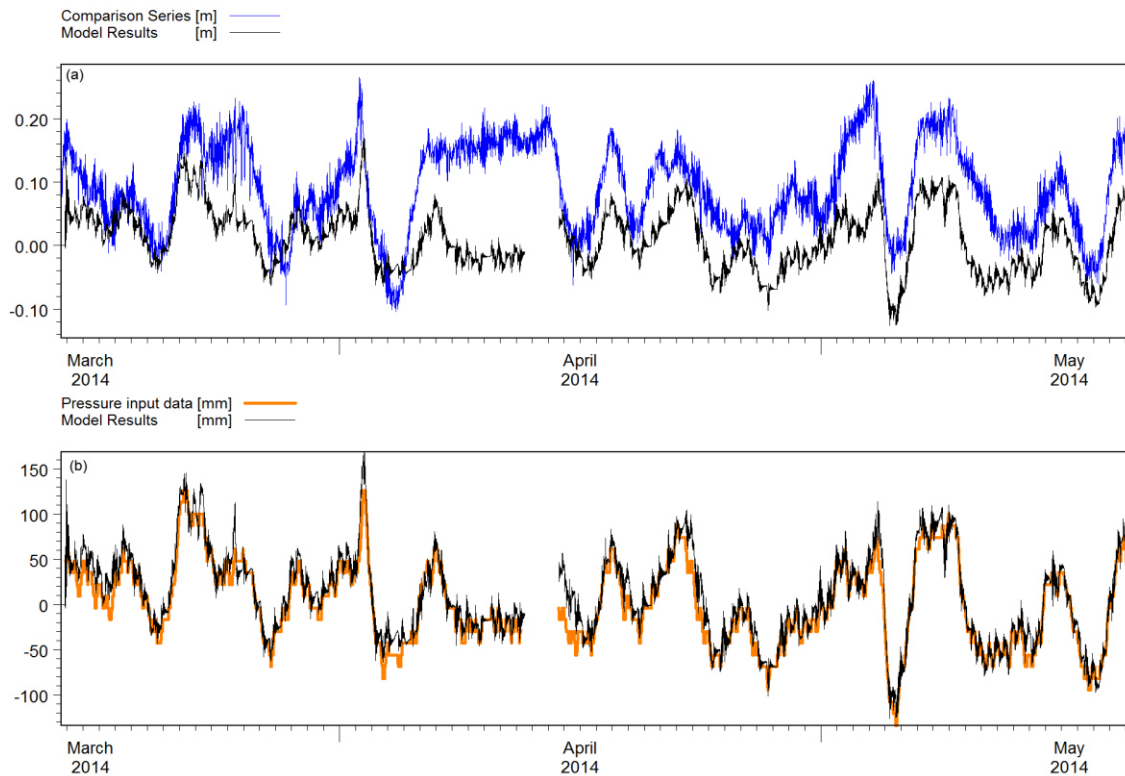


Figure 58: Modelled wind set up (Height in mm). (a) Model results shown against comparison series (b) Model results shown against pressure input

It is evident that, as expected, the static effects of pressure. i.e. the inverse barometer effect, is simply superimposed on the wind forcing. Hardly any additional dynamic effects are in fact produced by including the pressure in this way. It is therefore concluded that by including pressure effects to the model, as attempted here, does not solve for the dynamic components in the comparison series.

6.3.7 Calibration Scenarios: Local Wind Set-up

So far, properly calibrated results could not be obtained from any of the tested calibration runs described above. Furthermore, the sensitivity tests indicated that calibration is essentially unachievable between model results and the selected comparison series. It should be taken into account, however, that the comparison series, in all of these cases, included the so called dynamic effects of the time series analysis. What if the dynamic effects were to be excluded in the comparison series? With this question in mind, a comparison was subsequently made between the model results and a comparison series which consisted of wind components only and excluding the dynamic effects component. The model was set

up with the wind friction coefficient as well as the bottom friction coefficients as standard recommended values as discussed previously.

Figure 59 shows plots of modelled results and a comparison series for data series No.1. The comparison series here consists of wind setup only.

Much better results were achieved in the model run as described above than with the previous comparison series. The modelled surface elevations closely resemble that of the comparison series in that the heights of the positive spikes from both series are of similar magnitudes. The 99th percentile maximum heights of positive surface elevations (representative of maximum values but excluding sharp spikes) are 30.4mm and 32.2mm for the modelled results and the comparison series respectively. While it is true that the magnitudes of the elevation spikes are similar, it is noted that the comparison series contains more densely varying fluctuations than the modelled series. There is also not a clearly identifiable temporal correlation between the modelled series and the comparison series. However, this may be explained as the result of unwanted noise that may have been filtered through along with the wind set-up oscillations when digital filtering was done in Chapter 3. Bearing in mind that all oscillations within the frequency range of 8.86 -21.38 cpd were accepted as “wind effects”, the likelihood of having captured unwanted noise is highly probable. It is thus accepted here that despite this problem, the model run under consideration is suitably calibrated to the comparison series.

Similar model runs were also done for data series No.2 and No.3 and results are similar. Results are shown in **Figure 60**, **Figure 61** and **Table 27**.

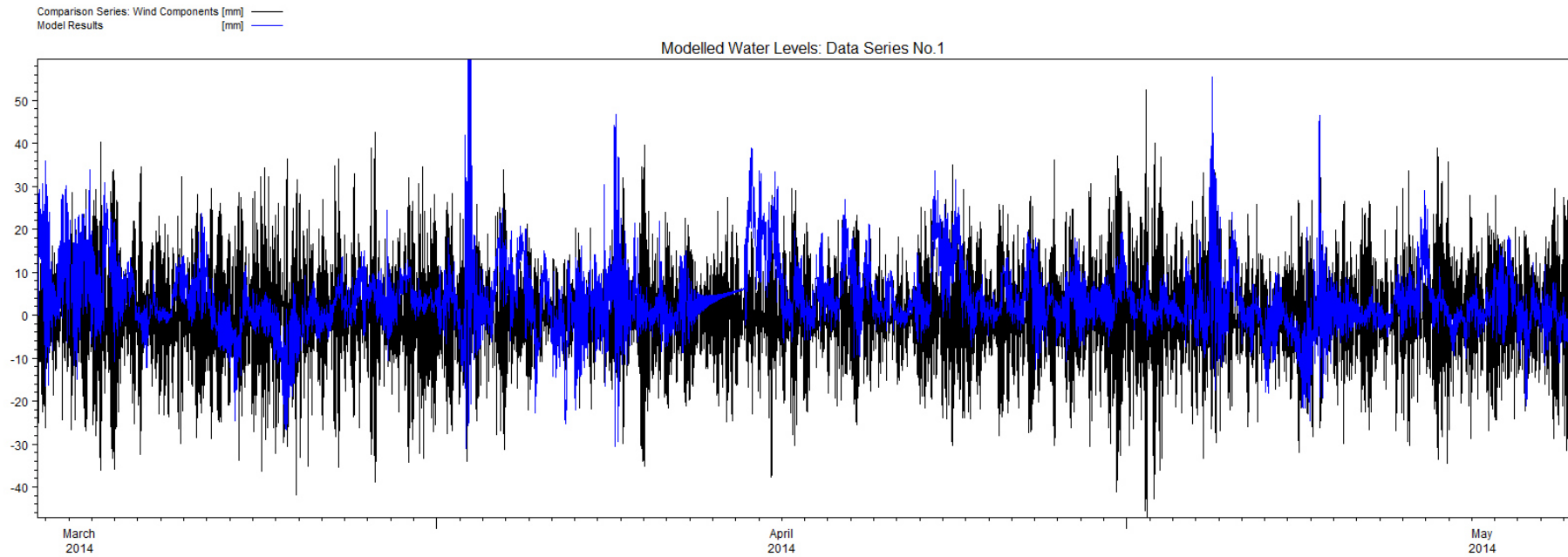


Figure 59: Modelled wind set up (Height in mm for data set No.1. The comparison series (black) consists of wind setup components only.

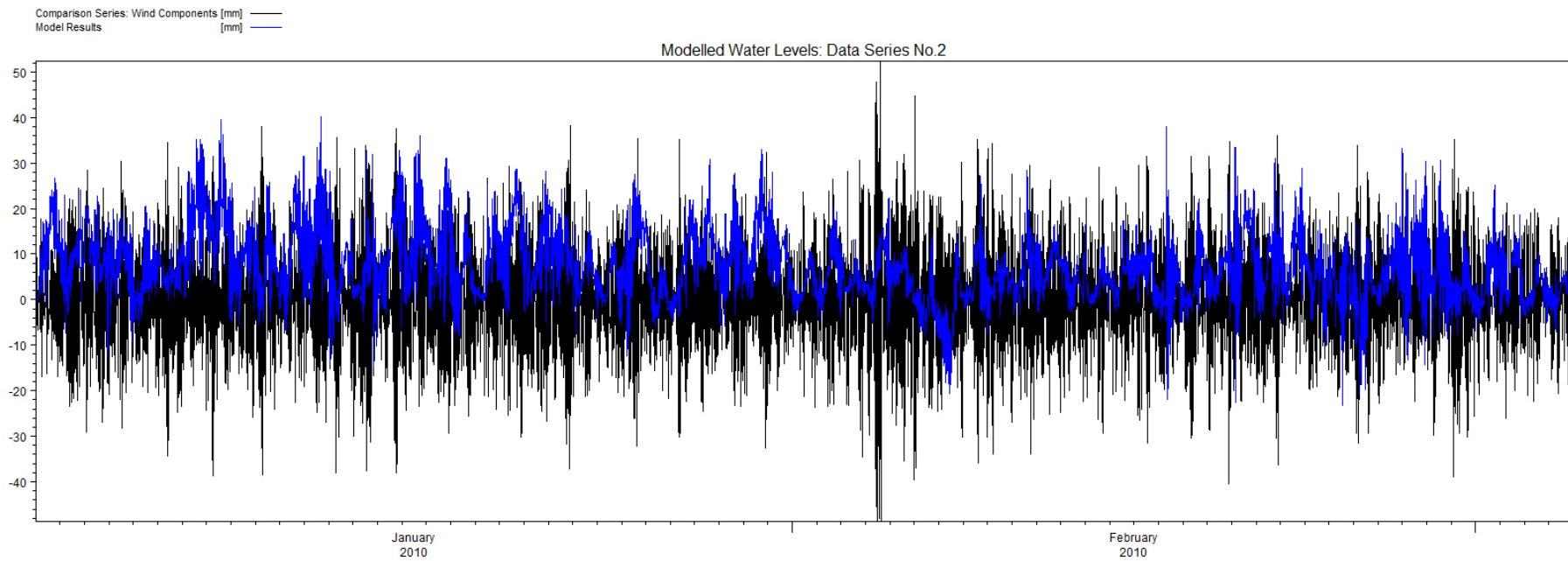


Figure 60: Modelled wind set up (Height in mm for data set No.2. The comparison series (black) consists of wind setup components only.

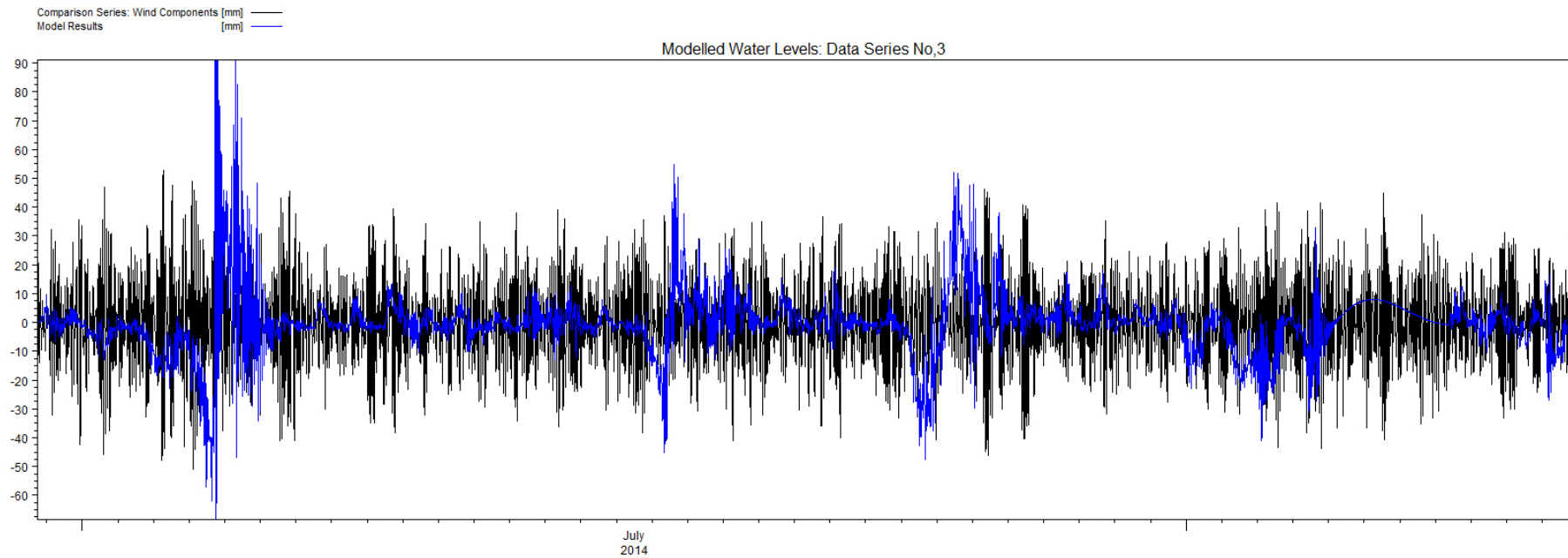


Figure 61: Modelled wind set up (Height in mm for data set No.3. The comparison series (black) consists of wind setup components only.

Table 27: Calibration results for modelled wind setup as compared with wind components of the time series analysis (Time series analysis results (B) extracted from Table 11)

Data series	95% Model (A)	95% TS Anal. (B)	A/B
1	20.6mm	23.6mm	87.1%
2	21.9mm	22.8mm	96.1%
3	26.9mm	28.4mm	94.4%
Average	23mm	25mm	92.5
	99% Model (A)	99% TS Anal. (B)	A/B
1	30.4mm	32.2mm	94.4%
2	28.4mm	30.5mm	93.4%
3	50.7mm	37.7mm	134.4%
Average	36.5mm	33.5mm	108.9%

6.4 MODEL RESULTS AND DISCUSSION

From the results of the calibration tests, it may be concluded that the numerical model succeeds satisfactorily in modelling the local effects of wind setup. However, one of the desired outcomes of the numerical model was that it would resolve the large dynamic effects component that was left unaccounted for during the time series analysis. This was not the case and dynamic components were not resolved in the model as anticipated. Therefore, these so called dynamic effects components from time series analysis still remains unresolved. It is thus yet to be proven that these components are related to storm surge.

Despite having come to the conclusion that the dynamic effects still remain unresolved for, some interesting results were nevertheless obtained in the process. Since having established that the numerical model produces neatly calibrated results for local wind set-up (or static wind effects, for that matter), the spatial variability of local wind set-up across the bay could be looked at in more detail.

The description of the model setup, included the fact that time series outputs were extracted from six different points within and near the bay (see **Figure 51**). It is the output obtained at the tip of caisson 25 that has, up to now, been selected as the **study-area output point** and it is this same output that was used for calibration tests. Modelled wind set-up heights at this point were small – in the order of 20 to 50mm.

The results from the remaining five points were also extracted and compared with that of the study-area point as described above. Here, one has to bear in mind that output from these points are un-validated as no measured data had been available for the calibration of these points. Results are nevertheless as expected, with the points in shallower water resulting in higher wind set-up values. **Figure 62** shows

time series plots of modelled wind setup at all 5 points for data series No. 1, 2 and 3 respectively. It is obvious that the wind setup is the most prominent at the back of the Langebaan lagoon, particularly during periods of strong northwesterly winds. Here, positive fluctuations reach values in the region of 880mm in winter months associated with strong north westerlies. The negative fluctuations are limited to 200mm deep as this signifies the extents of the still water depth at the output point. (In hindsight, the output point was perhaps selected at too shallow a water depth and this may also have resulted in over-exaggeration of modelled water level heights.).

Water level fluctuations at the remaining four points vary within the range of about 25-90mm. These points are located in shallower water than the point located at the tip of caisson 25 and the higher wind setup levels thus seem logical.

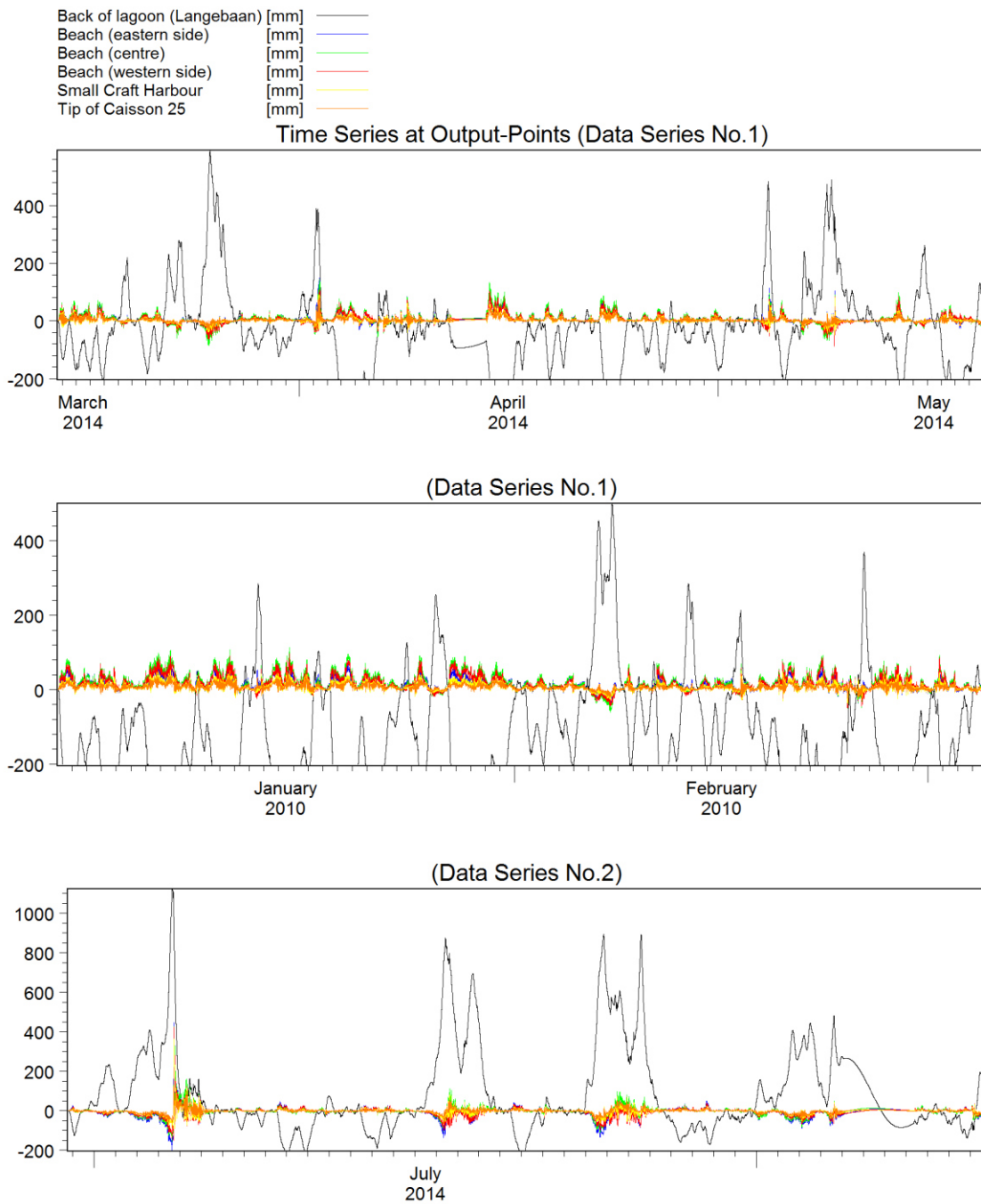
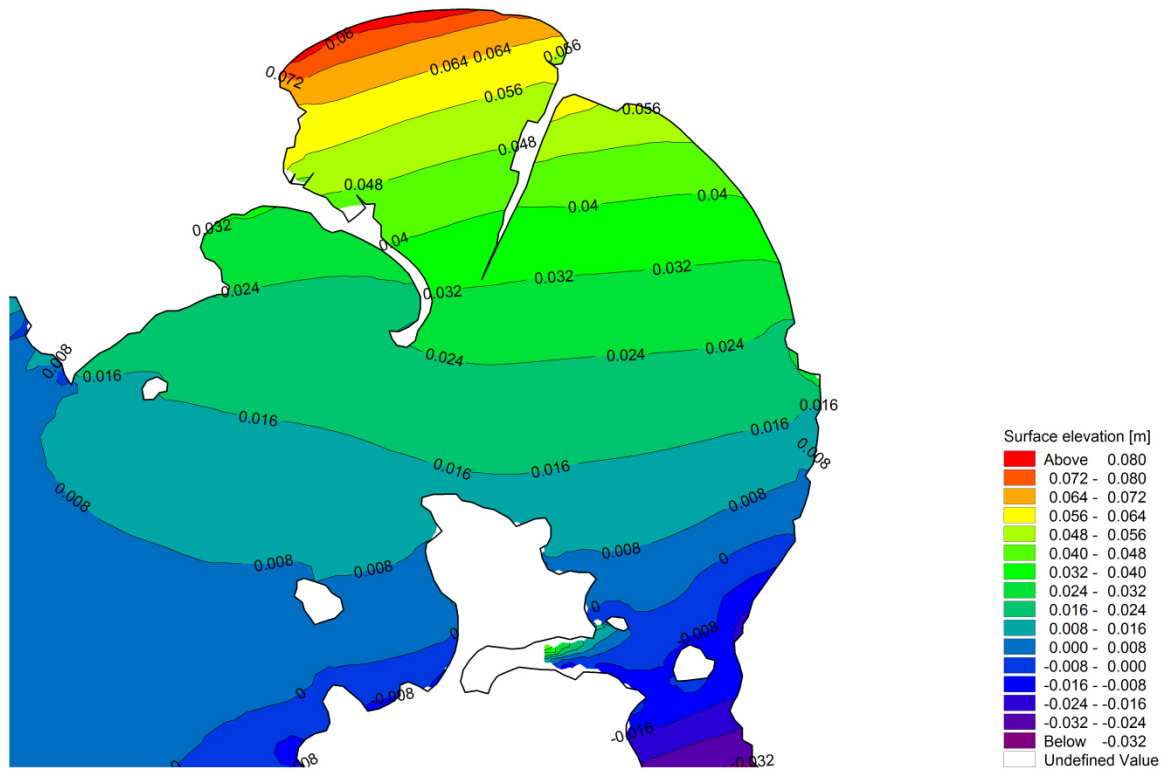


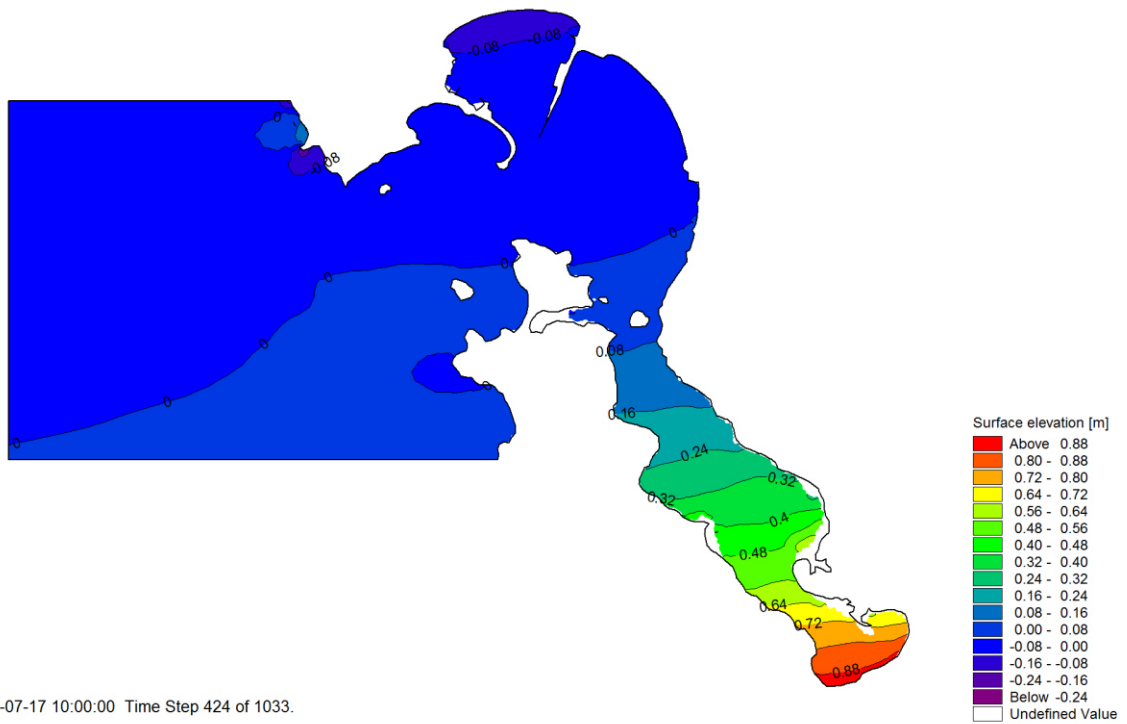
Figure 62: Modelled wind set up for data series no.1(top), no.2(middle) and no.3(bottom). Different collours represent results from diffent test points

Figure 63 and **Figure 64** show the spatial distribution of wind setup heights for a strong summer event and a strong winter event respectively. **Table 28** shows a summary of maximum modelled wind setup elevations at various points as corresponding to those shown on **Figure 51**.



2010-01-16 16:20:00 Time Step 376 of 1511.

Figure 63: spatial distribution of wind setup heights for a strong summer event



2014-07-17 10:00:00 Time Step 424 of 1033.

Figure 64: spatial distribution of wind setup heights for a strong winter event

Table 28: summary of modelled wind setup elevations at various points

No.1	Description	95 th Percentile Max. of Modelled Wind Setup		
		Data Set No.1	Data Set No.2	Data Set No.3
1	Tip of Caisson 25	20.6mm	21.9mm	26.9mm
2	Small Craft Harbour	24.0mm	28.6mm	23.9mm
3	Western end of beach	34.5mm	56.6mm	25.2mm
4	Centre of Beach	42.8mm	67.4mm	34.9mm
5	Eastern end of Beach	37.4mm	47.1mm	48.8mm
6	Back of Langebaan Lagoon	271.7mm	256.8	684.4mm

No.1	Description	99 th Percentile Max. of Modelled Wind Setup		
		Data Set No.1	Data Set No.2	Data Set No.3
1	Tip of Caisson 25	30.4mm	28.4mm	50.7mm
2	Small Craft Harbour	35.6mm	37.9mm	57.7mm
3	Western end of beach	48.6mm	70.3mm	63.3mm
4	Centre of Beach	58.4mm	83.6mm	83.8mm
5	Eastern end of Beach	53.0mm	59.7mm	93.7mm
6	Back of Langebaan Lagoon	378.6mm	421.2mm	880.7mm

6.4.1 Comparison with Results of Analytical Calculations

The results of the numerical model were compared with the analytically calculated wind setup. The comparison is summarised in **Table 29**. The differences between modelled and calculated setup values range between approximately 0% to approximately 176%. In some isolated cases, the values for wind setup as obtained from the two methods are almost an exact match. The values from the two methods matched particularly well in scenarios where wind blew from a south easterly direction. However, in some cases, particularly for results obtained from data series no.3, a significant difference was observed from one calculation method to the other.

Keeping in mind that data series no.3 involves the presence of strong northwest winds, it is clear that the area for wind setup generation, in this case, is limited to the short fetches inside of the inner bay. This explains why the analytical calculations, here, yielded (on average) smaller values than the numerical model. The analytical method assumes a simple two dimensional representation of the problem and does not include the complex three dimensional interactions of flows that occur in the bay as result of wind setup. The model does actually include the effects of these flows and therefore it makes sense that results may differ the way it does.

Table 29: Summary of comparison of modelled results and analytically calculated results

Test Position	Wind Setup (mm)			Difference (%)
	Model.	Calc.	Data Series	
Centre of Beach	58	37	1	57.8
	84	55	2	52
	84	34	3	146.5
Tip of Caisson 25		28		8.6
	30	23	1	32.2
		32		5
		27		5.2
	28	25	2	13.6
		69		58.8
Langebaan lagoon		46		10.2
	51	26	3	95
		19		166.8
AVERAGE	378.6	379	1	0.1
	421.2	367	2	14.8
	880.7	574	3	53.4
AVERAGE				48.0%

Having discussed the isolated cases of variations in similarity between the two methods, **Figure 65** goes on to illustrate a general and overall comparison of the two methods. From this plot it would appear that results from the two methods are, in general, well correlated ($R^2 = 949$).

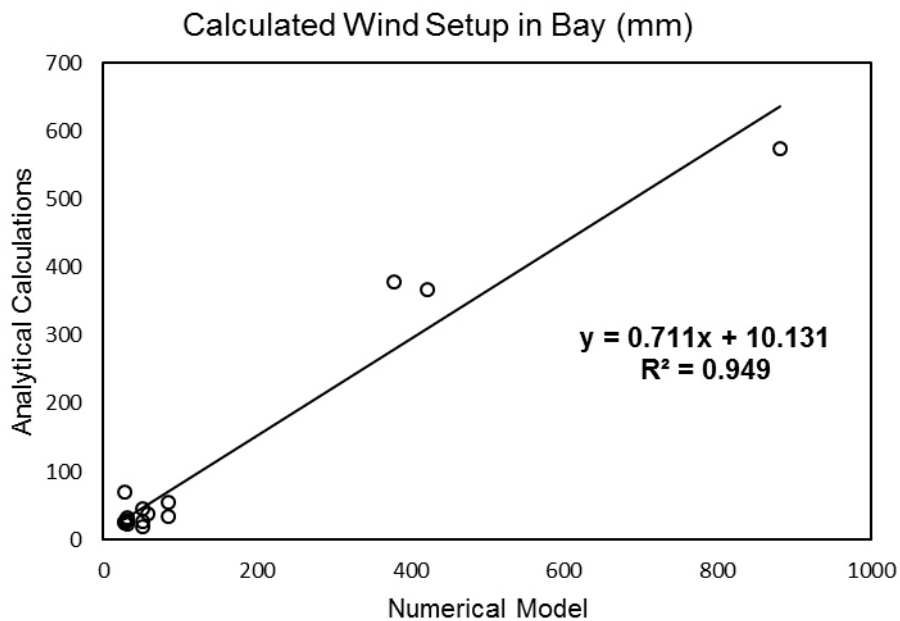


Figure 65: Comparison of modelled- and analytically-calculated wind setup heights

In conclusion, the results of the numerical model compare reasonably well with the results of the analytical calculations, although one should exercise caution in selecting which method to use. The analytical calculation is a good approximation of the model, but inside of small bays, especially, the simple assumptions made in the analytical calculations start to become evident in the results.

CHAPTER 7

7 Discussion of Results

7.1 GENERAL

Records of measured water levels were analysed for components resembling storm surge, or parts thereof. These components were then isolated for further analysis so that ultimately, all aspects of storm surges could be quantified. Thereafter, attempts were made to hindcast storm surge through the use of analytical methods and numerical modelling. Results from the analysis of the measured records were used in an attempt to validate the results of the calculated hindcasts. An extreme value analysis, in combination with the analytical calculations were also performed by which to predict long term maximum storm surge heights.

In this chapter, the results of these various analyses as mentioned above will be discussed and compared with one another. Finally, conclusions will be drawn and recommendations made.

7.2 DISCUSSION AND COMPARISON OF RESULTS

7.2.1 Static Storm Surge vs. Dynamic Storm Surge

It should be kept in mind that this study is based upon the assumption that there is a distinction between static storm surge and dynamic storm surge. Whereas static storm surge is considered as the wind setup and pressure setup manifesting in direct proportion to local winds and atmospheric pressure, dynamic surge is considered as that component of storm surge that arises from distant wind and pressure effects and which had propagated along a coastal shelf to the point of observation.

One of the key questions that were raised in earlier chapters is the question of the origin of the large unknown component identified during the time series analysis which, at that point in time, was hypothesised to be related to the dynamic effects of propagating storm surge. Subsequent analyses, however, did not succeed in delivering any kind of support to this suggestion.

In the case of the analytical calculations, it was always expected that the solutions yielded for wind setup and pressure effects would be entirely static and that the dynamic component of storm surge would be excluded from the results. While it was strongly anticipated that the numerical model would

yield such results (i.e. including dynamic effects), it had in fact failed to do so. Despite the fact that there had been small amounts of dynamic effects present in the outputs of the numerical models, the overall results had been mostly comparable to that of the analytical calculations in that no dynamic effects nearly as significant as those in question from the time series analysis were present. It must therefore be accepted that, due to a lack of substantial support coming from the analyses performed, that the large “dynamic effects” component of the time series analysis cannot be regarded as being related to storm surge. Perhaps, with the availability of data from a greater number of stations, including offshore stations, or synoptic charts, it would be possible to link the unknown components to wind or pressure (or some other phenomenon perhaps). Therefore, the possibility of the questioned components being related to storm surge is not ruled out but as far as what could be deduced within the constraints of this study and the available data, it cannot be regarded as storm surge.

Now with dynamic storm surge essentially being ruled out, it is concluded that storm surge as encountered in this study is predominantly static.

7.2.2 Storm Surge heights

Two components were looked into, namely wind setup and the inverse barometer effect (pressure setup):

Wind Setup

From the time series analysis, the maximum wind setup was determined to be in the range of 31 to 38mm (the analytical calculations suggested somewhat higher values of up to 64mm) Additionally, it was estimated that wind setup, on average, makes up a very small 6.4% of the total water level residuals. The process of obtaining this result involved filtering out wind-prone frequencies. It is possible that some unwanted noise is contained within this result. Therefore, it is noted here that this value for wind setup is given with a relatively low reliability. None the less, the value appears to be realistic when compared with the results of the subsequently performed analytical and numerical computations.

In this regard, a comparative analysis was done (Section 5.5.2) between the results of the analytical calculations and the values for wind setup as determined in the time series analysis. From this comparison, it was difficult to conclude the exact accuracy of the calculations with respect to the observed values. However, given the purpose of the study and the engineering application in mind, the results may well be accepted as satisfactory. A similar comparative analysis (Section 6.3.7) was performed between the modelled wind setup results and the observations if the time series analysis. This comparison showed that the modelled results very closely resembled the observations of the time series analysis (8% average deviation between the two).

With the similarity between the calculated and observed wind setup heights, one may want to argue that the wind setup outputs of the time series analysis are suitably validated. However, this should be done with caution. It is important to bear in mind that the analytical calculations involved the use of a friction coefficient which really should have been determined through field data for each site specifically. But, instead, a value for this coefficient was assumed because not enough field data was available for correctly determining the correct value. Similarly, for the numerical model, assumptions were made for the values of model input coefficients. Therefore, by comparing the results of the time series analysis to that of the analytical and numerical solutions, one is really comparing the results with two invalidated results. As a result, it would not be correct to imply that the time series analysis results are validated simply because the computations yielded similar results.

With that being said, it would appear nonetheless that assumptions made for the coefficients proved rather sufficient as results are consistent and realistic.

With regards to long term predicted outcomes for wind setup, extreme value analysis calculations based on NCEP data suggest that the 1 in 100 year expected wind setup, at this same point, could reach 163mm. Wind setup, even long term maxima, are thus fairly insignificant in Saldanha Bay. Unless this result will be used particularly for applications that are extremely sensitive to extreme sea levels, wind setup may be ignored all together.

Furthermore, it was observed that wind setup is highly variable within the bay. The analytical calculations and the numerical model unanimously showed a strong increase in wind setup heights over shallow stretches and long fetches. This is exactly as expected in terms of the theory. With this in mind, the wind setup calculated for the back of the Langebaan lagoon, in particular, is rather significant. According to calculations and models, short term expected wind setup height at this position could reach up to 720 to 880mm. A value such as this has serious design impacts and should not be ignored. Of even greater concern is the 1 in 100-year maximum predicted wind setup in the lagoon which was calculated as nearly 1.5m. These figures are not at all validated and have been determined in a fairly rudimentary manner, however it highlights the importance that shallow water bodies such as this is extremely susceptible to wind setup and this factor should form a definite part of such design.

Inverse Barometer Effect (Pressure Setup)

The second component of storm surge, namely the inverse barometer effect, yielded results that are somewhat more straightforward. Theoretically, as derived from analytical expressions, a 1mbar drop in ambient pressure at sea level, results in very near to 1cm in uplift of the sea level locally. However, from the time series analysis, there was strong evidence (strong statistical correlation) to suggest that contrary to the theory, 1mbar change in pressure resulted in as much as 1.7cm surface elevation change. Using the relationship as described above, it is concluded that pressure effects in Saldanha Bay is

relatively significant and is estimated to have reached heights in the range of 91mm to 268mm during the time periods corresponding to that of the three data sets analysed. Furthermore, the predicted maximum pressure-effect water level increase with a 1 in 100 year return period is 386mm.

Not much can be said about the spatial variability of the pressure effects, as the data required for such an evaluation was not available for this study.

7.2.3 Application of Study Outcomes

What is the significance of the results and how much of it is applicable in engineering practice and how is it applicable? These are the questions that need to be asked regarding the results that have been looked at thus far.

It is true that in this study, results were only obtained for Saldanha Bay, but having looked at the typical meteorological conditions for South Africa as a whole (Chapter 2), it may be said that Saldanha Bay actually is somewhat representative, meteorologically, of the greater part of the western and southwestern coastline. It is the same meteorological systems that affect Saldanha which so also affect the remainder of the west and southwestern coast. Furthermore, the continental shelf remains fairly uniform along most of the west and southwest coastline. As such, is clear that, in general, coastal waters of South Africa, even on the continental shelf, are deep enough to be unaffected by wind setup. With regard to water depths, Saldanha Bay really is a rare case in South Africa of a large, (relatively) shallow bay and even here, it was seen that wind setup is almost negligibly small. As such, the values of wind setup, as determined for Saldanha, if placed in the context of the South African coast as a whole, is perhaps even an over estimation of the reality, but should nevertheless yield safe and conservative estimates for engineering applications.

On the heights determined for storm surge, it may be reasonably accepted that the 23 to 64mm as determined for the short term and even the maximum predicted 163mm is small enough to be ignored for most practical and engineering applications. Pressure setup, on the other hand, was observed to reach 268 and predicted to reach 386mm. Although still small, this value is more noteworthy from a design perspective. This value should be taken into account in all designs where extreme high water levels are of interest. This value is moreover also not strictly site specific to Saldanha Bay, but may be applicable to any site along the western and southwestern coast that is susceptible to the cape cold front systems.

Another important point regarding storm surge levels that was highlighted in this study is that there are specific areas within the Saldanha Bay that are susceptible to significant wind setups. For instance, wind setup can reach up to 1.5m in the Langebaan lagoon. Admittedly, the wind setup heights that were determined for such points are given with a low reliability. However, it highlights the importance of treating such cases with special caution. Within the context of South Africa, there are several more

cases of shallow coastal waters like the one considered here. Examples include the large estuarine lakes such as St. Lucia, Bot, Kleinriver, Kosi to name a few.

Perhaps more important than the actual magnitudes of storm surge that was determined in this study, is the need to reflect on the usefulness concerning the methodologies and data sets that were used in determining these magnitudes.

As far as data is concerned, it is not uncommon in the South African-, or moreover, the African context, for engineers to have to design for areas where little to no recorded data is available. It was seen in this study that there were rudimentary calculation procedures which yielded relatively good results, without the need for any recorded data. For example, the NCEP data was found to represent surface air pressure fairly accurately. It also represented wind magnitude fairly accurately considering that wind is a process that is often rapidly varying. Unfortunately, in the case of Saldanha Bay, it was found that the NCEP data failed to accurately portray the wind directions as measured. Collectively though, wind and pressure is considered as being fairly well portrayed in the NCEP data and this type of data is freely available for the whole world. It can thus be recommended to make use of such NCEP data sets where required.

As for storm surge calculations; it is obvious that a detailed analysis such as the time series analysis that was performed in this study can only be replicated at sites where there are decent records available of water levels, wind data and pressure data. In the typical South African context, such data records are unavailable. With this in mind, and on the basis of the findings of this study, it may be concluded that numerical modelling succeeds in portraying wind setup reasonably well. Furthermore, even simple analytical calculations for wind setup, if applied within the framework of its assumptions and limitations, yields acceptable results. However, the analytical formulae should be used with caution and underlying assumptions and limitations should be respected. One may arguably rank the three methods of determining storm surge, in order of preference and accuracy, as follows: First analysis of time series data, second numerical modelling and third analytical calculations. Depending on the availability of data, the designer should make a decision accordingly.

CHAPTER 8

8 Conclusions and Recommendations

8.1 STUDY CONCLUSIONS AND APPLICATION OF RESULTS

Wind setup components of storms surge, applicable to the period of observation, was determined as reaching up to 64mm. This is based upon an analysis of data, numerical modelling and analytical calculations for the period between January 2010 and March 2015. An extreme value analysis of NCEP data indicated that wind setup values could reach 1 in 100 year maximum heights of 163mm. Inverse barometer effect components of storm surge, were identified as reaching 268mm. Extreme value estimates for this pressure component, derived from NCEP data, amounts to 386mm. From these results as summarised above, and from the outcomes of the various discussions undertaken in this study, the following recommendations and guidelines may be offered in terms of the application of the study results:

- Along the south and southwestern coastline of South Africa, wind setup components in coastal waters are small and may be ignored. This, however, does not apply to large estuarine bays.
- In some special cases, where designs are sensitive to small water level increases and where no data is available from which to calculated, a fixed value for wind setup height may be assumed of 65mm for the short term maximum and 165mm as an absolute maximum.
- For designs and studies concerning extremely shallow water bodies, such as lagoons and estuaries, wind setup could reach up to 1.5m. Detailed studies are recommended for such cases. Preferably, detailed numerical models should be considered for such studies.
- Along the south and southwestern coastline of South Africa, pressure setup components may be assumed as 270mm in the short term and a long term maximum of 390mm.

For designs and studies falling outside of the general south and southwest coast of South Africa, the following is recommended.

- The best estimate of storm surge is to analyse observed water levels at the point of interest. Wind and pressure data is also required for such an analysis.

- If water level data is not available for the point of interest, numerical modelling is recommended. Modelling requires the availability of water level data, detailed bathymetry data, wind data and pressure data. If wind and pressure data is not available, reasonably accurate estimated sets may be obtained from the NCEP data base.
- If neither water level data nor bathymetry data, nor wind and pressure data is available, the use of Bretschneider's simplified analytical method is acceptable. Wind inputs, in such circumstances, may be obtained from NCEP data sets.

8.2 RECOMMENDATIONS FOR FUTURE STUDIES

The following recommendations are made for future studies pertaining to storm surge heights in South Africa:

1. The outcomes of this study would suggest that wind setup components determined at Saldanha Bay are conclusive and indicative that wind setup, in general cases, are sufficiently small to be ignored. However, there would be logic in performing a similar study at a site with similar conditions in order to verify this outcome. A study of water levels in St Helena Bay and (at least a portion of) False Bay may provide useful results in this regard. A repeat study as mentioned here is however only recommended for the purpose of verifying the outcomes of this thesis and is not recommended for day to day engineering applications. For standard engineering and design applications, wind setup may simply be ignored (unless in the case of a particularly shallow lagoon or estuary).
2. Over and above the (single) repeat study as recommended above, it is recommended that for any scenario where storm surge is of particular interest, that a study such as in this thesis should be repeated. Such scenarios may include any study where the design is particularly sensitive to small changes in water level.
3. The shortcomings of this study is listed below so as to offer guidance towards better outcomes of a future study:
 - Water level data contained many gaps. As such, it was not possible to extract many data segments of long enough duration to perform accurate frequency domain analyses. Only three segments of decent length were extracted. This later limited the accuracy of verification of the analytical calculations.
 - Water level data was only available in one part of the Saldanha Bay. As a result, calibration of a numerical model was difficult to achieve

- Pressure setup could only be determined statically. There was still a large unresolved component of residuals in the time series analysis. Perhaps with spatially- and time-varying pressure data, a greater percentage of this unknown component could be positively linked to storm surge. However, this was not the case.
- Regarding the large unknown component that is mentioned in the point above, it would seem like a disappointing outcome to leave such a prominent component unaccounted for. However, this unfortunate outcome may be excused if one stays true to the objective of the study, which is, strictly, to quantify **storm surge** components (and not any or all of the other components which may be present). Within the limitations of this study, the unknown component could not be linked to storm surge with any confidence and therefore it may be dismissed within this context. This nevertheless raises obvious concerns and as such it would only be fair to list it as a shortcoming of this study. It also raises enough question to perhaps motivate for a further study into this unknown component on its own.
- The literature study did not provide results of storm surge heights from other areas of the world with similar meteorological and geographical conditions. Investing for the outcomes of such studies would have proved valuable.

9 References

- Bretschneider, C.L., 1967. Storm Surges. *Advances in hydroscience*, 4, pp.341–418.
- Brundrit, G., 2009. Global Climate Change and Adaptation : City of Cape Town sea- level rise risk assessment. Phase 5. *System*, (December), p.35.
- Brundrit, G., 2008. *Sea Level Rise Model for the City of Cape Town: Phase One Report*, Cape Town.
- Brundrit, G. et al., 2011. Understanding Sea-Level Rise and Variability. *African Journal of Marine Science*, 33:1(June 2015), pp.189–190.
- Brundrit, G.B., 1984. Monthly mean sea level variability along the west coast of southern Africa. *South African Journal of Marine Science*, 2(June 2015), pp.195–203.
- Brundrit, G.B., 1995. Trends of Southern african sea level: statistical analysis and interpretation. *South African Journal of Marine Science*, 16(June 2015), pp.9–17.
- CERC, 1984. *Shore Protection Manual*, Department of the Army, Waterways Experiment Station, Corps of Engineers, Coastal Engineering Research Center.
- Charles, D. & Stuart, A., 2013. *Characterizing Long Wave Agitation in the Port of Ngqura Using a Boussinesq Wave Model*, MSc Thesis. University of Stellenbosch.
- CIRIA, CUR & CETMEF, 2007. *The Rock Manual. The use of rock in hydraulic engineering (2nd edition)*, C683, CIRIA, London.
- Cloete, U., 2012. *Preliminary Investigation of Northern False Bay Storm Surge*, (BEng Disertation). University of Stellenbosch.
- De Cuevas, B.A., 1985. *Characteristics of sub tidal coastal trapped disturbances in sea level along the coasts of Namibia and South Africa*. MSc Thesis, University of Cape Town.
- Dean, R.G. & Dalrymple, R.A., 2002. *Coastal Processes with Engineering Applications*, Cambridge University Press.
- DHI, 2013a. *MIKE 21 & MIKE 3 Flow Model FM - Transport Module - Scientific Documentation*,
- DHI, 2013b. *MIKE Zero EVA Technical Reference and Documentation*,
- DHI, 2013c. *MIKE Zero EVA User Guide*,
- Fearon, G., 2014. *Extreme Wind Speeds for the South-West Indian Ocean using Synthetic Tropical Cyclone Tracks*. M.Eng Thesis, University of Stellenbosch.

- Fengshu, L. & Xinian, W., 1989. A review of storm-surge research in China. *Natural Hazards*, 2(1), pp.17–29.
- Glahn, B. et al., 2009. The role of the SLOSH model in National Weather Service storm surge forecasting. *National Weather Digest*.
- Gonnert, G. et al., 2001. *Global Storm Surges: Theory, Observations and Applications* German Coastal Engineering Research Council, ed., Die Kuste.
- Hellstrom, B., 1941. Wind effect on lakes and rivers. *Royal Swedish Inst. for Eng. Research Proceedings*, 158.
- Hunter, I., Stander, J. & Coning, E.D., 2007. The Storm Surge of 19 March 2007.
- Ippen, A.P. & Eagleson, P.S., 1966. *Estuary and Coastline Hydrodynamics*, New York: McGraw-Hill.
- Jury, M.R. et al., 1986. Meteorological and Oceanographic Aspects of a Winter Storm of the South Western Cape Province, South Africa. *South African Journal of Science*, 82, pp.315–319.
- Kamphuis, J.W., 2000. *Introduction to Coastal Engineering and Management* 2nd ed., Singapore: World Scientific Publishing.
- Karim, M.F. & Mimura, N., 2008. Impacts of climate change and sea-level rise on cyclonic storm surge floods in Bangladesh. *Global Environmental Change*, 18, pp.490–500.
- Keulegan, G.H., 1952. The form factor in wind-tide formulas. *National Bureau of Standards Report*, 1835.
- Keulegan, G.H., 1951. Wind tide in small closed channels. *Journal of the National Bureau of Standards*, 46(5).
- Knabb, R.D., Rhome, J.R. & Brown, D.P., 2005. *Tropical Cyclone Report Hurricane Katrina 23-30 August 2005*,
- Langhaar, H.L., 1951. Wind Tides in Inland Waters. In A. Arbor, ed. *1st Midwestern Conf. Fluid Mech.* Michigan: Michigan Press.
- LaquaR Consultants CC, 2008. *Sea-Level Rise Risk Assessment for the City of Cape Town. Phase Two Report*,
- Machutcheon, K.R., 2015. *An Introduction to Multifractal Geometry of Wave Sea States on the West and South-east Coasts of South Africa*. PhD Thesis, University of Stellenbosch.
- MacHutcheon, K.R., 2006. *The Characterisation of South African Sea Storms*. M.Eng Thesis, University

of Stellenbosch.

- Mather, A., Garland, G. & Stretch, D., 2009. Southern African sea levels: corrections, influences and trends. *African Journal of Marine Science*, 31(June 2015), pp.145–156.
- Mather, A.A. & Stretch, D.D., 2012. A Perspective on Sea Level Rise and Coastal Storm Surge from Southern and Eastern Africa: A Case Study Near Durban, South Africa. *Water*, 4, pp.237–259.
- Mather, A.A. & Theron, A., 2012. *Recent extreme events along the coast of South Africa DRAFT*,
- Mavume, A.F. et al., 2009. Climatology and Landfall of Tropical Cyclones in the South-West Indian Ocean. *Western Indian Ocean Journal of Marine Science*, Vol. 8(No. 1), pp.15–36.
- Nelson, R.C., 1975. Tropical Cyclone Storm Surges in Australia 1880 to 1970. In *Second Australian Conference on Coastal and Ocean Engineering, 1975: The Engineer, the Coast and the Ocean, The*. Sydney: Institution of Engineers, Australia, pp. 195–201.
- Netherlands Ministry of Infrastructure, Delft University of Technology & UNESCO-IHE, Coastal and River Engineering Support System (CRESS): Wind setup. Available at: <http://www.cress.nl/About.aspx>.
- NOAA, 2016. NCEP-DOE Reanalysis 2: Summary.
- OCDI, 2002. *Technical Standards and Commentaries for Port and Harbour Facilities in Japan* The Overseas Coastal Area Development Institute of Japan, ed., Japan: Daikousha Printing.
- Okal, E.A., Visser, J.N.J. & de Beer, C.H., 2014. The Dwarskersbos, South Africa local tsunami of August 27, 1969: field survey and simulation as a meteorological event. *Natural Hazards*, pp.251–268.
- Percival, D. & Mofjeld, H., 1997. Analysis of subtidal coastal sea level fluctuations using wavelets. *Journal of the American Statistical Association*, 92, pp.868–889. Available at: <http://www.jstor.org/stable/10.2307/2965551>.
- PRDW, 2010. *Climate Change Think Tank - Marine Inputs to Salt River Flood Model*, Cape Town.
- R Core Team, 2016. R: A Language and Environment for Statistical Computing. Available at: <https://www.r-project.org/>.
- Rossouw, J., 1989. *Design waves for the South African coastline*. University of Stellenbosch.
- Schumann, E.H., 1989. Coastal-Trapped Waves off the Coast of South Africa: Generation, Propagation and Current Structures. *Journal of Physical Oceanography*, 20, pp.1206–1218.

- Sebastian, A. et al., 2014. Characterizing hurricane storm surge behavior in Galveston Bay using the SWAN + ADCIRC model. *Coastal Engineering*, 88, pp.171–181. Available at: <http://dx.doi.org/10.1016/j.coastaleng.2014.03.002>.
- Singleton, A.T. & Reason, C.J.C., 2007. Variability in the characteristics of cut-off low pressure systems over subtropical southern Africa. , 310(September 2006), pp.295–310.
- Smith, A. et al., 2013. KwaZulu-Natal coastal erosion events of 2006 / 2007 and 2011 : A predictive tool? *South African Journal of Marine Science*, 109(3), pp.1–4.
- Smith, A.M. et al., 2007. Combined marine storm and Saros spring high tide erosion events along the KwaZulu-Natal coast in March 2007. *South African Journal of Science*, 103(August), pp.274–276.
- Sorensen, R.M., 1997. *Basic Coastal Engineering Basic Coastal* 2nd ed., Springer.
- Theron, A.K., 2016. *Methods for Determination of Coastal Development Setback Lines in South Africa, PhD Thesis*. University of Stellenbosch.
- Thomson, R.E. & Emery, W.J., 2001. *Data Analysis Methods in Physical Oceanography (Second Edition)*, Elsevier.
- Tyson, P.D. & Preston-Whyte, R.A., 2000. *The Weather and Climate of Southern Africa* 2nd ed., Oxford University Press.
- U.S. Army Corps of Engineers, 2002. *Coastal Engineering Manual (CEM), Engineering Manual 1110-2-1100*,
- U.S. Army Corps of Engineers, 1986. *STORM SURGE ANALYSIS AND DESIGN WATER LEVEL DETERMINATIONS*, Washington, DC.
- Watts, A., 2004. *The Weather Handbook* Second edi., Adlard Coles Nautical.
- Wijnberg, A.R., 1993. *Design Sea Levels for Southern Africa: A Probabilistic Approach*. PhD Thesis, University of Cape Town.